ADDIS ABABA UNIVERSITY

ADDIS ABABA INSTITUTE OF TECHNOLOGY

SCHOOL OF CHEMICAL AND BIO-ENGINEERING

ANALYSIS AND OPTIMIZATION OF PARA-XYLENE PRODUCTION PROCESS FROM SUGARCANE BAGASSE

BRHANU GEBRESLASSIE

ADVISOR: DR. ENG. HUNDESSA D. DEMSASH

A Thesis Submitted to School of Chemical and Bio-Engineering, Addis Ababa Institute of Technology in Partial Fulfillment of the Requirements for the Award of the Degree of Master of Science in Chemical Engineering under Process Engineering Stream.

ADDIS ABABA, ETHIOPIA

JUNE, 2018

ADDIS ABABA UNIVERSITY

ADDIS ABABA INSTITUTE OF TECHNOLOGY

SCHOOL OF CHEMICAL AND BIO-ENGINEERING

ANALYSIS AND OPTIMIZATION OF PARA-XYLENE PRODUCTION PROCESS FROM SUGARCANE BAGASSE

A Thesis Submitted to School of Chemical and Bio-Engineering, Addis Ababa Institute of Technology in Partial Fulfillment of the Requirements for the Award of the Degree of Master of Science in Chemical Engineering under Process Engineering Stream.

Approved by the Examining Board:

Name	Signature	Date
Dr. Ing. Abubeker Y. School Dean		
Dr. Ing. Hundessa D. Advisor		
Dr. Ing. Zebene K. External Examiner		
Dr. Ing. Anuradha J. Internal Examiner		

DECLARATION

I declare that this thesis entitled **"Analysis and Optimization of Para-Xylene Production Process From Sugarcane Bagasse"** has not been submitted in Addis Ababa university and an award at any university previously as well currently except for citations which have been appropriately acknowledged.

Name: Brhanu Gebreslassie

Signature:_____

Date: _____

This thesis has been submitted for examination with the approval of my Advisor Dr. Eng. Hundessa D. Demsash (Assistant Professor), instructor in School of Chemical and Bio-Engineering, Addis Ababa Institute of Technology, AAIT.

Signature:_____

Date:_____

ABSTRACT

Lignocellulosic biomass has a great potential for biofuel and fine chemical productions. This study focused on the effective conversion of the lignocellulosic biomasses, particularly sugarcane bagasse to the most valuable aromatic hydrocarbon called Para-xylene via two-step acid-catalyzed hydrolysis, dehydration, hydrogenation, and Diels-Alder cycloaddition reaction steps. Para-xylene is one of the most important aromatic hydrocarbons, which is used for the production of purified polyethylene terephthalate (PET), in which it is used for the production of world plastics. So, the production of fine chemicals from biomass helps to reduce the dependence of the imported oils as well as used to improve the overall economic and sustainability of the world. In this study, the effect of operating variables on the Diels-Alder cycloaddition reaction between the biomass-derived furan and the suitable dienophile, which is called Maleic anhydride, was investigated and optimized using the most reactive and selective Lewis acid catalyst ($AlCl_3$). In the Diels Alder cycloaddition reaction, the effects of reactant molar ratio, catalyst loading and reaction time on the conversion of DMF and the yield of dimethyl benzoic acid was investigated and optimized using Design expert®7 software. As the result, 41.4% conversion of DMF and 64.6% yield of dimethyl benzoic acid were obtained at the optimum values of the operating variables such as molar ratio of the reactant, catalyst loading and reaction time. And also, the effects of acid concentration and reaction time on the dehydration of dimethyl benzoic acid to Para-xylene were investigated, and 70.36% conversion of dimethyl benzoic acid and 49.66% yield of Para-xylene were obtained. In addition to this, the final product (Para-xylene) was analyzed using FTIR and GC-MS. As the result, the FTIR result is the same with the standard functional group of 1,4-dimethyl benzene, and 30.88% composition of Para-xylene were obtained using GC-MS.

ACKNOWLEDGEMENTS

Above all, I thank almighty God for all his blessings.

I would firstly like to express my deepest appreciation to my advisor, **Dr. Eng. Hundessa D. Demsash,** for his continued encouragement and guidance.

I would also like to thank School of Chemical and Bio-Engineering laboratory staff Henstaselassie for his support throughout the experimental work.

Lastly, I would like to thank for all lab assistants of Addis Ababa University College of natural science (Arat kilo), Department of chemistry, for their assistance in the FTIR analysis, and leather industry development institute (LIDI), for their assistance in the GC-MS analysis.

Table of Contents

LIST OF TABLES

LIST OF FIGURES

LIST OF ACRONYMS

ANOVA	Analysis of Variance
ASTM	American Society for Testing and Materials
BTX	Benzene, Toluene and Xylene respectively
CCD	Central Composite Design
DMA	Dimethyl Acetamide
DMF	2, 5-Dimethylfuran
DMSO	Dimethyl Sulfoxide
DMT	Dimethyl Terephthalate
DOE	Department Of Energy
DP	Degree of Polymerization
FT-IR	Fourier Transform Infrared Radiation
GC-MS	Gas Chromatography Mass Spectroscopy
GHG	Greenhouse gases
HMF	5-Hydroxymethyl Furfural
ILS	Ionic Liquid Solvent
LHW	Liquid Hot Water
MX	Meta-xylene
NREL	National Renewable Energy Laboratory
OX	Ortho-xylene
PET	Polyethylene Terephthalate
PTA	Purified Terephthalic Acid
PX	Para-Xylene
TAPPI	Technical Association Of Pulp And Paper Industries
THF	Tetrahydrofuran
XRD	X-Ray Diffraction

1. INTRODUCTION

1.1. Background

The production of biofuels and valuable chemicals from biomass has been increased due to increasing the need for sustainable products, as well as due to increasing environmental challenges (*Winner, 1994*). Aromatic hydrocarbons, including toluene, benzene and Xylenes are the most important compounds, which are used as a major feedstock for a large number of chemical production industries (*Eriksson, 2013*). Among the most important compounds of aromatic hydrocarbons, xylene is used as a major raw material for large chemical productions. The word "Xylene" comes from the Greek word "Xylose" which means that wood. Xylenes first were discovered from a wood spirit in 1850 G.C, and are called aromatic hydrocarbons, which contains benzene ring and two methyl groups, represented by (C_8H_{10}), and occurs in three forms of isomers, which are called meta-xylene, ortho-xylene, and p-xylene. P-Xylene is one of the most important isomers of xylene, which is utilized as a major feedstock for the production of terephthalic acid and dimethyl ester or dimethyl terephthalate which are used for the production of polyethylene terephthalate and these, which are commonly used for production of plastic bottles, clothing, automobiles and food packaging (*Barberio et al., 2015*).

Para-xylene has historically been produced from petroleum products via catalytic reforming of naphtha, which contains 0.5-1% of crude oil (*Aransiola et al., 2013*). At the time, many ideas have been created to decrease the amount of oil consumption and sustainable energy to produce renewable fuels and value-added chemicals. One of these creativities has been led to convert fructose to PX. Virent was built the earliest pilot plant in 2010 G.C, and the plant was originally trained to produce pure hydrogen (*Daramola, 2010*). In 2011, Virent has been developed the first bio-gasoline production plant from corn Stover and pine harvest forest residuals, and it was the time of the first for the Department of Energy's (DOE), and he received its largest federal award from the Department of Energy (DOE). These past accomplishments lead to development of biofuels and value-add chemicals such as p-Xylene from simple sugars, in an efficient, low-cost and utilizing sustainable production technologies. As a result of its low cost and availability, lignocellulosic biomasses are receiving significant attention worldwide as a feedstock for renewable liquid fuels and chemical production (*Biddy et al., 2016*).

Today, the market of P-xylene is mainly directed towards the production of various products such as fibers, films, and resins (*Fms, et al., 2017*). Since, P-xylene is used as a main raw material for the production of terephthalic acid and dimethyl terephthalate, which are used mostly for the production of plastic fabrics, the global demand for P-xylene has been steadily increasing, and this growth is expected to continue from time to time (*Tsai, 1999*).

According to the market report, the world Para-xylene demand is expected to increase at an average of 7% per year in the period of 2008-2013, driven mainly by PTA and PET demand increases in China, other Asian countries and in the Middle East. In addition to this, due to the applications of xylene used as a solvent in the printing (as component of ink), rubbers, leather industries (as component of adhesive, paints and varnishes), and in the laboratory used as a solvent to remove synthetic immersion oil from microscope objective during light microscopy. Furthermore, Nexant (i.e. the globally recognized software, consulting and services leader that provides innovative solutions utilities, energy enterprises, chemical companies and government entities worldwide) has estimated the U.S. market potential for renewable aromatic chemicals and materials starting from 2012 up to 2022 by assuming that renewable PET captures 5 percent of the U.S. PET bottle market by 2017 and 20 percent by 2022. However, due to these facts, the current production capacity of P-xylene is not sufficient. This implies, the demand for Para-xylene has been increasing continuously at a very fast pace throughout the world; therefore, this increment in its demand has created a challenge that needs to be addressed in the industrial sector (*Creation, 2014*).

In this study, lignocellulose biomass particularly sugarcane bagasse, which is the most abundant feedstock that is found around the sugar production industries such as Metehara, Wonji/Shoa and Tendaho, which is the most renewable resource is investigated to replace fuels and oil-based chemicals to produce Para-xylene via acid-catalyzed hydrolysis, dehydration, hydrogenation, Diels-Alder cycloaddition reaction, crystallization and decarboxylation processes (*Bogliano, 2016*).

1.2. Statement of the Problem

In the last decades, most fuels and fine chemicals have been commonly made from petroleum resources. As a result, petrochemical processes have reached maturity leading to the inexpensive production of the most commonly used chemicals. However, this leads to reducing oil reserves, increasing petroleum price and rising environmental burdens such as the continuous increment of atmospheric carbon dioxide and the resulting or expected climate changes, as a result, has led to the common agreement that the heavy dependence on fossil fuels is untenable. In addition to this, when we look at the biosphere, the most carbon sources organic materials are carbohydrates, particularly celluloses, which are the most problematic to solve in the biomass conversion to find favorable methods to convert these carbohydrates into biofuels and fine chemicals.

Around the sugar industry, we are dumping a lot of by-products into the environment such as sugarcane bagasse (i.e. the residue after the juice is extracted, which is not utilized for production of other value-added chemicals and inefficient for energy production) from which we can produce valuable products such as biofuels (e.g. furfurals) and fine chemicals (e.g. Para-xylene) by two-step acid-catalyzed hydrolysis, dehydration, hydrogenation, Diels-Alder cycloaddition reaction, crystallization and decarboxylation steps with economically feasible way.

Today, there is a higher awareness for a sustainable society, a growing concern about greenhouse gas effects, the fact that petroleum is a limited resource implies a business opportunity and an increased market interest for renewable raw materials, and for companies their long-term survival. In response to the increasingly urgent issue of sustainability, lignocellulose biomasses particularly celluloses are taken as the most potential alternatives for the production of high-volume and high-value fine chemicals by replacing mineral resources or fossils to overcome global warming and the major current environmental issues.

In general, this study is important as sugarcane bagasse is a widely available material which is the best alternative feedstock (rather than to use sugars, starches, sugarcane and oil-based materials) for Para-xylene production, and to overcome problems related to chemical product security, the creation of more sustainable environment, encourage rural development through job creation, and will reduce the greenhouse gas emissions.

1.3. Objectives

1.3.1. General objective

The general objective of this study is to analyze and optimize the Para-xylene production process from sugarcane bagasse.

1.3.2. Specific objectives

The specific objectives of this study were:

- To characterize the feedstock, such as proximity analysis (moisture content, volatile matter, ash content and fixed carbon), and chemical composition (extractives, hemicellulose, lignin, and cellulose);
- To investigate the effect of operating variables such as catalyst loading, reaction time and the molar ratio of reactants (DMF: Maleic anhydride) on the yield of dimethyl benzoic acid;
- To determine the optimum operating conditions such as catalyst loading, reaction time and the molar ratio of reactants that gives the maximum yield of dimethyl benzoic acid;
- To investigate the effect of acid concentration on the conversion of dimethyl benzoic acid and yield of Para-xylene in the dimethyl benzoic acid dehydration reaction to Para-xylene;
- To characterize the intermediate products using FT-IR; and
- To characterize the final product using GC-MS.

1.4. Significance of the Study

The main significance of this research is to transform from fossil fuel based economic system to a more sustainable economic system based on lignocellulose biomass. The production of high-value aromatic chemicals such as benzene, toluene and xylenes renewably from lignocellulose biomass-derived simple sugars will help to cover the way for future sustainability (*Loffler et al., 2009*). The transformation to biomass economy will be multiple drivers for the need to develop an environmentally, economically and socially sustainable global economy, desire of many countries to reduce an over dependency on chemical imports, the need to reduce atmospheric greenhouse gases emissions, and the need to motivate regional and rural developments. Production of Para-xylene directly from biomass is beneficiary and it will be directly integrated into existing chemical and production infrastructures. P-Xylene is one of the most important isomers of xylene, and it is used as key feedstock for the production of large-scale chemical industries. Para-xylene is primarily used as a key feedstock for the production of terephthalic acid; which is the building block for polyethylene terephthalate, which is used to manufacture plastic bottles, food packaging, clothing, and automobiles. This creates a unique aspect to make a commercially attractive process for renewable p- xylene production (*Weber et al., 2016a*).

1.5. Scope of the Study

In this study, characterization of the feedstock such as the proximate analysis and compositional analysis, different Para-xylene production steps such as pretreatment of the feedstock, acid-catalyzed hydrolysis reaction to convert cellulose to glucose, dehydration reaction of glucose to HMF, hydrogenation reaction of HMF to DMF, Diels-Alder cycloaddition reaction of DMF to Para-xylene, different investigations for the effects of the operating variables on the Diels-Alder cycloaddition reaction and dehydration of dimethyl benzoic acid to Para-xylene, optimization of dimethyl furan conversion and the yield of dimethyl benzoic acid, thermodynamics of the Diels-Alder cycloaddition reaction, and characterization of the intermediate product using FTIR and GC-MS were studied.

2. LITERATURE REVIEW

2.1. Introduction

Xylene is one of the most important aromatic hydrocarbon compounds, which is known as dimethyl benzene or methyl toluene, since it contains a benzene ring with two methyl groups, and is symbolized by the molecular formula of $C_6H_4(CH_3)_2$ or C_8H_{10}. There are three different structures of xylene in which the methyl groups vary on the benzene ring: meta-xylene, ortho xylene, and Para-xylene. These different forms are called isomers (*Yang et al., 2017*).

Xylene is primarily a synthetic chemical named in 1851, having been discovered as a consistency of wood tar. Industrially, xylene was produced from petroleum, and it occurs naturally in petroleum and coal tar and is formed during forest fires, to a small extent. It is a colorless, flammable liquid with a sweet odor. Para-xylene production from petroleum sources is a very energy intensive operation which involves many separations and distillation processes. Therefore, production of Para-xylene from renewable resources can be controlled and optimized through research, and it will help in the production of pure PX using a lower energy operation process in a more economically feasible way (*Settle et al., 2017*).

Generally, production of biofuels and fine chemicals from biomass is attractive, since there is a potential to reduce carbon emissions and environmental burdens. So, this study is concerned with the determination of sustainability of producing a chemical which is called Para-xylene from biomass particularly sugarcane bagasse instead of fossil resources (*Pacheco et al., 2014*).

2.2. World Para-Xylene Production and its Utilization

The petroleum fractions, which include all of the crude oil components heavier than pentanes up to a final boiling point between 105 ℃ and 170 ℃, are the most widely used materials for xylene production process. In majority xylene isomers are produced by catalytic reforming via hydro-treating naphtha originated from the pyrolysis or hydrocracking of heavier distillate fractions (*Neto et al, 2011*). But, the production process is a very energy intensive process involving many separations and distillation processes. Since, Para-xylene has main importance, such as it is used as a solvent in the printing, rubber, leather, plastics, biofuels and medical industries, the market demand has been gradually increased from time to time throughout the world. From 1999, world seriously concerns over p-xylene supply due to increasing the capacity development of purified

terephthalic acid and polyester. According to *Yasuhiko*, (*2013*), about 98% annual consumption of PX is used for the production of PET and PTA. At the time, new capacity has been coming into operation, but it has not decreasing because of steadily increased demand and generally has 6-8% annual demand growth.

Table 2-1: World PX production capacity and demand, 1999-2010; Source: (*Ashraf, 2013*)

Years	Demand (Annual kilometric tons)	Capacity (Annual kilometric tons)
1999	16,000	19,000
2000	17,000	22,000
2001	17,100	22,500
2002	18,000	22,500
2003	19,000	22,800
2004	21,000	23,000
2005	22,000	23,000
2006	24,000	25,000
2007	26,000	28,000
2008	28,000	32,000
2009	30,000	35,000
2010	32,000	37,500

In the years of 1990 to 1995 and 1995 to 2000, the worldwide growth rates for Para-xylene production were 7% and 8.8% respectively. The differential increases for the world production and demand for xylenes between the year 2003 and 2009 also 4.7 and 10.1 million tons respectively. After a period of severe over-capacity during 1999-2002, global operating rates for p-xylene were above 90% in 2005 (*Weber et al., 2016b*). World production capacity of xylene isomers in 2010 is approximately 44 million tons. And also as experts expected that, the world demand is annually increased from 2011 to 2015 and from 2015 to 2020 by 4.4% and 3.2% respectively. The capacity utilization, however, is predicted to reduce from 2011 to 2014, but begin an upward tendency afterward. This shows the global demand for xylene isomers has been steadily increasing with p-xylene leading the way (*Tsubaki et al., 2017*).

In the world; North America (NA), Western Europe (WE), South America (SA), Eastern Europe (EE), Middle East (ME) and Asian total (which includes Taiwan, China, South Korea, ASEAN, India and Japan) countries are the higher growth outlook for Para-xylene production and consumption. But, this is limited in scale due to increasing demand for the PET container resin market (*Neto et al., 2011*). Generally, global Para-xylene production growth and market demand has been dominated by the Asian Pacific regions and accounted around 80%, followed by North America and accounted about 11.7% of the overall world global demand in 2014. And also, China alone currently accounts for around two-thirds of the world PET fiber container resins (*Araujo et al., 2001*).

2.3. Feedstocks for Para-Xylene Production

Biomass and crude oils are mostly used as feedstock for Para-xylene production, and there are many similarities between them compared as chemical feedstock's, such as; both are multi-component mixtures, both require fractionation or separation into easily manageable building blocks before conversion to products and both require a methodology for conversion of these building blocks into useful products. And the main difference between them is, biomasses are the renewable and sustainable source of carbon in the form of polysaccharides such as; cellulose, starch, lignin, hemicellulose, protein, and monomer organic compounds such as; carbohydrates, oils, amino acids and plant extractive components (*Williams, 2014*).

Approximately $77x10^9$ tons per year of renewable carbon is created at the biosphere, due to this understanding, many researchers have been aimed at achieving an effective and efficient waste management scheme to convert these wastes to valuable fuels and chemicals. Lignocellulosic biomass-derived chemical products are renewable and can help to achieve sustainable development, and also, biomass resources are often available locally and the process is feasible without high capital investment. Furthermore, dependence on biomass chemicals can help to reduce greenhouse gas emissions (*Eriksson, 2013*). According to *Mcfarlane et al.,* (*2007*), have been reported that approximately 30 billion lb/year of chemical products are produced from renewable components. One important among BTX chemicals, requiring a low-cost, thermochemical process for renewable production is p-xylene. Production of p-xylene or PTA directly from biomass has the most important processes, that it can be directly integrated into the existing chemical and product infrastructures. Currently, new processes are being realized to

produce p-xylene from renewable resources using a process of two-step acid-catalyzed hydrolysis, dehydration, hydrogenation, crystallization and decarboxylation processes. Those new processes can be able to find the current market applications for the production of renewable PET and its monomer (*Lin, 2015*). The following materials are mostly used in the manufacturing of fuels and fine chemicals such as PX:

2.3.1. Sugars

Sugars, particularly C-6 (Hexose) involves in the process to produce furan groups using acid catalyzed dehydration before obtained the final product (Para-xylene). Therefore, sugars containing a high level of glucose materials are easiest for fuels and chemical production. But, it is difficult to use these materials as a feedstock for fuels and chemical production, because they are too expensive due to the advantages to use as human food chain (*Amarasekara et al., 2008*).

2.3.2. Starches

Starch is another important and potential feedstock that uses for Para-xylene production. Starch molecules are made up of long chains of glucose molecules, and also require reaction of starch molecules with water (hydrolysis) to break down the starch into fermentable sugars. Starch and cellulose can be hydrolyzed under the acidic condition or enzymatic condition to convert into glucose, in which the process is normally taking place at a temperature of 453-513K, and also this product can be dehydrated under acid catalyst to produce platform 5-HMF next to liquid fuels and chemical production (*Wang, 2014*).

2.3.3. Lignocellulosic Biomass

Agricultural wastes such as sugarcane bagasse, corn Stover, corn cob, rice hulls, woody crops, citrus peel waste, sawdust, paper pulp, municipal solid waste, and paper mill sludge's and others are a great source of lignocellulosic biomass, in which they are renewable, useless, non-edible and inexpensive. Today, these biomasses are the most abundantly used renewable materials on the earth, and so far, they are the most suitable and favorable materials used as a feedstock for production of green chemicals and biofuels (*Salminen et al., 2012*).

Lignocellulose biomasses can be categorized into three main components such as; cellulose, hemicellulose, and lignin. These components in the lignocellulose materials have different functions and chemistries. And also, lignocellulose biomass is the major renewable organic

matter with an estimated production of about 200 x 10^9 tons per year. And around 90 wt% of the dry matter in lignocellulosic biomass is made up of polymeric carbohydrates such as cellulose (20-60 wt%), hemicellulose (15-30 wt%) and lignin (10-25 wt%), and also (1-12 wt%) of extractives depends on the nature of the plant, and they occur in complex structure each other (*Sn, 2008*).

2.3.3.1. Cellulose

Cellulose is the main component of plant cell wall which contains approximately 20-60% depends on the nature of the plant. It is an un-branched polysaccharide, which is made up of a long chains of simple sugars particularly glucose molecules (β-D glucose units), which is linked by β-1,4-glycosidic bonds at a different degree of polymerization by intermolecular hydrogen bond (*Souza et al., 2012*). Cellulose is one of the main important abundant materials on the earth and plant cell wall widely used for chemical production, and also it occurs in bacteria, fungi, algae, and animals. In nature, cellulose has a degree of polymerization (DP) with approximately 10,000-15,000 glucopyranose units and each glucose unit is rotated at 180^O, relative to the adjacent units, and aggregates in the form of three-dimensional micro-fibrils. As mentioned before, these units of molecules are stabilized with hydrogen and Vander Waals forces, in which each glucose unit (cellobiose units) is linked by two intermolecular hydrogen bonds. And those intermolecular bond makes packed and stable configuration between molecules, or each hydroxyl group of molecules can create an ordered crystalline structure of cellulose and keeps cellulose thermally and chemically stable (*Maria et al., 2011*).

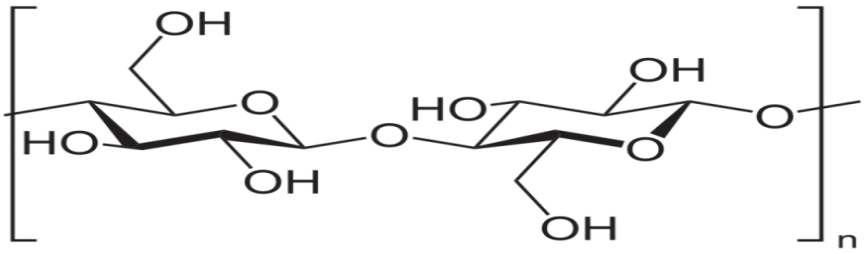

Figure 2-1: Chemical structure of cellulose (*Eriksson, 2013*).

2.3.3.2. Hemicellulose

Hemicellulose is another component of plant cell wall, and it is the most abundant heterogeneous group of polysaccharides next to cellulose. It is made up of pentose's (xylose, arabinose), hexoses (mannose, glucose, and galactose) and acetylated sugars. Hemicellulose is an amorphous

matrix material which binds the cellulose fibrils non-covalently through hydrogen bonding. In lignocellulose biomass, hemicellulose occurs with the composition of approximately 15-35% depends on the nature of the plant. In contrast to cellulose, hemicelluloses are differed by the composition of various sugar units, lower degree of polymerization (around 100-200), low strength and easy to hydrolysis, shorter and branched molecular chains and are lower crystalline than of celluloses. Due to these reasons, it can easily hydrolyze by dilute acid or base, as well as hemicellulose enzymes (*Amin et al., 2017).*

Table 2-2: Composition of various agricultural lignocellulosic biomasses; Source: (*Hong, 2013*)

Lignocellulose waste	**Composition (wt. %, dry basis)**		
	Cellulose	**Hemicellulose**	**Lignin**
Hardwood stems	40-55	24-40	18-25
Softwood	45-50	25-30	25-35
Corn fiber	14.3±0.5	16.8-35	8.4±0.6
Corn Stover	36.8-39	14.8-25	15.1-23.1
Cotton seed hairs	80-95	5-20	0
Ota straw	31-35	20-26	10-15
Rice Husks	28.7-35.6	12-29.3	15.4-20
Rice straw	35-45	18-25	10-25
Rye straw	37.6±0.4	30.5±0.5	19±0.8
Wheat straw	38-45	20-32	7-10
Soya stalks	34.5±0.5	24.8±0.2	19.8±0.4
Sugarcane bagasse	32-44	27-32	19-24
Switch grass	35-40	25-30	15-20

2.3.3.3. Lignin

Lignin is the third most abundant component of lignocellulosic biomass next to cellulose and hemicellulose, and they are complex, amorphous, hydrophobic, three- dimensional and cross-linked aromatic polymers of phenyl propane unit building blocks. And they make extremely resistant to chemical and biological degradation. Lignin is a composition of monomeric components such as; p-coumaryl, coniferyl or sinapyl alcohols, and these components are inter-linked in between lignin and hemicellulose as well as between lignin and cellulose. Due to strong inter-linkage between the components, such as ester, ether, or glycoside bonds, lignin's are extremely resistant to biodegradation and they occur in the form of three-dimensional in the plant cell wall in nature (*Petre et al., 1999*).

2.3.3.4. Extractives

Extractives are other components of lignocellulose biomass, which includes, the non-structural aromatic compounds, such as volatile oils, chlorophyll, fatty acids, waxes, resins, tannins, terpenes, sterols, inorganic compounds and so on, and they can be extracted with polar and non-polar solvents. These components can occur in the plant cell wall in small quantities, approximately 1-12% of the total lignocellulosic biomasses (*Edhirej et al., 2017*).

2.4. Sugarcane Bagasse as a Feedstock for Para-Xylene Production

Industrial productions of fuels and chemicals heavily depend on the fossil resources, but decreasing of these resources together with their increasing environmental effects, such as global warming and other problems have started to threaten the future of chemical industries (*Wijaya et al., 2015*). However, the competitive price advantage of fossil fuels during the last century has disappeared. After crossing the oil production peak, the decreasing of fossil resources will further boost the oil price and this situation will drastically impact the cost-effectiveness and competitiveness of fuels and chemicals. Alternative solutions are discovered to develop sustainable fuels and chemicals from renewable natural resources for decreasing the dependence on fossil resources. Biomass-derived feedstock's have been publicized as one of the most likely alternatives (*Meuwese, 2013*). Therefore, these materials have been well-chosen as the most sustainable source of organic carbon in the earth to replace the petroleum-based resources for the production of fuels and fine chemicals with net zero carbon emissions. In addition to this, those materials have vital advantages over other biomass stocks, since they are the non-edible sections

of the plant, and therefore, they do not interface with food supplies. Moreover, those materials are produced quickly and they are inexpensive than of the petroleum-based feedstock's and other agricultural biofuel feedstock's such as corn starch, soybeans and sugar cane (*Jenness, 2015*).

Figure 2-2: Waste sugarcane bagasse (Science. A, 2015).

Therefore, in this study, lignocellulose materials, particularly sugarcane bagasse was used for the production of value-add chemicals particularly for Para-xylene production. Sugarcane bagasse is obtained after the juice extraction in the sugar production industries, and approximately 540 million tons per year of sugarcane bagasse is produced in the world (*Betancur, 2010*).

2.5. Overview of Para-Xylene Production Process

The processes for Para-xylene production from lignocellulose biomass consists six steps. These are pretreatment to enhance biomass digestibility (i.e. extraction of cellulose from biomass), hydrolysis reaction of cellulose to sugar (i.e. Cellulose degradation to simple sugar particularly glucose), dehydration reaction of glucose to HMF, Hydrogenation reaction of HMF to DMF, Diels-Alder cycloaddition reaction of DMF to dimethyl benzoic acid, and crystallization and decarboxylation of dimethyl benzoic acid to Para-xylene (*Aqilah et al., 2014*).

2.5.1. Pretreatment of Lignocellulosic Materials

Lignocellulose biomass has a complex and rigid structure. Therefore, pretreatment is one of the most important process steps for biochemical conversion of lignocellulosic biomass into biofuels and fine chemicals. The main importance of pretreatment process is to remove lignin and hemicellulose (i.e. to extract cellulose), to reduce the crystallinity of cellulose, de-polymerization of hemicellulose, to increase the availability of the enzymes or acids to carbohydrates by increasing the surface area and porosity. After pretreatment and hydrolysis, cellulose from wood

or agricultural residues must be converted to simple sugars particularly glucose, either by acid or alkali hydrolysis or by the action of cellulose enzymes (*Delidovich et al., 2016*).

In general, Pretreatment methods can be classified into four common categories. Those are physical pretreatment, chemical pretreatment, physicochemical pretreatment and biological pretreatment (*Singhvi et al., 2014*).

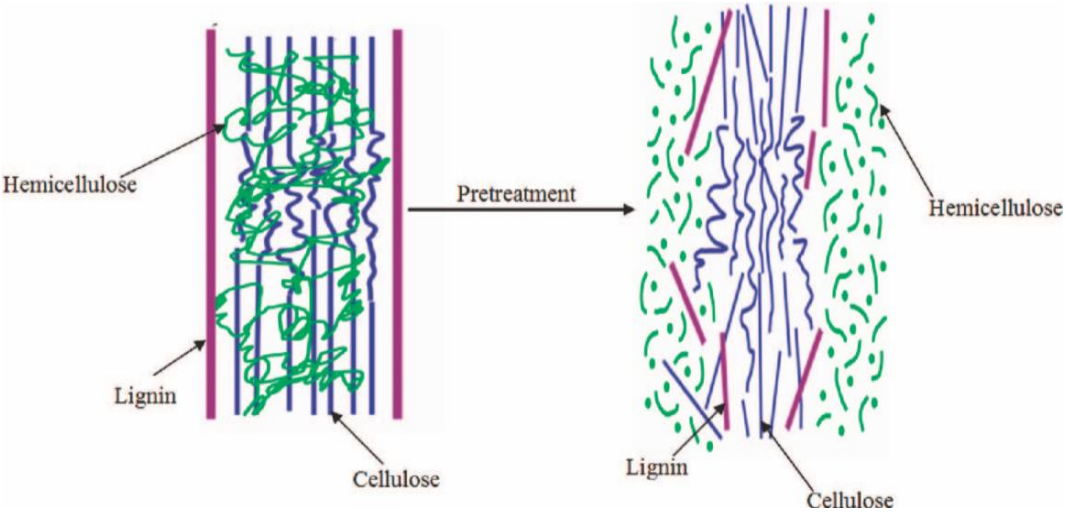

Figure 2-3: Pretreatment effect on lignocellulosic materials (*Zheng et al., 2009*)

2.5.1.1. Physical Pretreatment

This method includes size reduction by mechanical methods such as grinding or milling, different types of high energy irradiation and ultrasonic pretreatment methods and is used to increase the accessibility to hydrolyze long-chain polymers of lignocellulosic materials (*Winner, 1994*). In this method, there is no need of chemical agents. According to *Amin et al.,* (*2017*), mechanical pretreatment is a physical pretreatment which is broadly used for waste materials such as agricultural or forestry residues. Reduction of particle size is needed to make material handling easier and to increase surface/volume ratio, and it can be done by chipping, milling or grinding. But, this method of pretreatment needs an extremely high amount of energy to reduce the size of the feedstock from large size to a particle size of a millimeter and fine particles of micrometers, which is undesirable from the engineering perspective (*Aigbodion et al., 2010*).

During harvesting, the size of lignocellulosic materials is reduced to the particulate size of about 10–50 mm, chipping reduces the biomass size to 10–30 mm, while grinding and milling can reduce the particle size to 0.2–2 mm. From the physical treatment methods, grinding and milling

methods are more effective at reducing the particle size and cellulose crystallinity than chipping probably as a result of the shear forces generated during milling. Generally, the mechanical pretreatment method is carried out before other processing steps to reduce the feedstock, because the desired particle size is dependent on these subsequent steps (*Miao, Grift, & Ting, 2014).*

Radiation is another physical pretreatment method, which includes γ-ray, ultrasound, electron beam, pulsed electrical field, UV and microwave heating using high energy radiations, and this method can take place using microwaves to penetrate and heat the feedstock, as the result, the digestibility of the lignocellulosic materials (i.e. Cellulose) can be enhanced (*Harmsen et al., 2010*).

2.5.1.2. Chemical pretreatment

Chemical pretreatment is another important lignocellulosic material pretreatment method, in which chemical reactions are taking place to break down the biomass structure using chemical agents. According to *Gallo et al.,* (*2017*), the chemical pretreatment method is better to use than of biological as well as physical pretreatment methods, because it is more effective to degrade the complex materials such as removal of lignin or hemicelluloses and reduction crystallinity of cellulose components within a short period of time as well as it gives higher yield of reducing sugars. Pretreatments such as using acids, bases, organic solvents, pH-controlled liquid hot water, and ionic liquid pretreatments are the most widely used chemical pretreatment methods (*Abdel-Halim, 2014*).

i. Acid pretreatment

Acidic pretreatment is the method, in which it uses dilute or concentrated acids to hydrolyze completely or partiality of lignocellulosic materials. The acidic pretreatment process can increase the cellulose extraction or solubilization of lignin and hemicelluloses by catalyzing the hydrolysis of intermonomer ether linkages in the hemicellulose and crystallites of cellulose fractions of the lignocellulose matrix, as well as some linkages in the lignin fraction (*Jönsson et al., 2016*).

According to *Agbor et al.,* (*2011*), concentrated strong acids such as H_2SO_4, HCl, HNO_3 and H_3PO_4 are the most widely used acids for treatment of lignocellulose materials, because they are

more effective and powerful agents for solubilization of lignin and hemicellulose as well as degradation of cellulose to glucose.

The advantages of using concentrated acid hydrolysis are, it gives a high yield of reducing sugars within a short period of time as well as it requires mild temperature (110-260 ℃) conditions for hydrolysis. But, using concentrated acids have drawbacks such as; toxic, corrosive and hazardous nature; consequently, it requires reactors that need high-priced material construction resistant to corrosion as well as it needs to recycle acids in order to lower the cost (*Gallo et al., 2017*).

Alternatively, many researchers have been attempted to develop using dilute acid pretreatments for lignocellulosic materials, and it has been developed successfully. Dilute acid hydrolysis is performed in two different conditions, namely, high temperature (T > 160 ℃) in continuous mode for low solid loading (5-10% substrate concentration) and lower temperature (T ≤ 160 ℃) in batch mode for high solid loading (10-40% substrate concentration) (*Maryana et al., 2014*). This method of pretreatment is mainly used for a wide range of feedstock such as softwood, hardwood, herbaceous crops, agricultural residues, and municipal solid wastes. As stated before, several acids such as sulfuric acid, hydrochloric acid, nitric acid and phosphoric acids are most commonly used for pretreatment of lignocellulosic materials. According to (*Journal, 2012*) investigation, dilute sulfuric acid is most commonly and widely used due to its effectiveness (i.e. effective in terms of hemicellulose solubilization and cellulose degradation), and inexpensive than of the others, which is economically feasible pretreatment technique.

ii. Alkaline pretreatment

In this method, the process is involved by the addition of bases such as NaOH, KOH, $Ca(OH)_2$ and others to the lignocellulosic feedstock's. The major effect of alkaline pretreatment is the removal of lignin from the biomass, and improving the reactivity of the remaining polysaccharides and it can be able to remove the acetyl and various uronic acid substitutions on the hemicellulose that lowers the accessibility of the enzyme to the hemicellulose and cellulose surface (*Agustina et al., 2013*).

The alkaline pretreatment method is generally applied and works in an effective way for the lower lignin content of lignocellulosic materials. In such a way that, the effectiveness of this method depends on the composition of the lignin content in the feedstock (*Tucker, 2017*). This

method can take place in relatively mild condition and longer reaction time. In addition to this, mostly it is used to hydrolyze small portion and for partial hydrolysis of the lignocellulosic feedstock (i.e. mostly used after first step hydrolysis by using acids or others) (*Bhaumik et al., 2014*).

iii. Organosolv

In this method, organic solvent or mixtures of organic solvents such as ethanol, methanol, acetone, ethyl glycol and others with water are used for removal of lignin and hydrolyze hemicellulose before enzymatic hydrolysis of the cellulose fractions. When lignin is removed from the lignocellulose material it decreases the cost of enzymes because the absorption of cellulose to lignin is decreased (i.e. it improves the enzyme digestibility of cellulose before fermentation or chemical degradation). In this pretreatment method, the biomasses can degraded at a temperature of greater than 200 ℃ depending on the type of the feedstock and the type of the catalyst used to degrade the specified feedstock's and the process requires recovery of solvent to reduce the cost and environmental challenges (*Zhao et al., 2009*).

iv. Oxidative delignification

Oxidative de-lignification is another method in which, strong oxidizing agents such as hydrogen peroxide, hypochlorite's, ozone and oxygen are used to discard the lignin portion of the lignocellulose components (*Lee, 2005*). Since these chemicals are highly reactive oxidizing agents with the aromatic rings of the lignin, they can be used to convert the lignin to carboxylic acids. This method is limited to lignin, but it is impossible to degrade hemicellulose and cellulose or it might be hemicellulose is degraded to a small extent. As the result of lignin removal from the biomass, the rate of enzymatic hydrolysis can be increased, and this process is particularly conducted at (120-150 ℃) for (20-40) minutes (*Ayeni.A et al., 2013*).

v. pH-controlled liquid hot water

This pretreatment process includes both physical and chemical pretreatment methods, and the process is taking place by liquid hot water, followed by adjusting the pH value of the substance in the reactor. In order to control the pH value of the liquid hot water approaching to neutral, bases such as KOH or NaOH must be added into the LHW pretreatment process with its role to maintain the pH value, not as a catalyst in alkaline pretreatment. This method is limited to the

degradation of cellulose, but it can solubilize the hemicellulose and lignin at a temperature of 150-170 ℃ for 30-60 minutes, and the dissolution of the lignocellulosic material also depends on the pretreatment temperature, time as well as the pH-value (*Mathematik et al., 2015*).

vi. Ionic liquid (ILs) pretreatment

Ionic liquid pretreatment is another method, which involves using efficient and green novel cellulose solvents, in which they can degrade a large amount of cellulose at mild conditions. In this method, the chemicals or the solvents have their own ability to recover nearly 100% to their initial purity and this makes them attractive (*Negi et al., 2014*). The advantages of this method are low toxicity, the broad selection of anion and cation, low hydrophobicity, low viscosity, enhanced electrochemical and thermal stability, high reaction rates, low volatility with minimal environmental impact and non-flammable properties. And also the disadvantages are the high cost of ILs, regeneration requirement, lack of toxicological data and knowledge about basic physicochemical characteristics of chemicals, action mode on hemicellulose and lignin contents of lignocellulosic biomass and inhibitor generation issues (*Singh et al., 2013*).

In this method, the dissolution mechanism of cellulose in ILs involves using the electron donor-acceptor interactions of the oxygen and hydrogen atoms of cellulose hydroxyl groups, and during the interaction of the cellulose-OH and ILs, the hydrogen bonds are broken, resulting in opening of the hydrogen bonds between molecular chains of cellulose, and finally the dissolution of cellulose is formed. Chemicals such as; 3-methyl-n-bytylpyridinium chloride (MBPCl), benzyl dimethyl (tetradecyl) ammonium chloride (BDTACl), 1-n-butyl-3-methylimidazolium chloride (BMIMCl), n-methyl morpholine-n-oxide and 1-alkyl-3-methylimidazolium are the most widely used ionic solvents to degrade the lignocellulosic biomasses (*Elgharbawy et al., 2016).*

2.5.1.3. Physico-chemical pretreatment

This method includes physical and chemical pretreatment methods such as the liquid hot water pretreatment method, in which water at high temperature and high pressure are used for degradation of lignocellulosic materials. According to *Kumar. A et al.,* (*2017*), Steam explosion pretreatment can be classified as catalyzed or un-catalyzed steam explosions, and the un-catalyzed steam explosion is similar to catalyzed steam explosion, except in catalyzed steam explosion catalysts such as SO_2, H_2SO_4, CO_2 and others are used to hydrolyze the lignocellulosic biomass prior to steam-explosion. In addition to this, the catalyzed steam explosion is more cost-

effective and can able to remove the lignin and hemicellulose completely than of the un-catalyzed one. Generally, this method uses high-pressure steam and high temperature (150-170 ℃) for softwood biomass, and (200-230 ℃) for hardwood and herbaceous biomass to under-goes hemicellulose degradation as well as lignin matrix disruption (*Michelin et al., 2016*).

2.5.1.4. Biological Pretreatment

Biological pretreatment is involved with the action of microorganisms such as fungus are used for producing enzymes that can be able to degrade the components of lignocellulosic biomass such as lignin, hemicellulose, and polyphenols. There are three types of fungus in which mostly used in biological pretreatment used to degrade the lignocellulose materials; those are white-rot, brown rot, and soft-rot. Brown and soft rot fungi are primarily can attack the cellulose part of the lignocellulosic material, whereas white-rot fungus can attack both lignin and cellulose via the production of enzymes such as lignin peroxidases, polyphenol oxidases, maganesse-dependent peroxidases, and laccases that degrade the lignin (*Jaiswal, 2015*). Therefore, depending on the degradation of lignocellulosic materials, the white-rot fungus is the most effective and widely used for bio-treatment of almost all lignocellulose feedstock's (*Srivastava et al., 2017*).

The advantages of biological pretreatment method are: it gives higher product yield of reducing sugars, no need of chemical agents, requires less amount of energy, it takes mild reaction conditions, less resistance to corrosion and it is environmentally-friendly technology. And, the main disadvantages of the biological delignification are; is taking place on a very low rate of biological hydrolysis, so it requires a long incubation period as long as weeks for substantial change in the structure of the lignocellulosic feedstock's, and finally, the hydrolysis process of cellulose and fermentation of sugar makes mismatch, it requires careful control growth conditions, some fractions of the carbohydrate is consumed by the microorganisms (i.e. significant loss of biomass during the process) as well as it is applicable mostly for low lignin composition of lignocellulosic materials. In general, when we looking to the techno-economic challenge, biological pretreatment is less attractive commercially than of the other pretreatment method (*Limayem et al., 2012*).

In this study, chemical pretreatment was selected rather than physical as well as biological methods to extract cellulose from the lignocellulosic biomass. Because, chemical methods is even it has non-advantages such as toxic, corrosive and hazardous nature, but it gives high yields

of reducing sugars and it is used to remove a high lignin portion of the plant. In this study, sugarcane bagasse has a high lignin portion, which requires chemicals to solubilize completely. In the physical pretreatment method, it requires an extremely high amount of energy which is undesirable from the engineering perspectives. And biological pretreatment produces a high amount of reducing sugars, it requires less amount of energy, it is less resistant to corrosion as well it is an environmentally friendly technology. But, it has drawbacks such as it takes place in a very low rate; it requires a long incubation period as long as weeks for substantial change in the structure of the lignocellulose materials, it requires careful control growth condition, some fractions of carbohydrate is consumed by microorganisms (significant loss of biomass), and it is applicable mostly for low lignin lignocellulosic biomasses. In this, the material utilized, which is called sugarcane bagasse is a high lignin material it requires chemicals to remove completely, implies that, it is non-effective to extract the cellulose portion of the plant using biological methods (*Kumar et al., 2009*).

2.5.2. Hydrolysis of the pretreated biomass (cellulose degradation to glucose)

The conversion of lignocellulosic biomass-derived cellulose into reducing sugars can be taking place after the pretreatment of the raw biomass, and which is called hydrolysis reaction. As mentioned in the pretreatment process, pretreatment of lignocellulose material is required before hydrolysis, because, it uses to increase the accessibility of lignocellulosic materials for hydrolysis process (*Dussán et al., 2014*). The hydrolysis reaction can degrade the pretreated material into fermentable sugars either by acid or enzymatic catalyze actions. Hydrolysis process using chemicals can take place either using dilute or concentrated strong acids such as H_2SO_4, HCl, H_3PO_4, and HNO_3. In this method, sulfuric acid is the most commonly used acid due to low cost, less corrosive strength and effectiveness of material degradation. In diluted acid (i.e. 1-4% of acid) hydrolysis process, a high temperature of (200-240 ℃) and pressure are required to degrade the cellulose to reducing sugars for an optimum reaction time of 1-2 hours depending on the nature of the material. Alternatively, concentrated acids are used in moderate reaction conditions such as a temperature of (80-200 ℃) for a short period of time (*Kumar.P et al., 2009*).

According to *Bujang et al.,* (*2013*), the dilute acid hydrolysis is more useful than of using a concentrated acid hydrolysis process, because it is inexpensive and effective. In addition to this, concentrated acids are more equipment corrosive, highly problematic to the environment as well

as it needs high cost in order to recover the acid to lowering the cost after the completion of the reaction, and which makes it commercially less attractive.

Enzymatic hydrolysis is another method, which can degrade the cellulose by using cellulases enzymes (i.e. mainly consists the endo-glucanases, exo-glucanases, and β-glucosidases enzymes) to fermentable sugars particularly, glucose at optimum operating conditions such as pH value of 4.5-5 and temperature of (45-50 °C) (*Neifar et al., 2016*). In enzymatic hydrolysis, either bacteria or fungus can be used to produce cellulase enzymes for degradation of the lignocellulose materials (i.e. particularly glucose) by the action of microorganisms. Cellulomonas, Bacillus, Ruminococcus, Thermomonospora, Clostridium, Bacteriodes, Microbispora, and Streptomyces are the most commonly used bacteria's' which can produce the cellulases enzymes. The main advantages of enzymatic hydrolysis are; it is used to produce a high yield of reducing sugars, less energy requirement, and it is an environmentally friendly process. And the main disadvantages of using enzymatic hydrolysis are; it is very expensive, takes long reaction time as well as it needs careful growth of microorganisms (*Badiei et al., 2014*).

The pretreated lignocellulosic material (i.e. particularly cellulose) into glucose degradation either using the acid or enzymatic catalyzed reactions can be represented by:

$$(C_6H_{10}O_5)_n + n * H_2O \rightarrow n * C_6H_{12}O_6 \ldots\ldots\ldots\ldots\ldots\ldots\ldots\ldots\ldots\ldots\ldots\ldots\ldots\ldots (2.1)$$

Where, $(C_6H_{10}O_5)_n$ is made up of long chain n glucose molecules, which is called glucan, and $C_6H_{12}O_6$ is the single glucose molecule.

In this study, dilute acid-catalyzed hydrolysis was selected to convert cellulose in to simple sugars particularly glucose. Because, concentrated acids are more effective, but they are more toxic, corrosive, expensive, high acid consumption, and needs a high cost in order to recover the acid after completion of the reaction than of dilute acids. And, in enzymatic hydrolysis, the microorganism needs careful control growth, low rate of hydrolysis reaction, and enzymes are very expensive than of dilute as well as concentrated acids (Ghasemzadeh et al., 2014).

2.5.3. Dehydration of glucose to 5-HMF

HMF is a renewable chemical feedstock, which is obtained from the hydrolysis and dehydration of cellulosic biomasses, which is available from plant waste matter (*Wang, 2014*). This is an important biomass-derived platform chemical, in which, it can be converted into biofuels and

fine chemicals, pharmaceuticals as well as furan-based polymers. HMF can be produced from bio-based materials, particularly hexoses (i.e. glucose or fructose) by removing three amounts of water using an acid-catalyzed dehydration reaction, and also it could be further transformed into liquid fuels and fine chemicals such as 2,5-dimethylfuran next to PX (i.e. later being promising building blocks for the production of plastics and fine chemicals) (*Saha et al., 2014*).

The synthesis of HMF is one of the main steps in the production of liquid fuels and fine chemicals, and it can be obtained by the dehydration of carbohydrates such as; fructose, glucose and cellulose catalyzed by mineral acids such as (HCl, H_2SO_4 and H_3PO_4) or solid metal halides such as $CrCl_3$, $AlCl_3$, $FeCl_3$, $CuCl_2$ in the presence of different solvents such as water, aqueous-organic mixtures, pure organic solvents, ionic liquids and biphasic solvents (i.e. a combination of two solvents) (*Zhou et al., 2017*).

The biphasic systems (i.e. two solvents together in one reactor) using strong acid catalysts such as HCl and H_2SO_4, which are the most reactive and selective catalysts is more effective for dehydration reaction of glucose to HMF (*Liu et al., 2012*). And also, as *Catrinck et al.,* (*2017*) investigated that, solvents such as tetrahydrofuran (THF), water, 1-propanol, dimethyl sulfoxide (DMSO), dimethyl formide, 1-butanol, 1-butyl-3-methylimidazolium chloride ([Bmim]Cl), and dimethyl acetamide (DMA) are the most used solvents with mineral acid catalysts to transform simple sugars such as glucose or fructose to HMF under the optimum operating parameters such as; temperature (130-170 ℃) for dehydration time of (30-90 minute). In addition to this, the dehydration of glucose in a biphasic system using strong acid catalysts is more effective in the presence of salt or NaCl (i.e. used to enhance the production of HMF) (*Upare et al., 2015*).

2.5.4. Hydrogenation of 5-Hydroxymethyl furfural to 2.5-dimethylfuran

The conversion of HMF to DMF can be taking place by the addition of hydrogen molecule either in gas or liquid phase, and the process is called hydrogenation reaction. In the gas phase hydrogenation reaction, hydrogen gas (H_2) is used to react with HMF to produce DMF under high temperature and pressure. Alternatively, liquid phase hydrogenation reaction is taking place by the addition of liquid reagents as hydrogen donor. Generally, hydrogenation reaction of HMF to DMF can be taking place by two intermediate products within the system of one reaction conditions. Initially, HMF is converted to 5-methyl furfural (MFAL) and MFAL is converted to 2-methylfuran (2-MF) next to 2,5-dimethylfuran in the presence of reactive and selective

catalysts (*Peleteiro et al., 2014*). Catalysts such as; metal halides (e.g. $AlCl_3$, $CuCl_3$, $FeCl_3$,$CrCl_2$, $CrCl_3$ and $SnCl_4$), carbon supported catalysts (e.g. Cu-Ru/C, Pt/C, Rh/C and Pd/C), and copper containing catalysts like $CuCrO_4$ are among the most powerful and selective catalysts for hydrogenation reaction to convert the platform HMF into liquid fuels such as DMF using an optimum operating parameters such as temperature (100-150 ℃) for reaction time of (10-20 hrs) under continuous stirring of 350-450 rpm (*Sheppard et al., 2016).*

According to *Dutta et al.,* (*2014*), the copper containing halides are more effective and selective catalysts for hydrogenation reaction to reduce the oxygen content of HMF in the presence of different organic solvents and ionic liquids such as dimethyl ether, dimethyl acetamide, 1,4-dioxane, methyl isobutyl ketone, formic acid, dimethyl formide, carbon tetra chloride, tetrahydrofuran (THF), 1-ethyl-3-methylimidazolium chloride([EMIM]Cl), 1-butanol, dimethyl sulfoxide etc. Those solvents (chemical reagents) are mainly used to dissolve the reaction mixtures, as well as they are used as hydrogen source by donating H_2 to react with HMF to produce DMF in the liquid phase hydrogenation reaction. During the hydrogenation reaction of HMF to DMF, hydrogen has used to reduce formyl and hydroxyl groups without affecting the furan ring of 5-hydroxymethyl furfural (*Goyal et al., 2016*).

2.5.5. Diels-Alder cycloaddition of 2, 5-Dimethyl furan to Para-xylene

In this chemical conversion, PX is produced from the biomass-derived 2, 5-dimethylfuran. This chemical reaction needs at least two carbon atoms to react with DMF to produce PX, and this process is called Diels-Alder reaction, which includes cycloaddition reaction, crystallization and decarboxylation steps. Diels-Alder cycloaddition reaction can be taking place either in gas or in liquid forms. In gas phase, particularly ethylene gas is used as a dienophile under the harsh condition to react with the biomass-derived DMF to PX at the higher temperature (225-300 ℃) and higher gas pressure (30-70 bar) (*Pacheco et al., 2014*). According to *Vardon*, (*2017*) report, high yield approximately 97% p-xylene have been obtained using phosphorous modified zeolite catalyst at 250 ℃ under 62 bar ethylene gas. This production method can give a high yield of Para-xylene within a short period of time, but the process needs high cost as well as it needs a higher amount of energy, this process also not recommendable from the engineering perspective. Alternatively, in the liquid phase Diels-Alder cycloaddition reaction, different chemical reagents

such as Acrolein, acrylic acid, maleic anhydride, Maleic acid, 2, 2, 2-trifluoroethyl acrylate and others are utilized as a dienophile to react with DMF to produce PX (*Lyons et al., 2012*).

The Diels Alder cycloaddition reaction of DMF with dienophile reagents to PX can be converted using different catalysts such as Lewis acid catalysts (e.g. $AlCl_3$, Et_2AlCl, $BF_3.Et_2O$, ZnI_2, $SnCl_2$, $ZnCl_2$, $SnCl_4$ and $TiCl_4$), d-block transition metal catalysts (e.g. $Sc(OTf)_3$, $Hf(OTf)_4$, $ScCl_3$, $HfCl_4$ and zeolites) and silica-alumina catalysts (e.g. SiO_2/Al_2O_3) in the presence of different organic solvents such as chloroform, benzene, diethyl ether, toluene, ethyl acetate, carbon tetrachloride, dioxane, acetone, petroleum ether, n-heptane and others. In this chemical reaction, fast reaction rate has occurred in the presence of Lewis acid catalysts. However, the catalytic capability of these catalysts can vary by the type of halogenation metals, since the Lewis acidity of metal halide catalysts and their coordination ability with the ligands play a great role in their catalytic actions (*Nikbin et al., 2013*).

According to *Pacheco et al.,* (*2014*) investigation, high yield (i.e. Approximately 83% and 91% yield) of dimethyl benzoic acid and Para-xylene respectively have been obtained using Acrolein as a reagent in the presence of $Sc(OTf)_3$ catalyst and using chloroform as a solvent, at a temperature of -60 ℃ for 3 days (after 69 hrs) reaction time, and also, approximately 82% of dimethyl benzoic acid have been obtained using $Hf(OTf)_4$, at the same operating conditions with the previous one. Furthermore, around 86% and 91% of dimethyl benzoic acid and Para-xylene respectively, have been obtained using Maleic anhydride as a reagent at room temperature for 12 hrs reaction time in the presence of $Sc(OTf)_3$ catalyst and using diethyl ether as a solvent. Due to the facts of the previous study, in this paper, Maleic anhydride was selected as a reagent for the cycloaddition reaction, because it gives approximately high yields at room temperature as well as short reaction time, and it is better to use Maleic anhydride than of Acrolein because the reaction using Acrolein needs cooling process, implies that, it is an energy intensive process. In addition to this, it is a very good dienophile because it contains two highly electron withdrawing carbonyl groups to react with the lignocellulosic biomass-derived DMF to afford the corresponding cyclohexane system such as PX (*Thiyagarajan et al., 2016*).

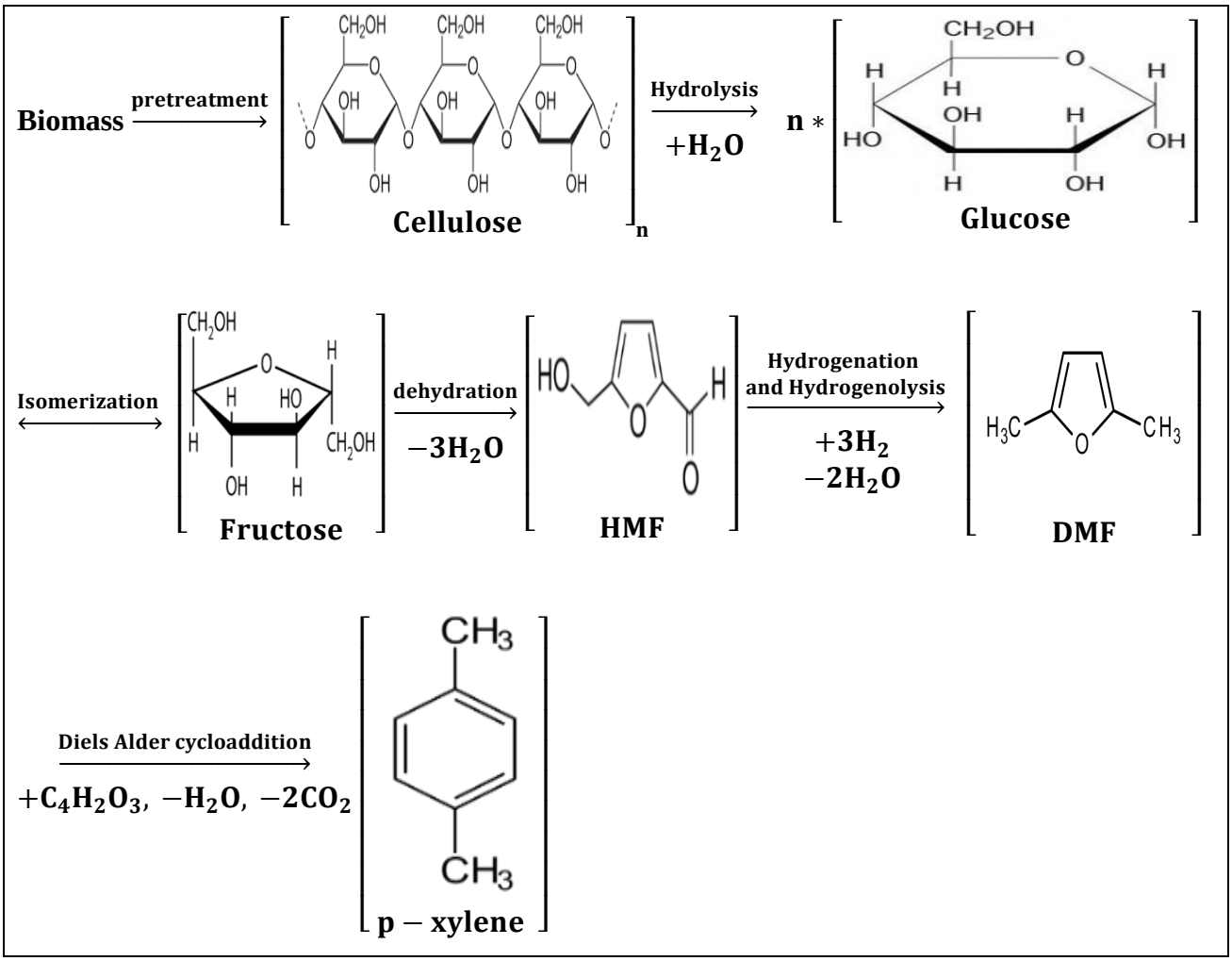

Figure 2-4: The overall reaction pathways for Para-xylene production from biomass, Source: (*Science. C et al., 2015*)

3. MATERIALS AND METHODS

3.1. Materials

The materials used during the experimental work were sugarcane bagasse, Acetone (C_3H_6O, min. assay 99%), Hydrochloric acid (HCl, min. Assay 35.4%), Sulphuric acid (H_2SO_4, min. assay 98%), Sodium hydroxide (NaOH, min. assay 98%), N_2 gas, Sodium chloride (NaCl, min. Assay 99.5%), Dimethyl sulfoxide (DMSO, C_2H_6OS, min. Assay 99.5%), Copper chloride ($CuCl_2$, min. assay 99.5%), Ethanol (C_2H_5OH, min. assay 99.5%), Formic acid (HCOOH, min. Assay 99%), Aluminum chloride ($AlCl_3.6H_2O$, min. Assay 99%), Dimethyl ether (CH_3OCH_3, min. assay 98%), Maleic anhydride (2, 5-furandione, $C_4H_2O_3$, 99% extra pure), Sodium sulfate (Na_2SO_4, min. assay 99%), Aqueous Hydrogen peroxide (30% H_2O_2, dalul pharmaceutical plc.), and Cupric oxide (Cu_2O, 99.5% extra pure). Sugarcane bagasse was collected from Wonji/Shoa sugar industry, 100 km south east of Addis Ababa (oromia region). And all the other chemicals were analytical reagents and bought from different chemical stores in Addis Ababa such as fine chemical general trading plc, micro international trading house plc, and wise team plc.

3.2. Equipments

The type of Equipments used during the experimental work includes digital mass balance, plastic bags, muffle furnace, grinder, sieves, desiccator, shaker, crucible, Soxhlet extractor, autoclave reactor, digital pH meter, three necked round-bottomed flask, vacuum filter, thermostat water bath, oil bath, hot plate, condenser, thermometer, different size conical and Erlenmeyer flasks, UV and FTIR spectrometer, and GC-MS.

3.3. Methodology

3.3.1. Sample collection and preparation

A suitable sample preparation method of the raw sugarcane bagasse for chemical production is suggested by (*ASTM E1757, 2008*), and the modified procedure is presented by (*Betancur, 2010*). In this study, the raw sugarcane bagasse (i.e. the feedstock) was collected from sugar production industries particularly Wonji sugar factory. After the sample is collected, it was sun dried for 10 days to reduce the moisture content. Then after, the dried sample was ground using a grinder to a particle size of less than 2 mm screen. Finally, the sample was sieved and the

fractions passing through the sieve (i.e. less than 2 mm) were collected and homogenized in a single lot, and stored in a plastic bag under dry conditions prior to use for the next experiments.

a) **b)**

Figure 3-1: Sugarcane bagasse before and after size reduction

3.3.2. Characterization of sugarcane bagasse

In this section, the proximate analysis and compositional analysis of the lignocellulose biomass was calculated. The measured values of proximate analysis such as moisture content, volatile matter, ash content and fixed carbon of feedstock's are important factors to understand the nature and the properties of the feedstock. And the measured values of compositional analysis, such as cellulose, hemicellulose, lignin and extractive contents are important to understand the structural compositions of the plant cell-wall.

3.3.2.1. Proximate Analysis of Sugarcane bagasse

The proximate analysis was performed gravimetrically to determine the moisture content (MC), ash content (AC), volatile matter (VM), and fixed carbon (FC) of the sample. The suitable method for characterization (i.e. for proximity analysis) of sugarcane bagasse is suggested by (*ASTM D 121*) and the modified procedure is presented by *Edhirej et al.,* (*2017*).

A. Determination of moisture content

The following procedures were used to determine the moisture content of the sample. Initially, about 4.23 g of ground sample sugarcane bagasse was weighted and placed in a pre-weighed dry Petri dish, and then, the sample was dried at 105 ℃ convection oven for 8 hours to remove the moisture content of the sample. Then after, the dried sample was cooled at room temperature for 30 minutes in a desiccator, and then, the sample was re-weighed and recorded. The drying-

cooling-reweighing procedure was repeated until a constant weight is recorded after 8hrs. Finally, the moisture content of the sample was determined using the following equation:

$$\text{Moisture content}(\%) = \frac{(W_1 - W_2)}{W_1} * 100 \ldots \ldots \ldots \ldots \ldots \ldots (3.1)$$

Where:

W_1 = the original mass of the sample before drying, and

W_2 = the final mass of the sample after drying.

B. Determination of volatile matter

The volatile matter of the sample was determined using the following procedures: Initially, about 3.93 g of ground sample sugarcane bagasse was weighed and placed in the empty pre-weighed crucible. Then after, the sample was incinerated in the muffle furnace at a temperature of 800 ℃ for 8 minutes, and then, the crucible was transferred into a desiccator to cool for 30 minutes in the free air atmosphere. Finally, the total weight loss of the sample and the crucible was weighted and recorded after cooling in the desiccator. Then, the volatile matter was determined by the following equation:

$$\text{Volatile matter}(\%) = \frac{(W_1 - W_2)}{W_1} * 100 \ldots \ldots \ldots \ldots \ldots \ldots (3.2)$$

Where:

W_1 = Mass of dry sample, and

W_2 = Mass left behind the sample is burned and followed by cooling in the desiccator.

C. Determination of Ash content

To determine the ash content of the sample, the following procedures were used: First, around 4.35 g of ground and dried sample sugarcane bagasse was placed in the pre-weighed crucible and it was incinerated at a temperature of 550 ℃ electrical muffle furnace for 4 hrs. After incineration, the crucible was transferred from the muffle furnace to the desiccator to cool in the free air atmosphere. Finally, the total weight of the sample and crucible was recorded after cooling for 20 minutes. The weight of the sample before heating and after heating was used to determine the amount of ash content present in the sample. In this test, the amount of residual substance is equal to the ash present in the sample. Then, the ash content was determined using the following equation:

$$\text{Ash content}(\%) = \frac{W_2}{W_1} * 100 \ldots\ldots(3.3)$$

Where:

W_1 = Mass of dry sample, and

W_2 = Mass left behind the sample is burned and followed by cooling in the desiccator.

D. Determination of fixed carbon

The fixed carbon of the sample was determined using the other previously determined values such as the ash content, moisture content and the volatile matter of the sample, and it was calculated using the following relationship in dry basis:

$$FC = 100 - \text{Ash}\ (\%) - \text{VM}\ (\%) - \text{MC}\ (\%) \ldots\ldots(3.4)$$

Where:

FC = fixed carbon,

MC (%) = percentage of moisture content

Ash (%) = percentage of ash content, and

VM (%) = percentage of volatile matter.

3.3.2.2. Chemical composition of sugarcane bagasse

The compositional analysis of lignocellulosic materials can be performed gravimetrically to determine the extractives, lignin, hemicellulose, and cellulose contents. The method for compositional analysis of sugarcane bagasse is supposed based on (*ASTM D 2015*) and the procedure is modified by *Karp et al.*, (*2013*).

A. **Extractives: -** The extractive portions of the lignocellulosic biomass particularly samples of sugarcane bagasse was determined as the following procedures: Initially, around 10 g of ground and dried sample sugarcane bagasse was entered into Soxhlet extractor setup using 360 ml of acetone as a solvent to extract the non-structural components of the plant cell-wall such as fatty acids, waxes, resins, volatile oils, tannins etc. Then after, the process was taking place at a temperature of 70 ℃ thermostat water bath for 4 hrs run period. And then, the solid part of the sample that remains after extraction of the non-structural parts were dried at room temperature for 15 minutes to remove the large portion of the solvent and it was dried in a convection oven at 105 ℃ overnight to remove the moisture content of the sample. Finally, the percentage extractive of the sample was determined using the following equation:

$$Extractive(\%) = \frac{(W_1 - W_2)}{W_1} * 100 \ldots\ldots\ldots\ldots\ldots\ldots\ldots\ldots (3.5)$$

Where:

W_1 = mass of the dry sample before extraction, and

W_2 = mass of dry sample after extraction.

Figure 3-2: Soxhlet extractor set up

B. Hemicellulose: -To determine the hemicellulose portion of the lignocellulosic material, the solid part remaining after extraction of the non-structural portion was utilized and the process was performed as follows: first, about 3 g of extracted and oven-dried sample was mixed with 120 ml of 0.1mol/L NaOH in a 250 ml flask, and the mixture was boiled in a thermostat water bath at 73 ℃ for 3.5 hrs. Then after, the sample was filtered using vacuum filter and the pH was adjusted using HCl until it was reached neutral, and then, the residue (solid remains after filtration) was dried in a convection oven overnight at a temperature of 105 ℃. Finally, the percentage hemicellulose content of the sample was determined using the following equation:

$$Hemicellulose(\%) = \frac{(W_1 - W_2)}{W_1} * 100 \ldots\ldots\ldots\ldots\ldots\ldots\ldots\ldots (3.6)$$

Where:

W_1 = the extracted and oven dried mass of the sample before treatment, and

W_2 = the mass of dry sample after treatment.

C. Lignin: -To determine the lignin portions of the lignocellulosic material, the solid part remaining after extraction of the non-structural portion was utilized and the process was

performed as follows: initially, about 3.0 g of extracted and oven dried sugarcane sample was mixed with 20 ml of 98% H_2SO_4 and it was shaken carefully using the electrical shaker of 200 rpm at room temperature for 2 hrs. And then, after complete mixing, it was added with 560 ml of distilled water in a 2000 ml glass beaker, and the second step of hydrolysis was taking place in an autoclave reactor at a temperature of 121 ℃ for 1hr. Then after, the hydrolysate sample was filtered using vacuum filter and the pH was adjusted using 0.1 mol/L of NaOH until it was reached neutral, and then, the solid fraction was oven dried at 105 ℃ overnight to remove the moisture content. Finally, the percentage lignin content of the sample was determined using the following equation:

$$\text{Lignin (\%)} = \frac{(W_1 - W_2)}{W_1} * 100 \quad \ldots \quad (3.7)$$

Where:

W_1 = initial dry mass of the sample before hydrolysis, and

W_2 = final dry mass of the sample after hydrolysis.

D. Cellulose:-The cellulose content of the sample was determined by assuming that, the lignocellulose material contains only the extractive, lignin, hemicellulose, and cellulose components. Therefore, the cellulose content was determined by subtracting the sum of the lignin, extractive, and hemicellulose composition percentages from 100 as the following relationship:

$$100 = W_C + W_H + W_L + W_E \quad \ldots \quad (3.8)$$

Where; $W_C, W_H, W_L,$ and W_E indicates, the weights of cellulose, hemicellulose, lignin, and extractives respectively.

3.3.3. Dilute Acid-catalysis Pretreatment (i.e. Cellulose extraction)

The following procedures were used for pretreatment of the sugarcane bagasse using a dilute acid catalyst. Initially, about 860 g of untreated sugarcane bagasse was socked in a 8600 ml total solution of distilled water with 98% H_2SO_4 (1% H_2SO_4, V/V, in distilled water), and the mixture was stirred using rod stirrer at 2000 rpm for 5 hrs before hydrolysis reaction is taking place in the autoclave reactor (the mixture is prepared using the solid to liquid ratio of 1:10, and stirring is used to homogenize the mixture as well as to reduce the crystalline nature of the biomass, which

makes easy for solubility of the biomass using dilute acid-catalyzed hydrolysis reaction). Then after, the first step for hemicellulose hydrolysis was performed in a batch, autoclave reactor using 2000 ml glass beaker at a temperature of 121 ℃ for 30 minutes. After the initial hydrolysis, the resulting solid material was separated by filtration using 100µm sieve through washing using distilled water to eliminate the excess acid (i.e. Until the pH reached neutral), and then, the solid material was dried in an oven drier at 105 ℃ overnight. Then after, the second step hydrolysis was performed using 1.5 W/V (g/L) of NaOH (i.e. gram of NaOH/volume of distilled water) ratio. The second step of hydrolysis is needed for removal of lignin portions of the lignocellulosic biomass (i.e. for material delignification, because alkaline are very reactive with the OH groups of lignin). In the second step hydrolysis, 537.5 g of initially pretreated bagasse were soaked in a 1075 ml of total solution (i.e. NaOH in distilled water) at room temperature for 1hr, and finally, the solid material was separated by filtration using 100µm sieve through washing using distilled water until the neutral pH was reached. Then after, the separated solid material was dried in a convection oven drier at 105 ℃ overnight prior to use for another experiment. The method (i.e. for pre-hydrolysis of raw sugarcane bagasse) is suggested by (*TAPPI, 1988*) and, the procedures with their optimum operating parameters were optimized by *Dussán et al.*, (*2014*).

a) **b)** **c)**

Figure 3-3: a) Sample homogenization using rod stirrer before initial hydrolysis; b) Autoclave reactor during pretreatment of raw sugarcane bagasse at 121 ℃ (cellulose extraction), and; c) The pretreated sample (cellulose)

3.3.4. Acid-catalyzed hydrolysis reaction of cellulose to glucose

Hydrolysis or degradation of cellulose (i.e. the hemicellulose and lignin free material) into reducing sugars particularly glucose was performed in a batch, closed autoclave reactor. And all the reactions were taking place in a 1000 ml of glass beaker using the following procedures: Initially, about 417.714 g of total extracted cellulose were utilized with 3579.43 ml total solution of distilled water with 98% H_2SO_4 (2%, V/V of H_2SO_4 in the total solution) using two 2000 ml glass beakers. Then after, the solid and the liquid was separated in a 1000 ml of glass beaker using the solid to liquid ratio of 1:9, and then, it was sterilized at a temperature of 150 ℃ for 1hr. The optimum operating conditions are previously presented by *Dhabhai et al*, (*2012*). After completed the reaction, the reaction mixture was cooled at room temperature to terminate the reaction. And then, the solid material was filtered using 32µm sieve through washing using distilled water and it was dried in a convection oven at 50 ℃ overnight to remove the moisture content prior to a dehydration reaction to convert into HMF.

a) **b)**

Figure 3-4: a) Acid-catalyzed hydrolysis of cellulose to glucose using Autoclave reactor at 150 ℃, and; b) Sample after hydrolysis (glucose)

3.3.5. Acid-catalyzed dehydration of glucose to HMF/HMF production procedure

The dehydration reaction of glucose to HMF was carried out in a batch, stirred, oil bath reactor. All the reactions were carried out in a 2000 ml of glass beaker and the procedure was as follows: initially, 230.357 g of dried glucose with 2M (49.45ml) of HCl and 15 g of NaCl were

subsequently dissolved in a biphasic reaction solvents (i.e. two solvents together in one system, such as 600 ml of DMSO with 200 ml of distilled water) as a reaction media prior to heating. Then after, the reaction mixtures were immersed in the preheated oil bath reactor using the 2000 ml of glass beaker under continuous stirring using rod stirrer at 200 rpm, and the dehydration reaction was taking place at a temperature of 150 ℃ for 1hr. After completed the reaction, the reaction mixtures were immediately removed from the oil bath and cooled at room temperature to terminate the reaction and it was sun dried for 3-days followed by oven drier at 50 ℃ for 12 hrs to remove the moisture content. The method is suggested by the (*NREL, 2017*), and the set of the operating conditions are previously optimized by *Dashtban et al.*, (*2015*).

a) **b)**

Figure 3.5: a) Acid-catalyzed dehydration of glucose to HMF using oil bath reactor at 150 ℃, and; b) Sample after dehydration (HMF)

3.3.6. Hydrogenation reaction of HMF to DMF/ DMF production procedure

All the hydrogenation reaction of HMF to DMF was performed in a 500ml three-necked bottom-round flask equipped with a condenser and magnetic stirrer under N_2 gas to purge the CO_2 using the following procedures. In this experiment, initially, about 205.786 g of HMF and 50 g of $CuCl_2$ as a catalyst were dissolved in 153.60 ml of dimethyl ether (CH_3OCH_3, i.e. the solvent), and 600 ml of formic acid was added as a solvent, as well as it is used as hydrogen sources (hydrogen donor to react with HMF). Then after, the reaction mixture was immersed in the preheated oil bath temperature of 120 ℃ for 15 hrs under continuous stirring of 400 rpm. These set of operating conditions were previously optimized by *Meng et al.*, (*2017*). After the reaction completion, the reaction mixture was immediately removed from the oil bath and cooled at room

temperature to terminate the reaction. Finally, the sample was filtered using vacuum filter followed by filtering off the solid particles prior to the Diels-Alder cycloaddition reaction.

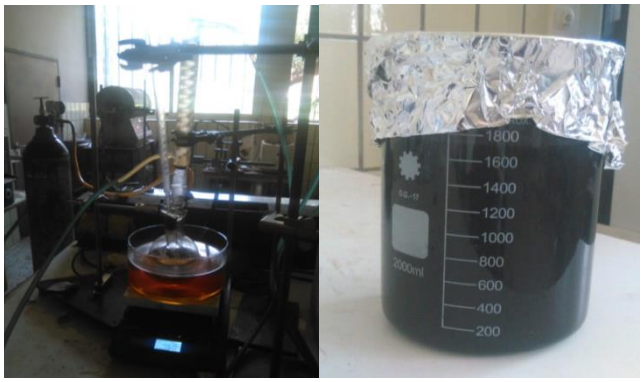

a) **b)**

Figure 3-6: a) Hydrogenation reaction of HMF to DMF at 120 ℃, and;

b) Sample after hydrogenation reaction (DMF)

3.3.7. Procedures for Conversion of DMF and Maleic anhydride to P-xylene

Researchers worked on the conversion of synthetic and lignocellulosic biomass-derived DMF with a common dienophile such as Ethylene, Maleic anhydride, Acrolein, Malic acid, Acrylic acid and others to Para-xylene, the process is called Diels-Alder cycloaddition reaction. The Diels-Alder reaction is facilitated by the presence of electron donating groups on the diene and by the presence of electron withdrawing groups on the dienophile. In this study, maleic anhydride was selected as a very good dienophile because it contains two highly electron withdrawing carbonyl groups to react with the lignocellulosic biomass-derived DMF to afford the corresponding cyclohexane system such as PX. Such a reaction is taking place under the variation of different operating parameters to know the optimum values of these parameters, such as reaction time (4-12 hrs), ratio of DMF to Maleic anhydride (i.e. DMF: MA from 1 to 5) and catalyst loading (0.1-0.5 moles), at a constant temperature (i.e. 50 ℃, at approximately the melting point of maleic anhydride) (*Barberio et al., 2015*).

The conversion of DMF and Maleic anhydride to Para-xylene, and optimization was performed by using Design expert®7 software CCD method. The method for the Diels Alder cycloaddition reaction of the biomass-derived fuels to valuable chemicals has been supposed based on the

(*NREL, 2017*). In this study, 27.78 g or 0.283 mol of reagent (i.e. Maleic anhydride) was used for each experiment and the factors are: reaction time with three levels (4, 8 and 12 hrs.), an amount of 2, 5-dimethylfuran with three levels (0.28, 0.85 and 1.42 moles) and loading of catalyst (i.e. $AlCl_3$; 0.10, 0.30 and 0.50 moles or 13.33, 40 and 66.67 g) was used throughout the experiment. And also, the procedures were as follows: initially, 27.78 g (0.28 moles) of maleic anhydride was placed in a 500 ml flask for each experiment, and then, different amount of DMF (0.28, 0.85 and 1.42 moles) and dimethyl ether as solvent with the ratio of DMF: dimethyl ether (1%, V/V), and the catalyst (i.e. $AlCl_3$; with 0.10, 0.30 and 0.50 moles) was added to each flask based on the order of the design experiment. Finally, all the reactions were carried out in a 500 ml of bottom-round flask equipped with a condenser and a magnetic stirrer of 200 rpm at a temperature of 50 ℃ for a reaction time (4, 8 and 12 hrs). After completing the reaction, the solid particles including the catalyst were separated from the liquid using vacuum filtration, and the liquid was utilized for the next experiment. From the experimental procedure of reaction mixtures DMF and maleic anhydride, dimethyl benzoic acid is formed. And this compound was used to produce the final product (i.e. Para-xylene) through a series of aromatization steps such as dehydration and decarboxylation steps.

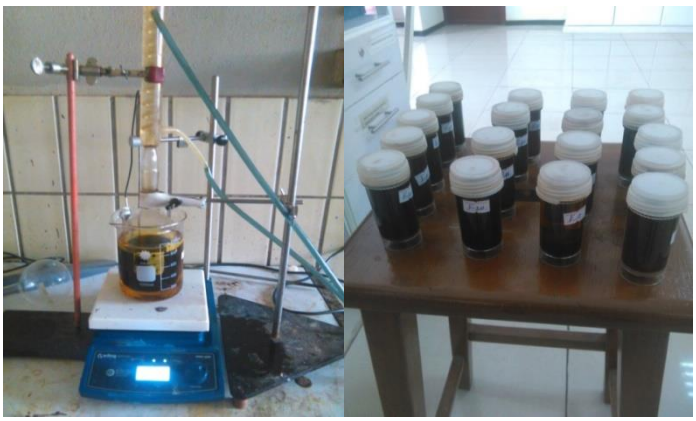

a) **b)**

Figure 3-7: a) Diels-Alder cycloaddition reaction setup at 50 ℃, and;
b) Samples of dimethyl benzoic acid

3.3.7.1. Procedures for Oxidation and dehydration of 2, 5-dimethyl benzoic acid

The Diels-Alder reaction of DMF and Maleic anhydride was conducted in 500 ml of glass beaker in different molar ratios and different loading of the catalyst at 50 ℃ reaction temperatures.

After different operation times, equal amount of H_2O (5ml) was added at room temperature for each experiment. And, the mixture was kept at 4 ℃ overnight to freeze by adding 30% H_2O_2 (7ml) and 1g of $NaClO_2$ as an oxidizing and bleaching agents. Then after, 2, 4 & 6 M, of 98% H_2SO_4 was added to investigate the effect of acid concentration on the dehydration reaction. And finally, the dehydration reaction was taking place in a 500 ml of glass beaker equipped with hot plate through continuous stirring of 200 rpm rod stirrer and 115 ℃ reaction temperatures for 1-3 hrs.

a) **b)** **c)**

Figure 3-8: a) Dehydration process of dimethyl benzoic acid at 115 ℃; b) Vacuum filtration to separate the liquid from the solid, and; c) Sample of dimethyl benzoic acid after dehydration

3.3.7.2. Procedures for decarboxylation (aromatization) of dimethyl benzoic acid to PX

Decarboxylation or aromatization of dimethyl benzoic acid into Para-xylene was carried out to remove the CO_2. This process was performed in a batch, three-necked 500 ml bottom round flask equipped with a magnetic stirrer under N_2 gas to purge the CO_2. The decarboxylation process to convert the benzoic acid into PX have been reported by different researchers under optimum operating conditions, such as: at a temperature of (120 ± 5), and 8-8.5 hrs operating time (*Lin et al., 2013*). The following procedures was used: the dehydrated samples of dimethyl benzoic acid was placed in a 500 ml three-necked flask, and then, 5 g of Cu_2O and 3 ml of degassed solvent (i.e. DMSO) was added and heated at 120 ℃ (i.e. oil bath temperature) for 8 hrs equipped with a magnetic stirrer of 200 rpm and N_2 gas to purge the CO_2. After completing the reaction, the reaction mixture was immediately removed from the oil bath to cool at room temperature, and then, the mixture was washed with acetone and dried over Na_2SO_4.

a) **b)**

Figure 3-9: a) Decarboxylation process setup at 120 ℃, and; b) Dimethyl benzene samples.

3.3.8. Preparation of stock solution for dimethyl benzoic acid determination

The standard stock solution of dimethyl benzoic acid was prepared by dissolving 4 mg/mL in ethanol. This means that, 400 mg of dimethyl benzoic acid is dissolved completely in a 100 ml of 99.5% ethanol after 10 minutes sonication. This corresponds to 400 ppm of dimethyl benzoic acid. Standard stock solutions of 100, 150, 200, 250, and 300 mg dimethyl benzoic acid was placed in a 500 ml volumetric flasks, and then 100 ml of 99.5% ethanol were added to dissolve the standard dimethyl benzoic acid and prepare for calibration curve (i.e. The linearity levels were prepared by subsequent dilution from these stock solutions using ethanol as a reference). Then after, the absorbance of the dimethyl benzoic acid was measured at λ = 228 nm using UV-absorption spectrometer. And then, the concentrations of dimethyl benzoic acid present in the sample were determined using the measuring absorbance from the calibration curve of the standard solution. And it was determined as follows: First, the standard solution calibration curve for dimethyl benzoic acid was plotted using the equation:

$$Y = mx + b \quad \ldots\ldots (3.9)$$

Where: Y is absorbance,

X is concentration,

m and b are the slope and y-intercepts respectively.

Then after, the unknown concentration of the sample dimethyl benzoic acid was calculated by:

$$\text{Unknown Conc. Of sample} = \frac{((\text{Absorbance of the sample}) - (\text{y} - \text{intercept})) * \text{Df}}{\text{Slope}} \quad \ldots\ldots 3.10$$

Where: DF is the dilution factor

Finally, the conversion of dimethyl furan, and yield of dimethyl benzoic acid was calculated by:

$$\text{Conversion of DMF} = \frac{[\text{n}_{\text{DMF},0} - \text{n}_{\text{DMF}}]}{\text{n}_{\text{DMF},0}} * 100 \ldots\ldots\ldots\ldots\ldots\ldots\ldots\ldots\ldots\ldots\ldots\ldots\ldots\ldots\ldots\ldots\ldots\ldots\ldots\ldots\ldots 3.11$$

Where, $n_{DMF, 0,}$ and n_{DMF} are the amounts of DMF initially and left un-reacted respectively.

$$\text{Dimethyl benzoic acid yield} = \frac{[\text{gams of dimethyl benzoic acid produced}]}{[\text{grams of DMF utilized per sample}]} * 100 \ldots\ldots\ldots .3.12$$

3.3.9. Preparation of stock solution for dimethyl benzene determination

The standard stock solution of dimethyl benzene was prepared by dissolving 1.62 mg/mL in ethanol. This means that, 162 mg of dimethyl benzene was dissolved completely in a 100 ml of 99.5% of ethanol in thermostat water bath at 75 ℃ for 10 minutes. This corresponds to 162 ppm of dimethyl benzene. Standard stock solutions of 100, 150, 200, 250, and 300 mg dimethyl benzene was placed in a 500 ml volumetric flasks, and then 100 ml of 99.5% ethanol was added to dissolve the standard dimethyl benzene and for preparing the calibration curve (i.e. The linearity levels were prepared by subsequent dilution from these stock solutions using ethanol as a reference). Then after, the absorbance of the dimethyl benzene was measured at λ=192 nm using UV-absorption spectrometer. And then, the amount (i.e. the concentration) of dimethyl benzene present in the sample was determined using the measuring absorbance from the calibration curve of the standard solution. And it was determined using the same formulas with the previous equations 3.9, 3.10, 3.11, and 3.12. First, the standard solution calibration curve for dimethyl benzene was plotted using the equation:

$$\text{Y} = \text{mx} + \text{b} \ldots\ldots\ldots\ldots\ldots\ldots\ldots\ldots\ldots\ldots\ldots\ldots\ldots\ldots\ldots\ldots\ldots\ldots\ldots\ldots\ldots\ldots\ldots\ldots\ldots\ldots\ldots\ldots\ldots\ldots\ldots\ldots\ldots\ldots . (3.13)$$

Where: y is absorbance,

X is concentration,

m and b are the slope and y-intercept respectively.

Then after, the unknown concentration of the sample was determined by:

$$\text{Unknown Conc. Of sample} = \frac{(\text{Absorbance of the sample}) - (\text{y} - \text{intercept}) * \text{Df}}{\text{Slope}} \ldots\ldots (3.14)$$

Where: DF is the dilution factor

Finally, the conversion of dimethyl benzoic acid and yield of Para-xylene was determined by:

$$\text{Conversion of dimethyl benzene} = \frac{[n_{DMBA} - n_{DMBA}]}{n_{DMBA,0}} * 100 \ldots\ldots\ldots\ldots\ldots\ldots\ldots\ldots\ldots\ldots\ldots\ldots (3.15)$$

Where, $n_{DMBA,\,0}$ and n_{DMBA} are the amounts of dimethyl benzoic acid initially and left un-reacted respectively.

$$\text{And, para} - \text{xylene yield} = \frac{[\text{grams of para} - \text{xylene produced}]}{[\text{grams of dimethyl benzoic acid utilized}]} * 100 \ldots\ldots\ldots\ldots (3.16)$$

Figure 3-10: UV-spectroscopy when measuring the absorbance

3.3.10. Experimental Design

Data analysis was performed by Design expert®7 software using the central composite design method. In the Diels-Alder cycloaddition reaction, we have three most common factors, such as; reaction time, catalyst loading and the molar ratio of the reactants (i.e. DMF: Maleic anhydride), and the responses were the conversion of the main reactant (i.e. DMF conversion) and the yield of dimethyl benzoic acid. The experimental error and the productivity of the data were analyzed by three factors-three level with 4-replicate center points, the factorial points become, $2^n = 2^3 = 8$, 6 axial points and 4 centers; a total of 18 experiments required to perform the experiment. This design of the experiment helps us to differentiate the significance of the main and the interaction factors as well to optimize the process variables. And, the significance of the result was analyzed from the analysis of variance (ANOVA).

3.3.11. Fourier Transform Infrared Spectroscopy (FT-IR)

FTIR spectroscopy is one of the most widely used and most effective method to identify the functional group characteristic of the chemical compounds. The infrared spectroscopy probes the molecular vibrations and the functional groups can be associated with characteristic infrared

absorption bands, which correspond to the fundamental vibrations of the functional groups. The infrared spectra were interpreted according to *Gobinath et al.,* (*2017*). FTIR analysis works based on the selective chemical reagents such as, KBr was used for powder samples and NaCl plate for liquid samples by thin film deposition technique. And finally, the instrument was recorded the spectra of the sample using spectrum 65 FT-IR equipped with powder KBr for the powder sample and NaCl for the liquid sample as beam splitter from frequency of 4000 to 400 cm^{-1} with a resolution of 4 cm^{-1}, and 24 scans was averaged. Finally, the resulted data was plotted using origin lab pro 8.0 and the functional group was determined based on the interpretation of the infrared spectrum obtained by comparing it with the standard spectrum group vibrations. This analysis was performed in Addis Ababa University College of natural science, chemistry department.

3.3.12. Gas chromatography-Mass spectrometry (GC-MS)

Gas chromatographic-mass spectrometry (GC-MS) is a very powerful analytical technique with a very sensitive and information-rich mass spectrometer (MS). It is used to separate the volatile components of complex mixture species based on their interactions with a stationary phase and a mobile phase, and also it is used to determine the mass spectrometer of each component present within the sample. This instrument provides two separate dimensions of information about the components in the sample, these are the GC retention times and electron ionization (EI) mass spectra. The GC retention time specifies the chemical properties of the molecules such as volatility, polarity, presence of specific functional groups, and the electron ionization mass spectra indicates the atomic composition of the sample. The chromatograms were recorded on a gas chromatograph coupled to the polarized mass spectrometer; the mass spectral data were recorded with electron impact ionization at 70 eV. The temperature of ionization was fixed at 200 ℃ and the injector temperature was set at 250 ℃. Then, the column oven temperature was held at 40 ℃ for 2 min, and then it was increased to 250 ℃ at a heating rate of 5 ℃/ min. The volatile and semi-volatile species was vaporized and flow into a mobile phase (i.e. helium, which is used as carrier gas, at a flow rate of 1.00 ml/min) and blown through a fused silica open tubular capillary (stationary phase). This analysis was performed in Addis Ababa leather industrial development institute (LIDI).

4. RESULTS AND DISCUSSION

This chapter includes the results of all the laboratory activities, such as characterization of the feedstock (e.g. Proximate analysis, which includes: the percentage of moisture content, ash content, volatile matter as well as fixed carbon of the sample, and the compositional analysis, which includes: the percentage of extractives, lignin, cellulose and hemicelluloses of the sample) gravimetrically. And also, it includes different analysis and investigations with the most operational parameters, which affects the conversion of DMF and the yield of the intermediate products such as 2,5-dimethyl benzoic acid as well as Para-xylene in the Diels-Alder cycloaddition reaction using Design expert®7 software. Furthermore, it includes the characterization results of different intermediate products in the process and the final product using FTIR and GC-MS respectively.

4.1. Characterization of sugarcane bagasse

4.1.1. Proximate Analysis of Sugarcane bagasse

The proximate analysis of different types of lignocellulosic materials including sugarcane bagasse was previously defined by works of literature *Toribio-cuaya,* (*2014*). According to *Ferreira et al.,* (*2017*), 3.26% moisture content, 7.7% ash content, 74.27% volatile matter, and 14.03% fixed carbon was reported. In addition to this, 6.85% moisture content, 8.02% ash content, 85% volatile matter, and 13% fixed carbon of sugarcane bagasse was reported by *Beers,* (*2005*).

In this study, about 4.15% moisture content, 8.06% ash content, 75.04% volatile matter, and 13.45% fixed carbon was obtained as shown below in figure 4.1, which is within the literature and is nearly the same result with the previous researchers. Therefore, the standard method (i.e. ASTM D 121) is used for characterization of the lignocellulosic materials such as sugarcane bagasse, which gives nearly the same result with the methods used by the previous researchers.

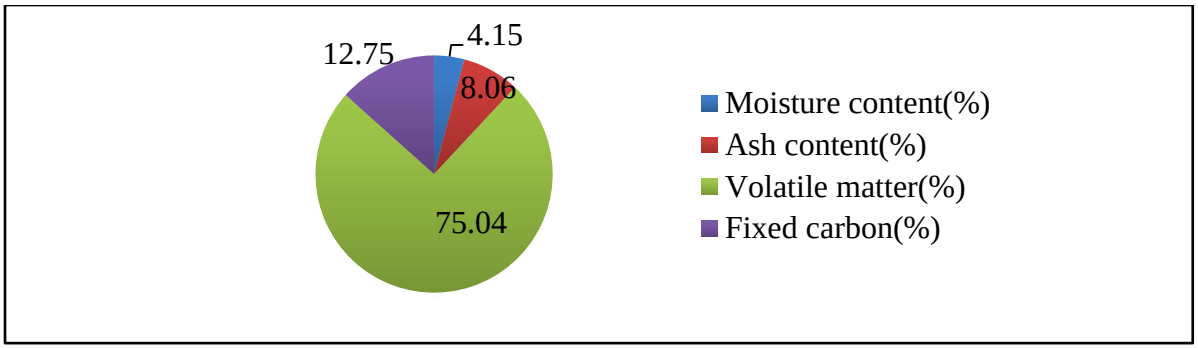

Figure 4-1: The proximate analysis results of sample sugarcane bagasse

4.1.2. Chemical composition of sugarcane bagasse

The chemical composition of various agricultural lignocellulosic materials including sugarcane bagasse have been defined by *Hong,* (*2013*), and was reported that sugarcane bagasse contains, cellulose (32-44%), hemicellulose (27-32%), lignin (19-24), and extractives (2.08-2.24%). In addition to this, 43.89% of cellulose, 33.38% hemicellulose, and 19.10% lignin have been reported by *Toribio-Cuaya et al.*, (*2014*). And also, according to *Augustine et al.*, (*2015*), 43% cellulose, 31% hemicellulose, 21% lignin and 2.14% extractives was reported. In this study, around 43.80% cellulose, 33.2% hemicellulose, 20.8% lignin and 2.205% extractives was obtained, which is approximately the same results with the previous researchers. Therefore, the standard method (*ASTM D 2015*) that was used for determination of the cellulose content is possible to apply for production of platform bio-fuels (e.g. HMF) and value-add chemicals (e.g. Para-xylene).

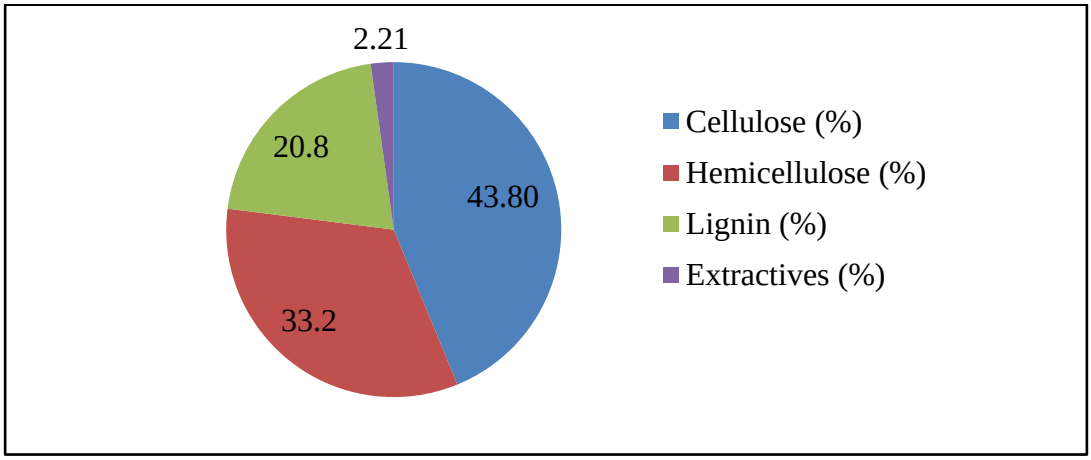

Figure 4-2: Chemical composition analysis results of sample sugarcane bagasse

4.2. Measurement of dimethyl benzoic acid and dimethyl benzene

The total concentration of dimethyl benzoic acid and dimethyl benzene produced per sample was determined from the absorbance versus concentration of the standard solution that was measured using the UV-spectrometer after the Diels-Alder cycloaddition reaction and aromatization steps respectively. To determine the concentration of the dimethyl benzoic acid and dimethyl benzene, first, the standard curve was plotted using the known concentrations of standard solutions dimethyl benzoic acid and dimethyl benzene, using ethanol references as shown in figures 4.3 a and b. Finally, the conversion of dimethyl furan, yield, and conversion of dimethyl benzoic acid as well yield of dimethyl benzene was determined using equations 3.11, 3.12, 3.15 and 3.16 respectively.

Table 4-1: Dimethyl benzoic acid and dimethyl benzene, standard solution and their absorbance

The same amount of standard dimethyl benzoic acid and dimethyl benzene Concentration, mg/100ml	0.000	100	150	200	250	300
Absorbance for dimethyl benzoic acid	-0.001	0.30	0.48	0.65	0.83	0.99
Absorbance for dimethyl benzene	0.001	0.20	0.29	0.37	0.45	0.54

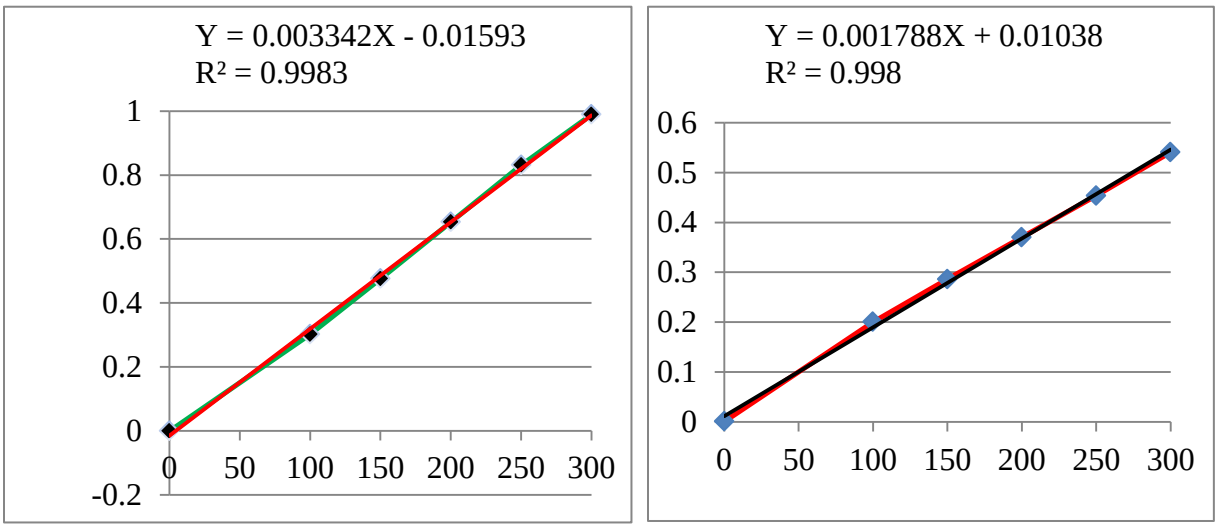

a) **b)**

Figure 4-3: a) Calibration curve for the standard solution of dimethyl benzoic acid, and; b) Calibration curve for the standard solution of dimethyl benzene.

The unknown concentrations of dimethyl benzoic acid in the sample were determined from the above standard calibration curve figure 4.3 a. In this study, experimental design technique (i.e. Design expert®7) was used to analyze and investigate the parameters that affect the process. According to *Nizamoff,* (*2012*), in the Diels-Alder cycloaddition reaction we have three operating parameters that mostly affects the process, such as the molar ratio of the reactants, the load of catalyst, and reaction time. So, the design expert tool is used to analyze and investigate for all parameter effects on the responses as shown below in table 4.2.

Table 4-2: Results of DMF conversion and the yield of dimethyl benzoic acid using Design expert®7 software.

Run №	**Factor 1 A:DMF: MA (mole)**	**Factor 2 B:Catalyst loading (mole)**	**Factor 3 C: Reaction time (hrs)**	**Absorbance @ 228 nm**	**Response 1 Conversion (%)**	**Response 2 Yield (%)**
1	1	0.1	4	0.40	26.53	41.45
2	5	0.1	4	0.87	11.37	17.76
3	1	0.5	4	0.62	40.41	63.14
4	5	0.5	4	0.99	12.82	20.03
5	1	0.1	12	0.60	39.12	61.12
6	5	0.1	12	0.99	12.83	20.04
7	1	0.5	12	0.62	40.46	63.21
8	5	0.5	12	0.89	11.57	18.08
9	1	0.3	8	0.63	41.34	64.57
10	5	0.3	8	0.91	11.82	18.47
11	3	0.1	8	0.87	18.96	29.62
12	3	0.5	8	0.99	21.40	33.43
13	3	0.3	4	0.71	15.53	24.27
14	3	0.3	12	0.89	19.35	30.23
15	3	0.3	8	0.89	19.35	30.23
16	3	0.3	8	0.89	19.29	30.14
17	3	0.3	8	0.89	19.30	30.16
18	3	0.3	8	0.89	19.30	30.15

The resulting data in the above table 4.2 were obtained using Design expert®7 software to investigate the effects of operating parameters such as the molar ratio of DMF: $C_4H_2O_3$, catalyst loading, and reaction time on the conversion of DMF and the yield of dimethyl benzoic acid (i.e. the responses, which are called the dependent variables, they are obtained using equations 3.11 and 3.12). Generally, this technique uses to differentiate the significance of the main and interaction effects of the reaction parameters on the responses. And all the experiments were carried out in a randomized order to minimize the effect of the variability on the responses.

Table 4-3: Design summary of the experiments

Study type	Response surface
Initial design	Central composite design
Design model	Quadratic polynomial
Center point	4
Runs	18
Number of responses	2
Blocks	No blocks

In this study, the quadratic polynomial model was used to analyze the results, and to show whether the model is significant or non-significant, first it is extremely important to perform the analysis of variance as shown in table 4.4 and 4.5 for the two responses (i.e. the conversion of DMF and the yield of dimethyl benzoic acid) respectively. From these tables, the significance or non-significance of the individual factors as well as interaction effects were performed on the probability values (p-value). The smaller the p-value of the variables indicated that, the bigger significance of the corresponding coefficient (i.e. the variable is more significantly affects the process).

Table 4-4: Analysis of variance for response surface quadratic model

Response 1: Conversion					
Source	**Sum of Squares**	**df**	**Mean Square**	**F-Value**	**p-value Prob>F**
Model	1.92E+003	9	214.00	72.2	< 0.0001*
A-DMF: $C_4H_2O_3$	1.62E+003	1	1.62E+003	548.00	< 0.0001
B-Catalyst loading	31.9	1	31.9	10.8	0.011
C-Reaction time	27.7	1	27.7	9.37	0.016
AB	28.2	1	28.2	9.52	0.015
AC	19.3	1	19.3	6.52	0.034
BC	29.1	1	29.1	9.82	0.014
A^2	126.0	1	126.0	42.5	0.0002
B^2	0.47	1	0.47	0.16	0.70
C^2	14.6	1	14.6	4.93	0.057
Residual	23.7	8	2.96		
Lack of Fit	0.0058	5	0.012	5.63	0.110**
Pure Error	0.022	3	0.007		
Cor Total	1.95E+003	17			

N.B: *represents model is significant, and ** represents lack of fit is non-significant

Table 4-5: Analysis of variance for response surface quadratic model

Response 2: Yield					
Source	**Sum of Squares**	**df**	**Mean Square**	**F-Value**	**p-value Prob>F**
Model	4.69E+003	9	522.00	72.2	< 0.0001*
A-DMF:$C_4H_2O_3$	3.96E+003	1	3.96E+003	548.00	< 0.0001
B-Catalyst loading	77.9	1	77.9	10.8	0.011
C-Reaction time	67.7	1	67.7	9.37	0.016
AB	68.8	1	68.8	9.52	0.015
AC	47.2	1	47.2	6.52	0.034
BC	71.0	1	71.0	9.82	0.014
A^2	307.0	1	307.0	42.5	0.0002
B^2	1.15	1	1.15	0.158	0.70
C^2	35.6	1	35.6	4.93	0.057
Residual	57.8	8	7.23		
Lack of Fit	0.0046	5	0.0046	4.63	0.120**
Pure Error	0.0053	3	0.0018		
Cor Total	4.75E+003	17			

N.B: *represents model is significant, and ** represents lack of fit is non-significant

To compare the model variance with residuals (error) variance look at the F-values. When the variances are close to the same values, the ratio will be close to one and it is less likely that any operating parameter has a significant effect on the response. And the calculation is performed by the ratio of the model mean square to residual mean square. In this study, for the two responses, as shown in the above tables 4.4 and 4.5, the model F-value of 72.2 implies the model is significant. There is only a 0.01% chance that a "Model F-Value" this large could occur due to

noise. Values of "Prob > F" less than 0.05 indicates model terms are significant. In this case, A, B, C, AB, AC, BC, A^2 are significant model terms. Values greater than 0.10 indicate the model terms are not significant.

If there are many insignificant model terms (not counting, those required to support hierarchy), the model reduction may improve the model. The "Lack of Fit F-value" of 5.63 for conversion and 4.63 for yield implies the lack of fit is not significant relative to the pure error. There is 11.00% for conversion and 12.00% for yield, chances that a "Lack of Fit F-value" this large could occur due to noise. Non-significant lack of fit is good.

In addition to this, to decide whether the model is preferably used or not it is important to check based on the values in table 4.6 and 4.7, such as coefficient of Variation, the standard deviation expressed as a percentage of the mean; Predicted-Residual Error Sum of Squares, which is a measure of how the model fits each point in the design; R-Squared, which measures the amount of variation around the mean explained by the model; Adj R- squared and Pred R-Squared, which measures the amount of variation in the new data explained by the model, and Adequate Precision, which measures the signal to disturbance ratio due to random error.

Table 4-6: Model adequacy measures for conversion

Std. Dev.	1.72	R-Squared	0.988
Mean	22.3	Adj R-Squared	0.974
C.V. %	7.73	Pred R-Squared	0.807
Press	376.00	Adeq precision	25.3

Table 4-7: Model adequacy measures for yield

Std. Dev.	2.69	R-Squared	0.988
Mean	34.8	Adj R-Squared	0.974
C.V. %	7.73	Pred R-Squared	0.807
Press	917.00	Adeq precision	25.3

The quality of the model developed could be evaluated from their coefficients of correlation. From the above two tables 4.6 and 4.7, the "Pred R-Squared" of 0.8071 is in reasonable agreement with the "Adj R-Squared" of 0.9741 in less than 0.2 difference. The difference between Adj R-Squared and Pred R-Squared is 0.167 (i.e. they are close to each other), and this indicates the close fit of the model to the actual response data. In addition to this, the value of R-squared for the developed correlation is 0.988; this indicates 98.8% of the total variation in the percentage of conversion or yield is the success to experimental studies. "Adeq Precision" measures the signal to noise ratio, and when the ratio is greater than 4, it is desirable. Therefore, in this study, the ratio of 25.254 indicates an adequate signal and this model can be used to navigate the design space. In addition to this, the regression coefficient and 95% CI (confidence interval) high and low as shown below in tables 4.8 and 4.9, can measure the effectiveness of the given parameters. If a zero value is occurring in the range of 95% CI high and low, the parameters have no effect and high value of regression coefficient can be affected highly in the process. In this study, the regression coefficients for molar ratio, catalyst loading, reaction time and their interactions each other are highly significant effect in the Diels-Alder cycloaddition reaction for the production of dimethyl benzoic acid next to Para-xylene.

Table 4-8: Regression coefficients and the corresponding 95% CI High and Low

Factors	Coefficient Estimate	df	Standard Error	95% CI Low	95% CI High
Intercept	19.5	1	0.68	18.0	21.1
A-DMF:$C_4H_2O_3$	-12.7	1	0.54	-14.0	-11.5
B-Catalyst loading	1.79	1	0.54	0.53	3.04
C-Reaction time	1.67	1	0.54	0.41	2.92
AB	-1.88	1	0.61	-3.28	-0.47
AC	-1.55	1	0.61	-2.96	-0.15
BC	-1.91	1	0.61	-3.31	-0.50
A^2	6.82	1	1.05	4.40	9.23
B^2	0.42	1	1.05	-1.99	2.83
C^2	-2.32	1	1.05	-4.73	0.09

From the above table 4.8, the quadratic polynomial model for conversion of DMF can be represented in terms of coded and actual factors as shown below:

Final Equation in Terms of Coded Factors:

Conversion of DMF = +19.5-12.7*A + 1.79*B + 1.67*C -1.88*A*B -1.55*A*C

-1.91*B*C + 6.82*A^2 + 0.42*B^2- 2.32*C^2…….(4.1)

And,

Final Equation in Terms of Actual Factors:

Conversion of DMF= +25.0 -13.6*(DMF: $C_4H_2O_3$) + 35.8*Catalyst loading + 4.04*reaction time -4.69*(DMF: $C_4H_2O_3$)*Catalyst loading -0.194*(DMF: $C_4H_2O_3$)*reaction Time-2.38*Catalyst loading*reaction time + 1.70 *$(\text{DMF: } C_4H_2O_3)^2$ +10.4*Catalyst loading^2 -0.145*reaction time^2……(4.2)

Table 4-9: Regression coefficients and the corresponding 95% CI High and Low

Factors	**Coefficient Estimate**	**df**	**Standard Error**	**95% CI Low**	**95% CI High**
Intercept	30.5	1	1.06	28.1	33.0
A-DMF:$C_4H_2O_3$	-19.9	1	0.85	-21.9	-18.0
B-Catalyst loading	2.79	1	0.85	0.83	4.75
C-Reaction time	2.60	1	0.85	0.64	4.56
AB	-2.93	1	0.95	-5.12	-0.74
AC	-2.43	1	0.95	-4.62	-0.24
BC	-2.98	1	0.95	-5.17	-0.79
A^2	10.6	1	1.63	6.88	14.4
B^2	0.65	1	1.63	-3.12	4.42
C^2	-3.63	1	1.63	-7.39	0.14

From the above table 4.9, the quadratic polynomial model for the yield of dimethyl benzoic acid was represented in terms of coded and actual factors as shown below:

Final Equation in Terms of Coded Factors:

$$Yield = +30.5 - 19.9*A + 2.79*B + 2.60*C - 2.93*A*B - 2.43*A*C - 2.98*B*C + 10.6*A^2 + 0.650*B^2 - 3.63*C^2 \quad \ldots\ldots(4.3)$$

And,

Final Equation in Terms of Actual Factors:

$$Yield = +39.1 - 21.3*(DMF: C_4H_2O_3) + 56.0*Catalyst\ loading + 6.30*Reaction\ time - 7.33*(DMF: C_4H_2O_3)*Catalyst\ loading - 0.303*(DMF: C_4H_2O_3)*Reaction\ time - 3.72*Catalyst\ loading*Reaction\ time + 2.66*(DMF: C_4H_2O_3)^2 + 16.3*Catalyst\ loading^2 - 0.227*Reaction\ time^2 \quad \ldots\ldots (4.4)$$

Diagnostic Plots

The graphical analysis of residuals is a very effective way to investigate the adequacy of fitting regression models and to check the underlying assumptions (i.e. the assumption of analysis of variance such as assumptions of an experimental error is normally distributed, the constant variance between treatments, independent of samples or randomized sample design). To see whether the assumptions of the analysis of variance well satisfied the model or not, it is better to check based on the following plots:

1) Normal probability plot of the studentized residuals to check for normality of residuals and the predicted versus actual plots to check the close relationship between predicted and the actual values.
2) Studentized residuals versus predicted values to check for constant error.
3) Externally Studentized Residuals and the plot of Diffts versus the number of experiments to look for outliers (i.e., influential values).

The actual versus predicted values/data's using models in the above equations 4.2 and 4.4 (i.e. in terms of actual factors) are tabulated in tables 4.10 and 4.11 for the conversion of DMF and the yield of dimethyl benzoic acid respectively. These data's are used to draw the plots of the normal probability of residuals, residual versus predicted, residuals versus run number, actual versus predicted plots and so on. But, it is enough to check based on the above common characteristics such as normal probability plot (i.e. to check for normality of the residuals) and the actual versus predicted plots, residual versus predicted plots (i.e. to check the error of the experiment), and the

run number versus externally Studentized residuals as well run number versus difft (i.e. to look the influential values or outliers).

Table 4-10: Actual versus model Predicted for the conversion of DMF

Response 1: Conversion								
Diagnostics case statistics								
Run №	Actual Value	Predicted Value	Residual	Leverage	Internally Studentized Residual	Externally Studentized Residual	Influence on fitted Value	Cook's Distance
1	26.5	28.4	-1.87	0.79	-2.39	-4.20	-0.26	0.21
2	11.4	9.77	1.60	0.79	2.04	2.76	0.42	* 1.61
3	40.4	39.5	0.87	0.79	1.12	1.14	0.23	0.48
4	12.8	13.4	-0.58	0.79	-0.75	-0.72	-1.42	0.21
5	39.1	38.7	0.47	0.79	0.60	0.57	1.13	0.14
6	12.8	13.8	-0.99	0.79	-1.26	-1.32	-1.59	0.61
7	40.5	42.2	-1.71	0.79	-2.19	-3.23	* -6.34	* 1.85
8	11.6	9.81	1.76	0.79	2.25	3.47	-1.81	0.95
9	41.3	39.1	2.24	0.51	1.85	2.28	* 2.30	0.35
10	11.8	13.6	-1.78	0.51	-1.47	-1.61	-1.63	0.22
11	19.0	18.2	0.79	0.51	0.65	0.63	0.63	0.044
12	21.4	21.7	-0.34	0.51	-0.28	-0.26	-0.27	0.008
13	15.5	15.5	-0.02	0.51	-0.01	-0.01	-0.01	1.74E-005
14	19.3	18.9	0.47	0.51	0.39	0.37	0.37	0.0153
15	19.3	19.5	-0.19	0.16	-0.12	-0.11	-0.05	0.0003
16	19.3	19.5	-0.25	0.16	-0.16	-0.15	-0.06	0.0005
17	19.3	19.5	-0.23	0.16	-0.15	-0.14	-0.06	0.0004
18	19.3	19.5	-0.24	0.16	-0.15	-0.14	-0.06	0.0004
*Exceed limits, which means, values that going beyond the limit, this indicate that, the model will give reasonable performance in prediction.								

Table 4-11: Actual versus model Predicted for the yield of dimethyl benzoic acid

Response 2: Yield								
Diagnostics case statistics								
Run №	Actual Value	Predicted Value	Residual	Leverage	Internally Studentized Residual	Externally Studentized Residual	Influence on fitted Value	Cook's Distance
1	41.4	44.4	-2.92	0.79	-2.39	-4.20	-0.26	0.21
2	17.8	15.3	2.49	0.79	2.04	2.76	0.42	* 1.61
3	63.1	61.8	1.36	0.79	1.12	1.14	0.23	0.48
4	20.0	20.9	-0.91	0.79	-0.75	-0.72	-1.42	0.21
5	61.1	60.4	0.73	0.79	0.60	0.57	1.13	0.14
6	20.0	21.6	-1.54	0.79	-1.26	-1.32	-1.59	0.61
7	63.2	65.9	-2.67	0.79	-2.19	-3.23	* -6.34	* 1.85
8	18.1	15.3	2.74	0.79	2.25	3.47	-1.81	0.95
9	64.6	61.1	3.50	0.51	1.85	2.28	* 2.30	0.35
10	18.5	21.3	-2.79	0.51	-1.47	-1.61	-1.63	0.22
11	29.6	28.4	1.24	0.51	0.65	0.63	0.63	0.04
12	33.4	34.0	-0.53	0.51	-0.28	-0.26	-0.27	0.01
13	24.3	24.3	-0.03	0.51	-0.01	-0.01	-0.01	1.74E-005
14	30.2	29.5	0.73	0.51	0.39	0.37	0.37	0.02
15	30.2	30.5	-0.29	0.16	-0.12	-0.11	-0.05	0.0003
16	30.1	30.5	-0.39	0.16	-0.16	-0.15	-0.06	0.0004
17	30.2	30.5	-0.37	0.16	-0.15	-0.14	-0.06	0.0004
18	30.1	30.5	-0.37	0.16	-0.15	-0.14	-0.06	0.0004
* Exceed limits, which means, values that going beyond the limit, this indicate that, the model will give reasonable performance in prediction.								

From the above tables 4.10 and 4.11 the following diagnostic curves was plotted to check whether the assumptions of the analysis of variance (ANOVA) satisfy the model or not.

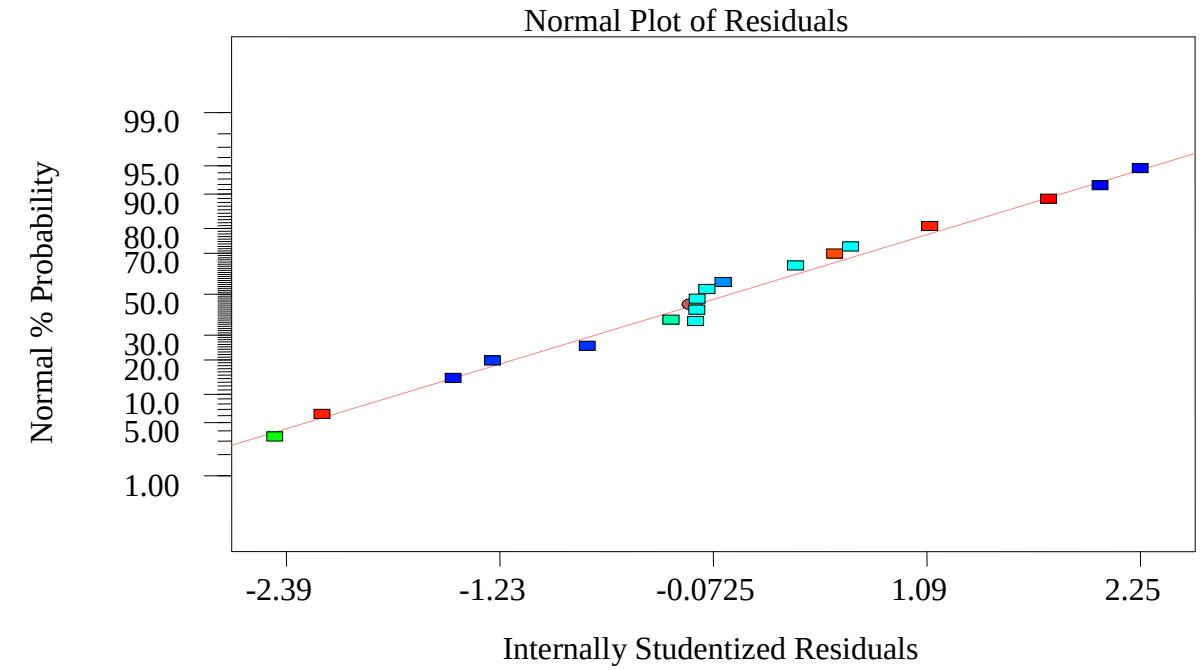

a)

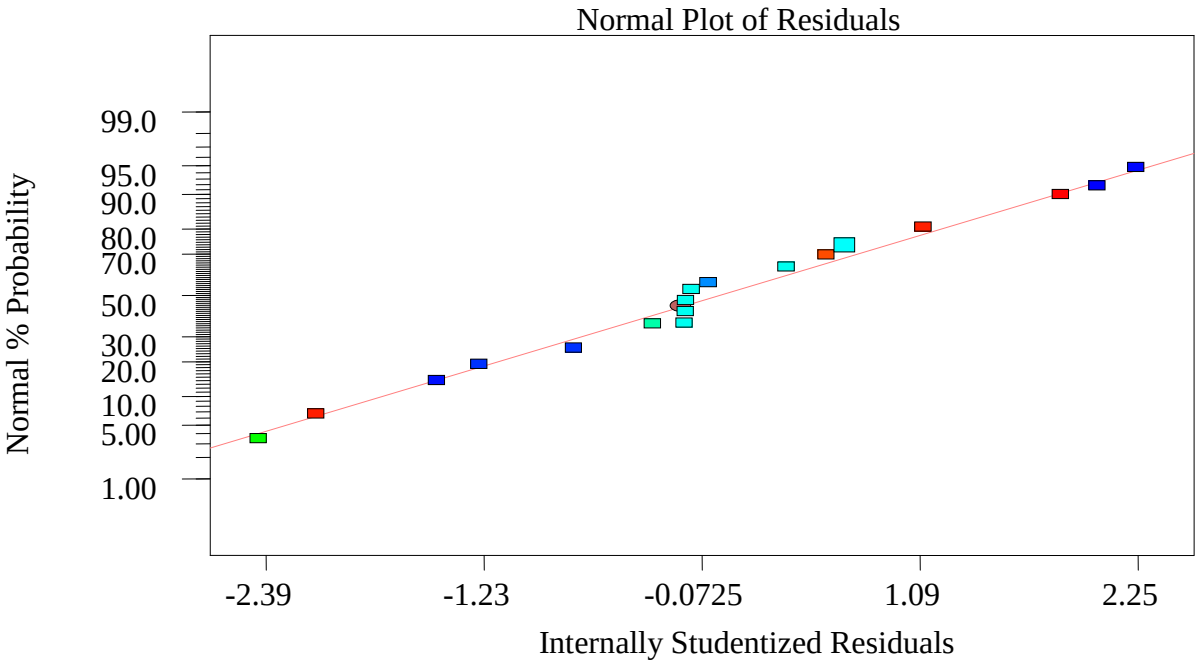

b)

Figure 4-4: a) Normal probability plot of residuals for the conversion of DMF, and; b) Normal probability plot of residuals for the yield of dimethyl benzoic acid.

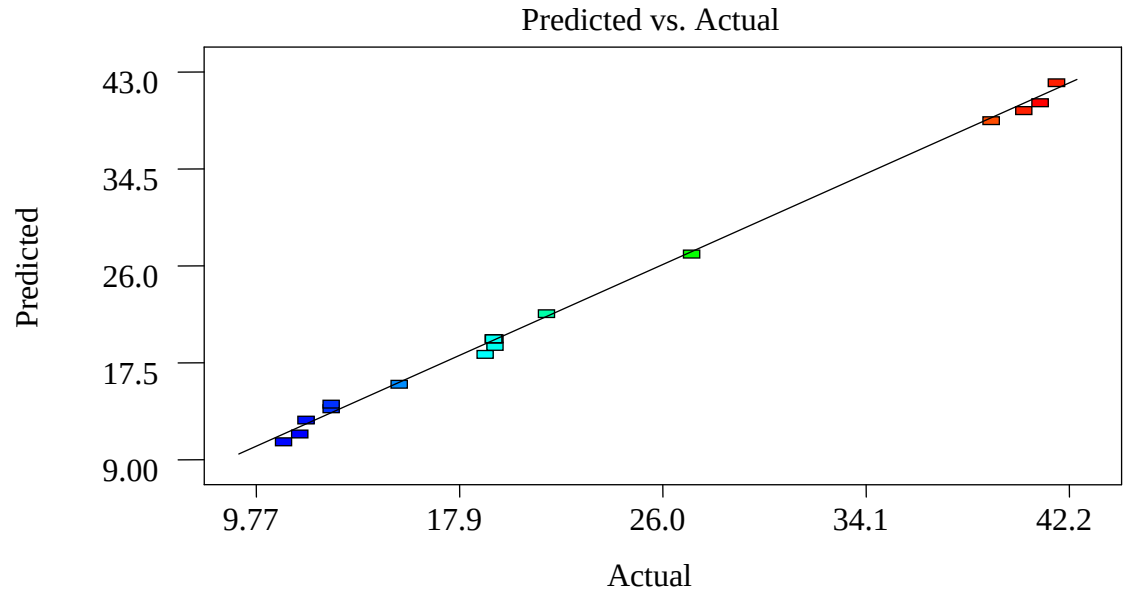

a)

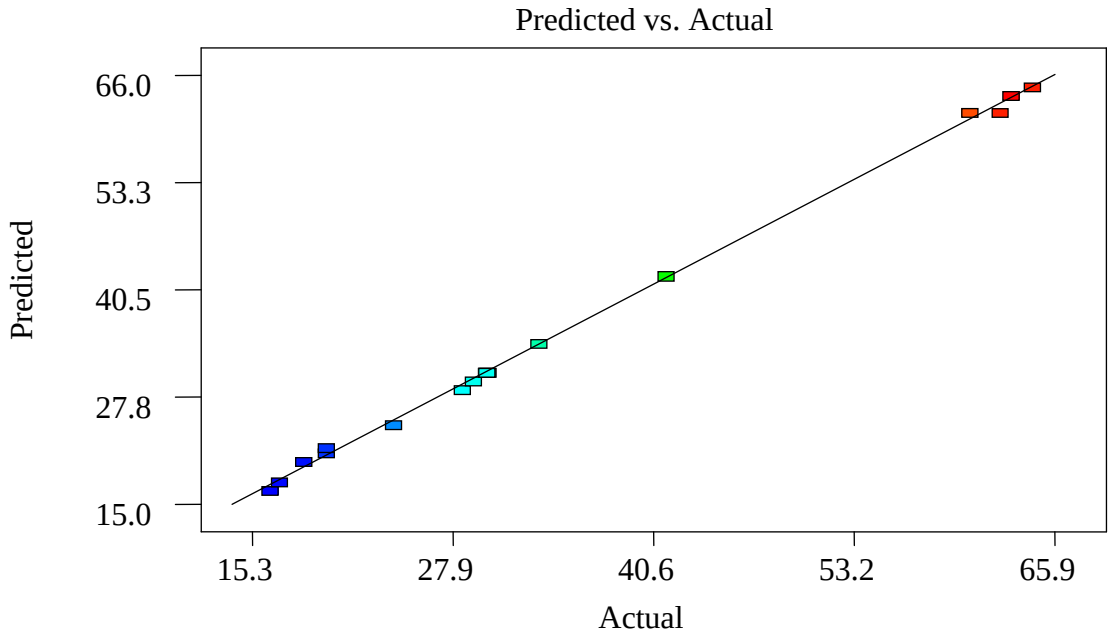

b)

Figure 4-5: **a) A**ctual versus predicted plot for the conversion of DMF, and;

b) **A**ctual versus predicted plot for the yield of dimethyl benzoic acid.

The normal probability plot is a graphical technique for assessing whether or not a data set is approximately normally distributed, and the assumption of disturbance is very much needed for

the validation of the results for testing of hypothesis, confidence intervals, and prediction intervals. The data are plotted against a theoretical distribution in such a way that the points should form approximately a straight line. The correlation coefficient associated with the linear fit to the data in the probability plot is a measure of the goodness of the fit. And a departure from this straight line indicates that, the departures from the specified distribution (i.e. if the points on the plot depart from the straight line, the normality may be invalid). In this case, the normal probability plot of the data is used to check the assumption of normality with the residuals. The plot as shown above (i.e. Figures 4.4 a and b) represent the normal probability plot of the residuals following a normal distribution, and the points in the plot shows to fit close to a straight-line in the figures, this shows that the quadratic polynomial model satisfies the assumptions for analysis of variance (ANOVA) (i.e. The error distribution is approximately normal). And, the predicted versus actual plots as shown in the above figures 4.5 a and b, in which all the points are very close to the line of perfect fit. This indicates to an adequacy agreement between the real data and the outputs from the model, and also, this represents the regression model equation gives an accurate description of the experiment. The color of the points such as dark blue, light blue, green, and red in the actual versus predicted plots represents a continuous increasing value of residuals from dark blue to red color respectively.

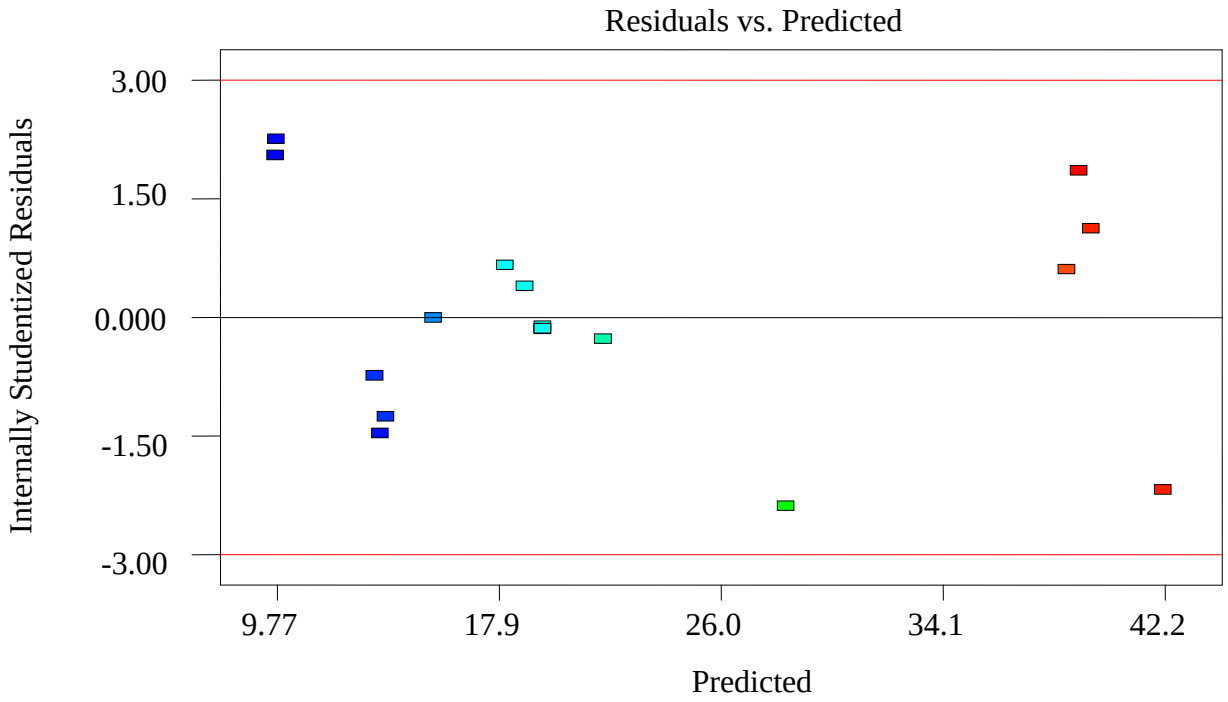

a)

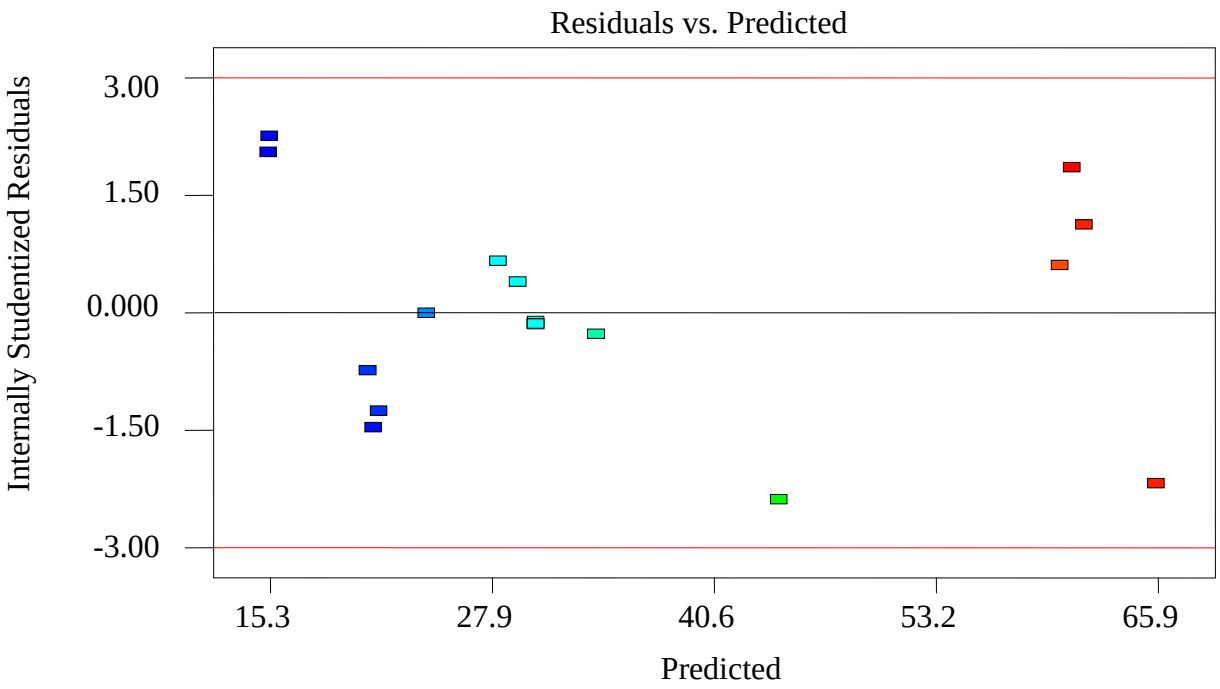

b)

Figure 4-6: a) Residual versus predicted plot for the conversion of DMF, and; b) Residual versus predicted plot for the yield of dimethyl benzoic acid.

The residual versus predicted plots as shown in the above figures 4.6 a and b simply used to check whether the model is correct or not, based on the assumption of variance (i.e. it is checked based on the assumption of constant variance). This plot shows a random pattern of residuals on both sides of zero. The plot is used to detect non-linearity, unequal error variances, and outliers. Generally, if the model is correct and the assumptions of variances are satisfied, the residuals should be non-structural (i.e. the variables are unrelated to each other at any point including the predicted response). Therefore, in this study as shown in the above figures 4.6 a and b for both conversions of DMF and the yields of dimethyl benzoic acid shows a random scatter, which justifying no need for an improvement to minimize personal error.

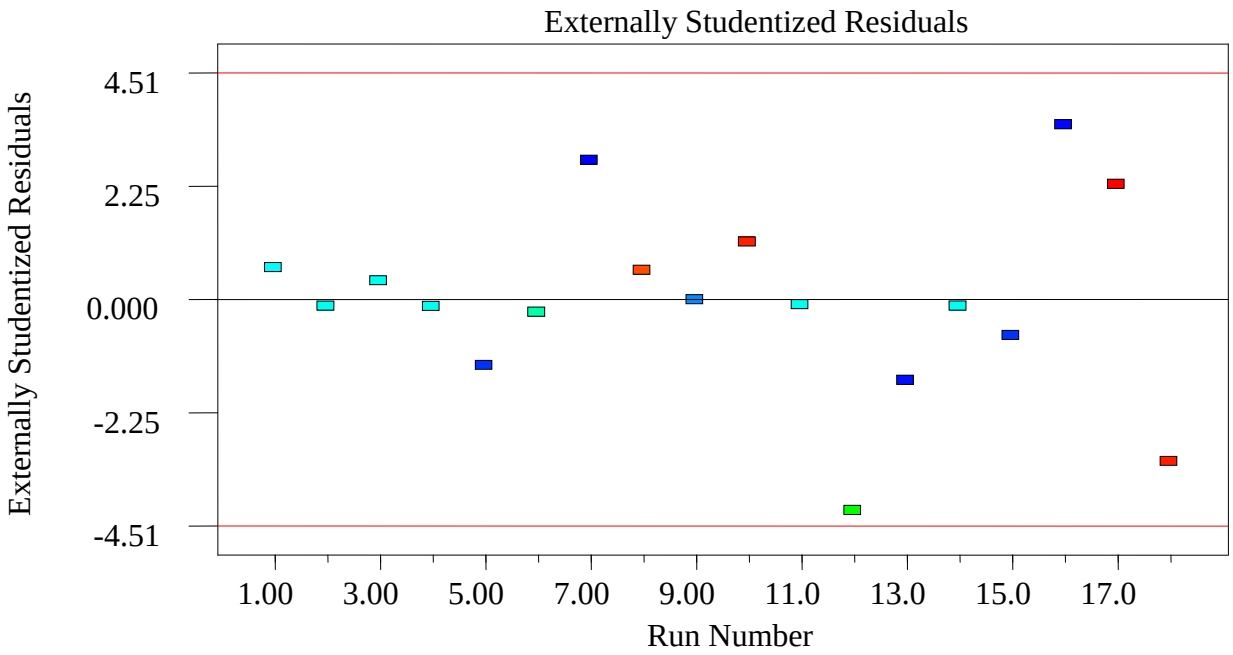

a)

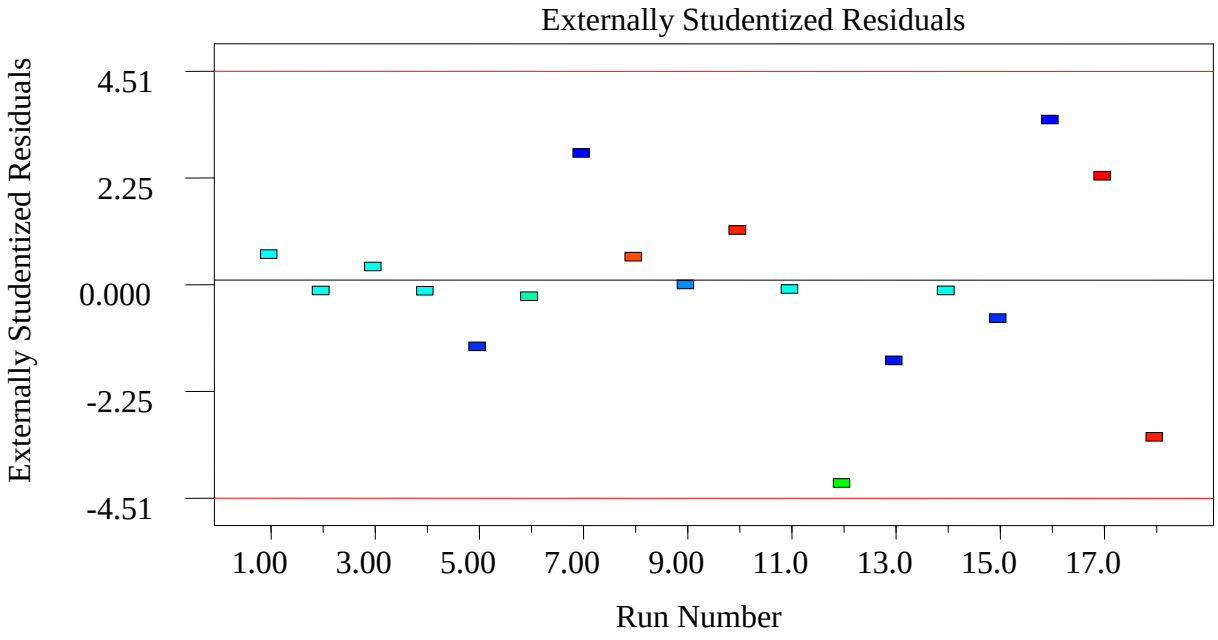

b)

Figure 4-7: a) Residual versus run number for the conversion of DMF, and;

b) Residual versus run number for the yield of dimethyl benzoic acid.

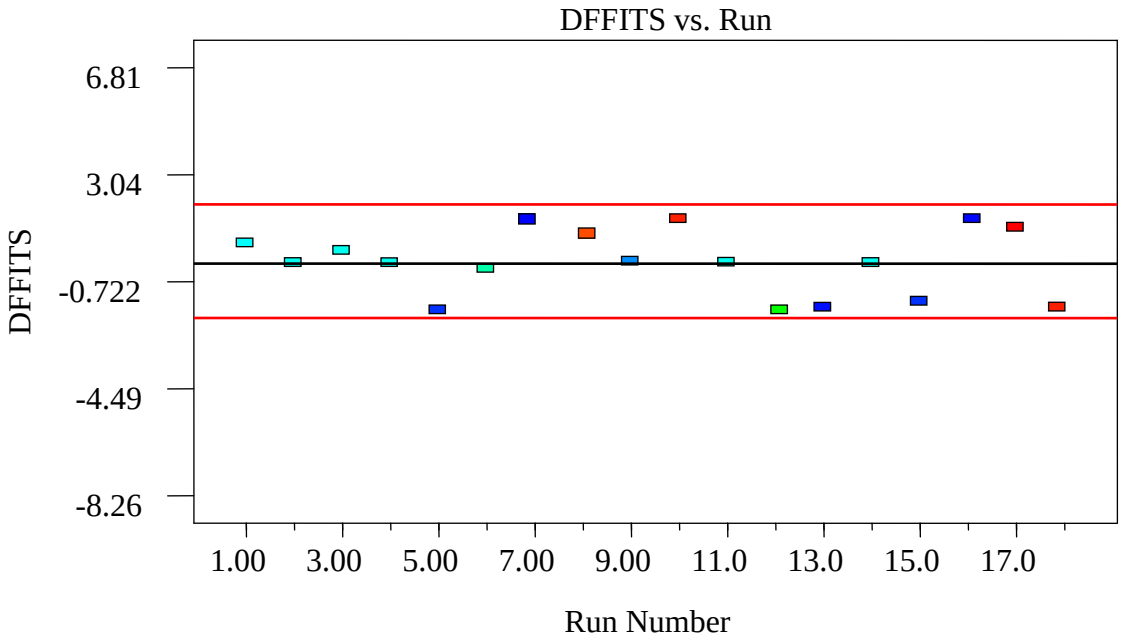

a)

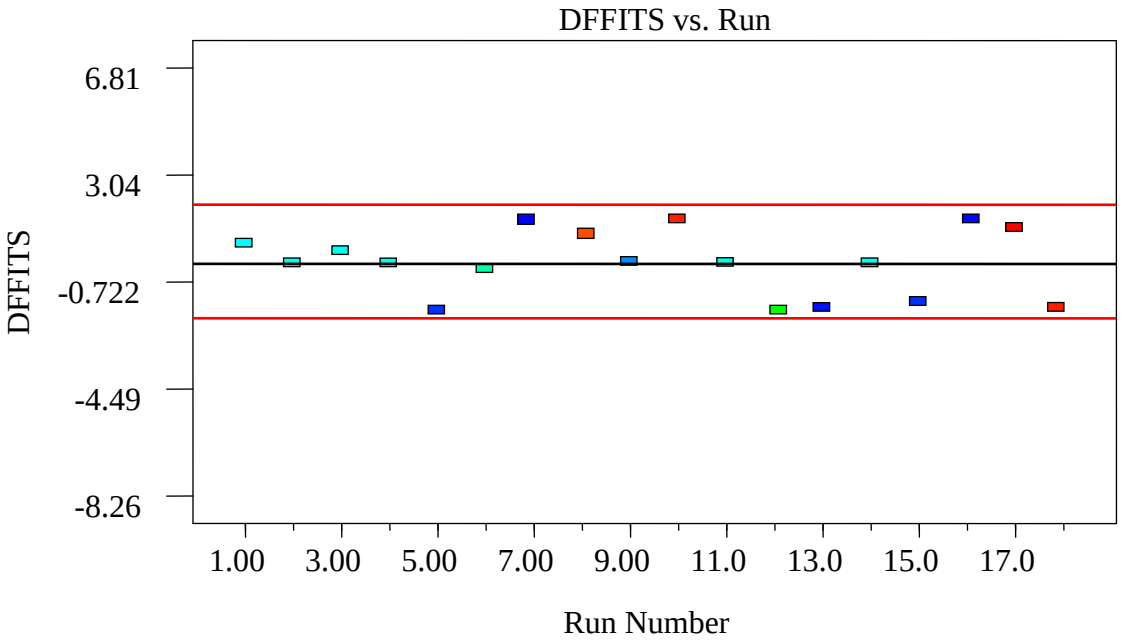

b)

Figure 4-8: a) Plot of run number versus difft for DMF conversion, and; b) Plot of run number versus difft for the yield of dimethyl benzoic acid.

The plots of all the residual versus orders of the experiment and number of experiment versus difft can be used to find the non-random error. These plots help to check the assumption that the residuals are uncorrelated with each other (i.e. based on the assumption of independence of samples or randomized sample design) and to check the outliers (influential values). The presence of outliers can lead to inflated error rates and substantial distortions of parameters (data points are far outside the norm for a variable or points that are considered to be larger than the absolute value of the standard points). In this study, as shown in the above figures 4.7 a and b and figures 4.8 a and b, all the points are less than the absolute value of the standard points of the design. If points are outside the norm, which indicates there is an experimental error due to faulty measurement, the incorrect recording of data, failure of measuring instruments, personal error, etc., but, in this study no point is outside the standard values, which indicates, these plots are a random scatter, which justifying no need for an improvement to minimize personal error.

4.3. Effect of experimental variables on the Diels-Alder cycloaddition

Dimethyl benzene production can be affected by a number of operating parameters, starting from the sample preparation up to aromatization process. In this study, the most common operating parameters that affect the conversion of DMF and the yield of dimethyl benzoic acids were analyzed and investigated in the Diels-Alder cycloaddition reaction section. In this section, the operating parameters, such as reactant molar ratio, catalyst loading and reaction times are highly affected to the process. The best way of showing the significant effects of these operating parameters for the conversion of DMF and the yield of dimethyl benzoic acid is to generate the response surface plots of the equation and also to determine the optimum operating condition (i.e. Parameters which give a high conversion of reactants and yield of products). To show the effects of the variables to the common response look at the plots of single effect, interaction effect, contours and the three dimensional surface effects as the function of the single or interactions of any two of the variables by holding the other value of the variable at the center.

4.3.1. Effect of reactant molar ratio on the conversion of DMF and yield of dimethyl benzoic acid

In this study, the effects of the operating conditions on the conversion of DMF and the yield of dimethyl benzoic acid were investigated by considering the process is affected by single effect as

the other parameters are constant (when catalyst loading and reaction times are an actual factors or at the center point).

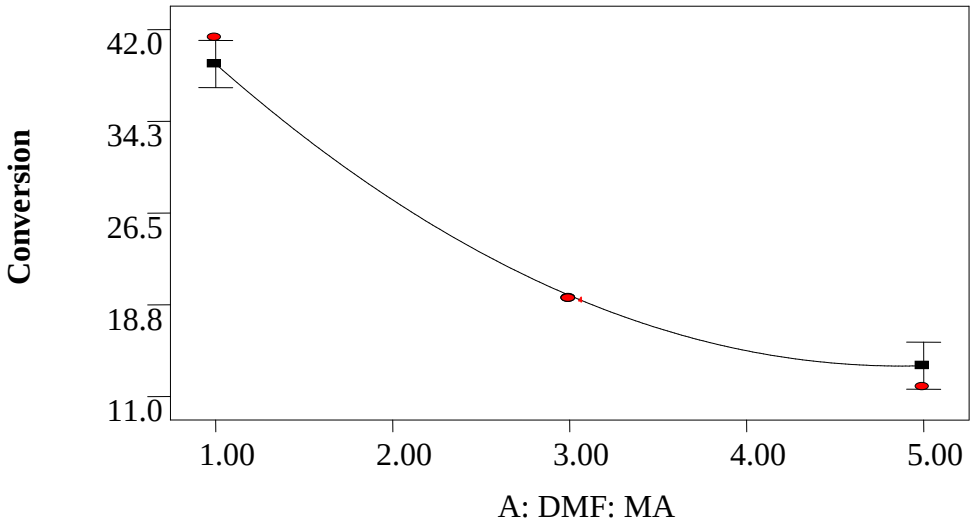

a)

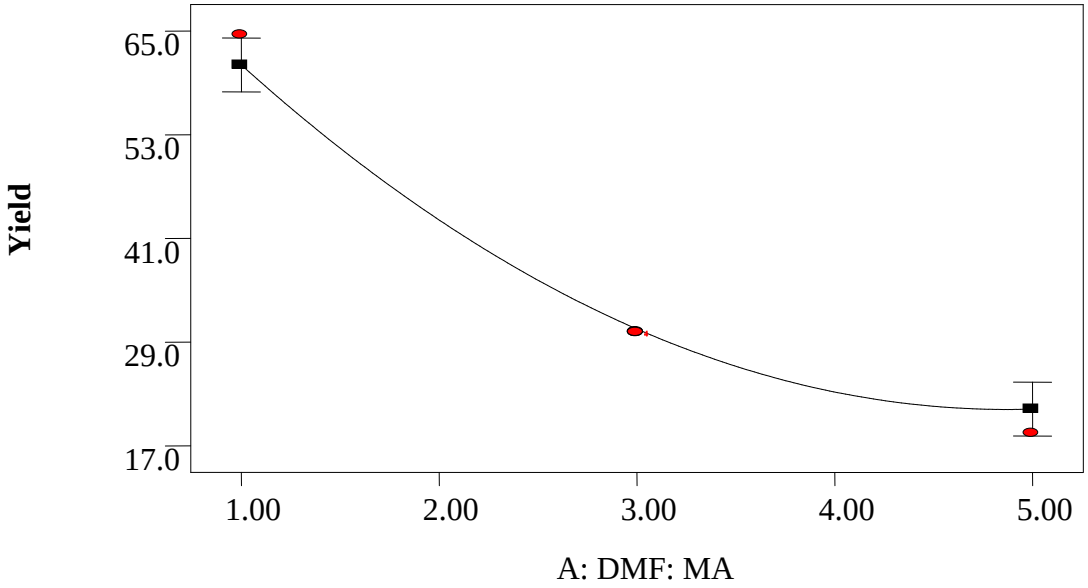

b)

Figure 4-9: a) Effect of reactant molar ratio on the conversion of DMF, and; b) Effect of reactant molar ratio on the yield of dimethyl benzoic acid respectively, at 0.3 mol of catalyst, and 8 hrs reaction times.

The most effective variable, which affects the conversion of 2, 5-dimethyl furan and dimethyl benzoic acid production yield during the Diels-Alder cycloaddition reaction, is the molar ratio of DMF to maleic anhydride. Since Diels-Alder cycloaddition reaction is an equilibrium reaction, a large excess of DMF is required for the reaction to move forward and avoid the reversible reaction. The dimethyl benzoic acid production has been investigated over the studied reactants molar ratio of DMF to Maleic anhydride from 1:2 to 5:1. From the resulting plots of the above figures 4.9 a and b, the molar ratios of reactants versus conversion as well as yield, as the molar ratio of reactants increased from 1 to 5 mol, both the conversion of the main reactant (DMF conversion) as well as the yield of the intermediate product (i.e. the yield of dimethyl benzoic acid) was slowly decreased from 41.3 to 11.8, and 64.6 to 18.5% respectively at constant catalyst loading and reaction time (i.e. When the catalyst loading and reaction times are at the center point). As the molar ratio of the reactants was increased above 1.03, the reduction in reactant conversion, as well as the yield of the intermediate product, may happen due to the reversibility behavior of the Diels-Alder cycloaddition reaction. In addition to this, it is in fact that, cooking on the catalyst surfaces leads to catalyst deactivation. Therefore, the optimum molar ratio (i.e. DMF: $C_4H_2O_3$ = 1.03) has been obtained, which gives a maximum conversion of DMF as well as the yield of dimethyl benzoic acid in the Diels-Alder cycloaddition reaction. This result proved that increasing the molar ratio higher than 1.03 is unflavored for the Diels-Alder cycloaddition reaction.

4.3.2. Effect of catalyst loading on the conversion of DMF and yield of dimethyl benzoic acid

Catalyst loading is another factor which affects the Diels-Alder cycloaddition reaction (i.e. for both conversions of the main reactant and the yield of the product). The effect of catalyst loading was studied at 50 ℃ (i.e. at an approximately the melting point of Maleic anhydride) at 3 mol/mole ratio of reactants for 8 hours reaction time. Five different amounts of catalyst (starting from 0.1 to 0.5 moles of $AlCl_3$) were taken to investigate the effects on the reactant conversion and yield of the product, with the molar ratio of reactants and the reaction time was kept constant (i.e. when reactant molar ratio and the reaction times are an actual factors or at the center point). And the effects are as shown in the following representations.

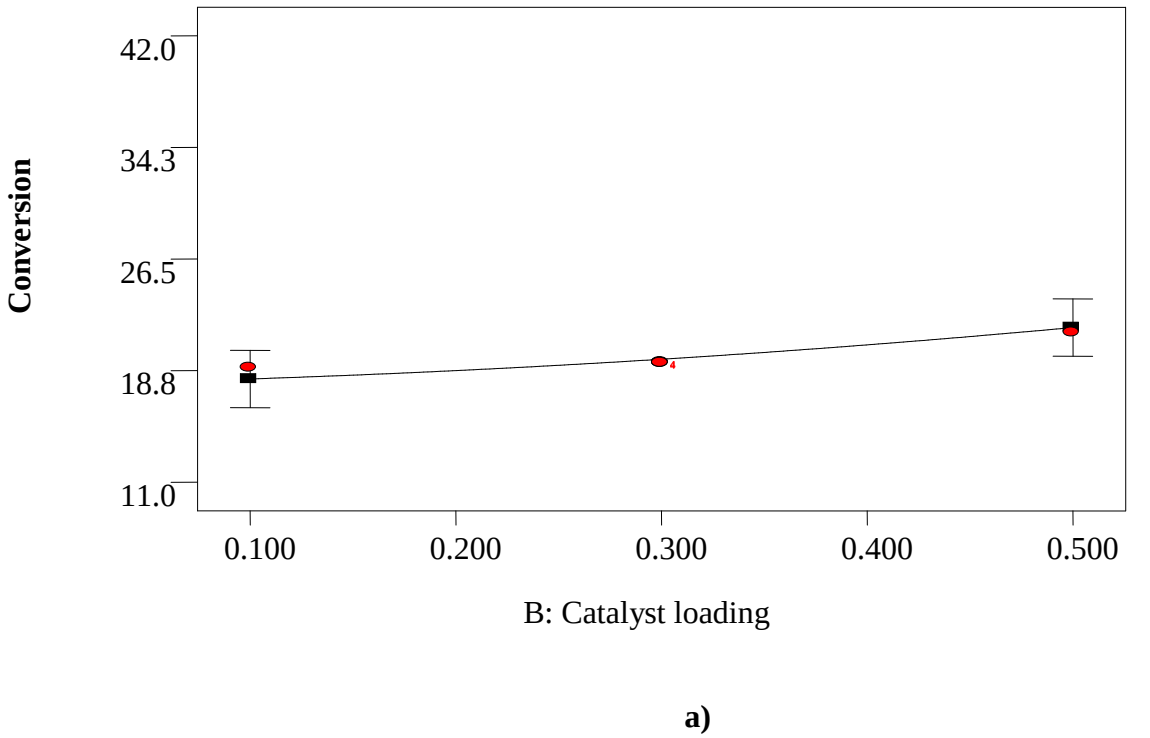

a)

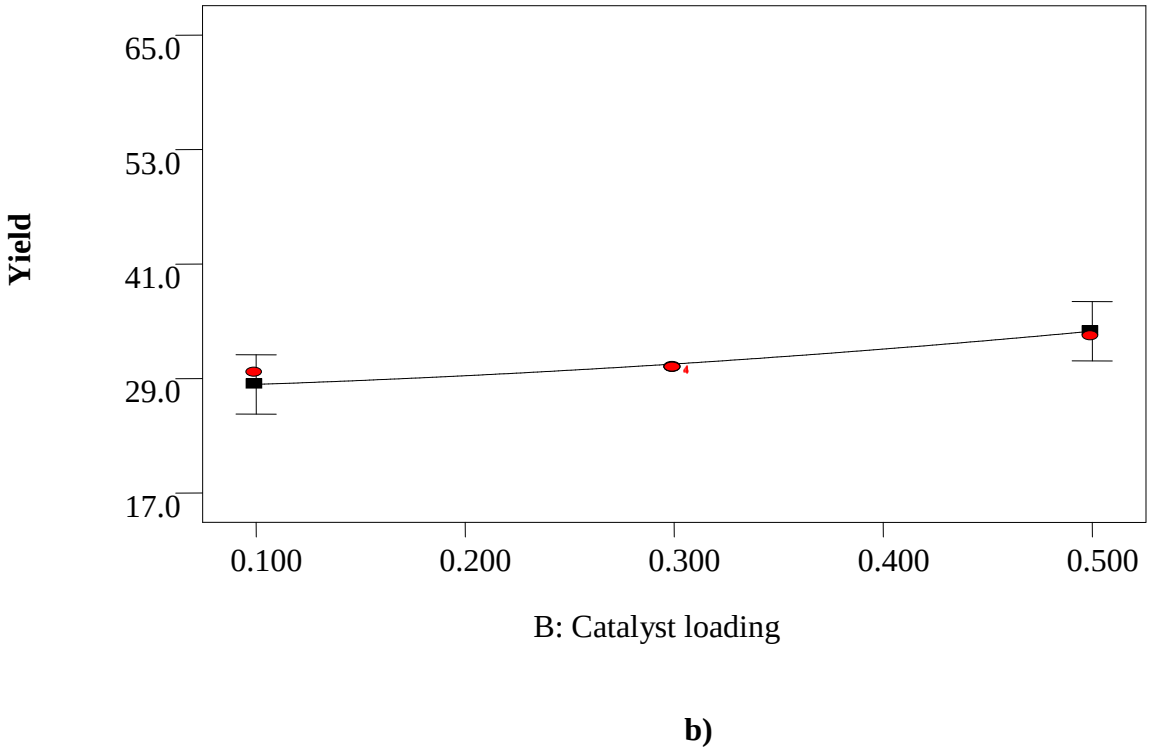

b)

Figure 4-10: a) Effect of catalyst loading on the conversion of DMF, and; b) Effect of catalyst loading on the yield of dimethyl benzoic acid respectively, at 8 hrs reaction time, and 3 mole/mole ratios of reactants.

A fast reaction rate of Diels-Alder cycloaddition reaction has occurred in the presence of Lewis acid catalysts (metal halides) like $AlCl_3$, Et_2AlCl, $BF_3.Et_2O$, ZnI_2, $SnCl_2$, $ZnCl_2$, $SnCl_4$, and $TiCl_4$, because they react with the DMF to break them apart. So that Maleic anhydride can bond with the DMF and produce dimethyl benzoic acid next to Para-xylene. However, aluminum chloride was selected and utilized as a catalyst in this investigation due to its reactivity, low cost, and availability. As shown in the above figures 4.10 a and b, at constant reactant molar ratio and reaction time (i.e. when they are at the center point), the conversion of the main reactant and the yield of the intermediate product was slowly increased with increasing the catalyst loading. Generally, as the catalyst loading is increased from 0.1 to 0.5 mol, both the conversion of the DMF and the yield of dimethyl benzoic acid are increased from 18.2 to 21.7 and 28.4 to 34% respectively. However, both the conversion of the reactant and the product yield are insensitive to different catalyst loadings. Higher catalyst loading, above 0.3 moles leads to increase the conversion and yield in the Diels-Alder cycloaddition reaction of furan to produce the cyclohexane, which could further lead to increased coking formation. It is supposed that cooking on the catalyst surfaces leads to catalyst deactivation, but with increased the catalyst loading above 0.3 moles, further leads to increase the cooking formation. Therefore, 0.5 mole of the catalyst is an optimum value, because it gives a higher conversion of reactants as well as maximum yield of the product in a short period of time. The reason is catalysts are substances they can speed up the rate of the chemical reaction without consuming itself.

4.3.3. Effect of reaction time on the conversion of DMF and yield of dimethyl benzoic acid

Reaction time is another factor, which affects the Dies-Alder cycloaddition reaction (i.e. for both conversions of the main reactant and the yield of the intermediate product) at 50 ℃ reaction temperatures starting from 4 to 12 hrs. Five reaction times were taken to investigate the effects on the reactant conversion (i.e. Conversion of the DMF) and product yield (i.e. the yield of dimethyl benzoic acid), with the reactant molar ratio (i.e. DMF: Maleic anhydride) and the catalyst loading (i.e. the amount of $AlCl_3$) was kept constant (i.e. When they are an actual factors or at the center point). And the effects are as shown in the following representations.

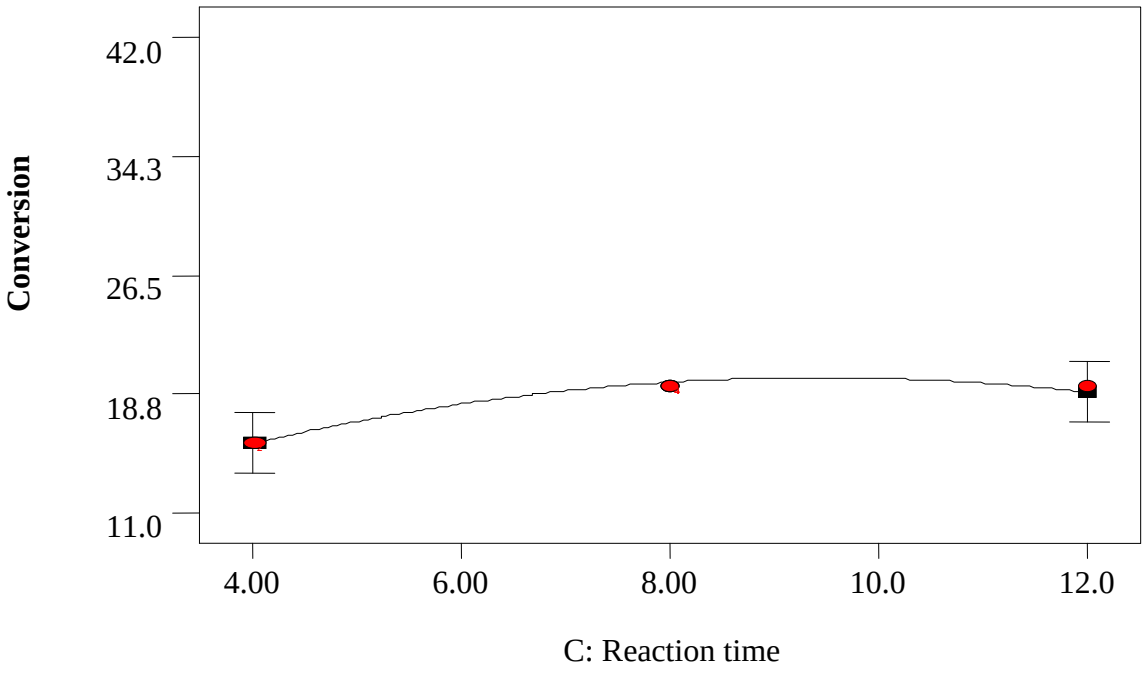

a)

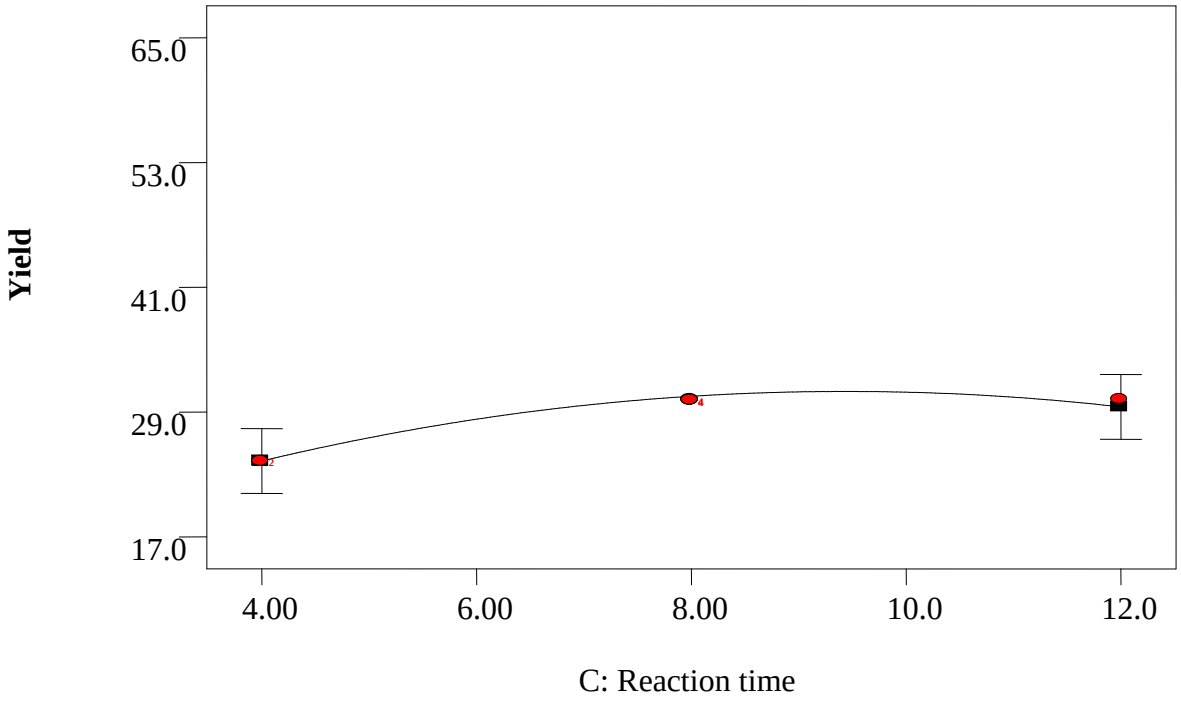

b)

Figure 4-11: a) Effect of reaction time on the conversion of DMF, and; b) Effect of reaction time on the yield of dimethyl benzoic acid respectively, at 0.3 mole of catalyst, and 3 mole/mole reactant molar ratios.

From the resulting plots of reaction time versus DMF conversion and yield of dimethyl benzoic acid as shown in the figures 4.11 a and b, when the molar ratio of reactants and the catalyst loading were actual factors (i.e. When they are at the center point), both the conversion of DMF and the yield of dimethyl benzoic acid were increased for some reaction time (i.e. Until reaction time reaches 9 hrs). As the reaction time further increases above 9 hrs, both reactant conversion and yield of the intermediate product was slowly decreased. The reason is, since Diels-Alder cycloaddition is a reversible reaction, in which products are favored at some reaction condition and turn them back into the reactants (i.e. The reversible reaction can under certain conditions, reach what we call 'equilibrium' and then turn them back into the reactants, which is called 'Le Châtelier's Principle'). In addition to this, since the reaction is taking place in a closed system, one where no substances are being added or lost. Therefore, at the beginning of the reaction, we have only the reactants. Once the reaction starts, the amounts of the reactants were starting decreasing and the amounts of the products were beginning to increase. After a time, a reversible reaction in the closed system reaches equilibrium. This is where the forward reaction (reactants reacting to produce the products) and the backward reaction (products reacting to reform the reactants) are occurring at the same rate. Finally, as cooking time increased, it leads to catalyst deactivation (it may be occurring due to the instability nature of the catalyst), as the result, the corresponding responses were decreased.

4.3.4. Effects of reactant molar ratio and catalyst loading on the conversion of DMF and the yield of dimethyl benzoic acid

In the Diels-Alder cycloaddition reaction, there are three main factors which affect the process such as the molar ratio of the reactants, catalyst loading and the reaction time. As shown in the tables 4.4 and 4.5 all the factors/parameters and their interactions can affect the process. The effects of the single factors has been discussed starting from figures 4.9 up to 4.11, and in this section, the interaction effects of variables were investigated. As shown in the following figures 4.12, 4.13, and 4.14, represented as interaction, contour and surface response plots, the effects of two different operating variables on the responses such as DMF conversion and dimethyl benzoic acid yield was investigated by considering the value of the third variable is kept at the center point.

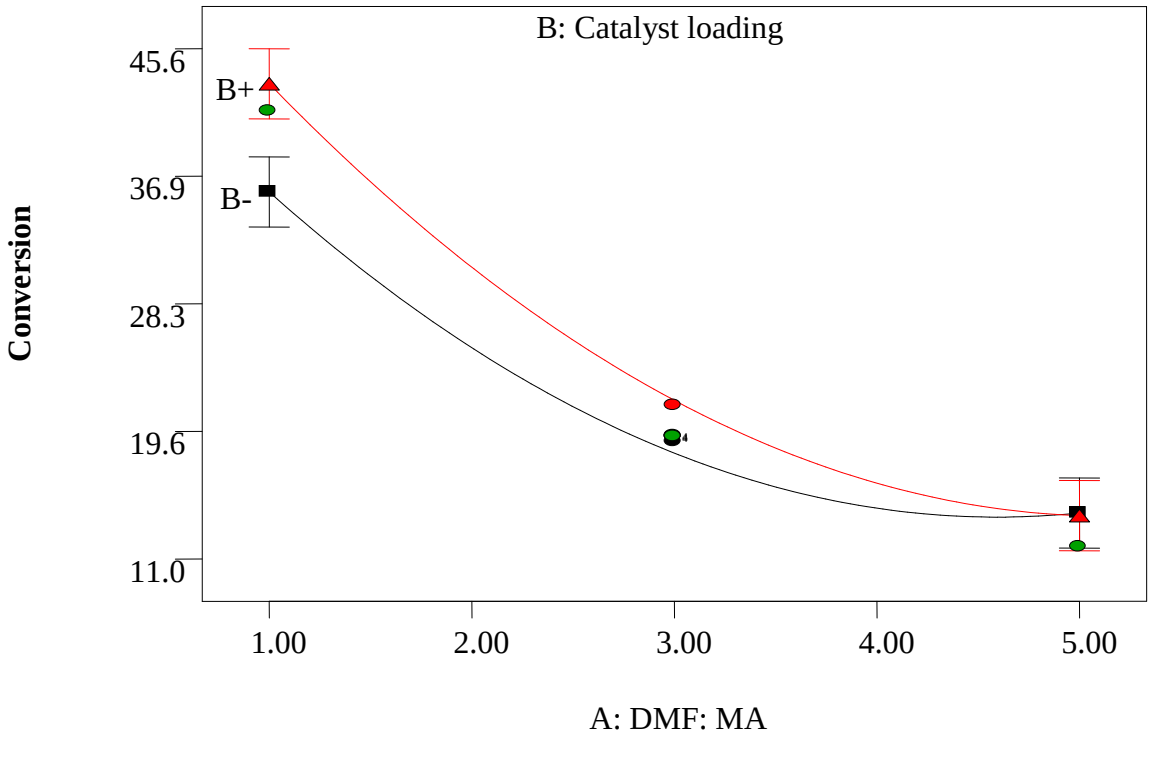

a)

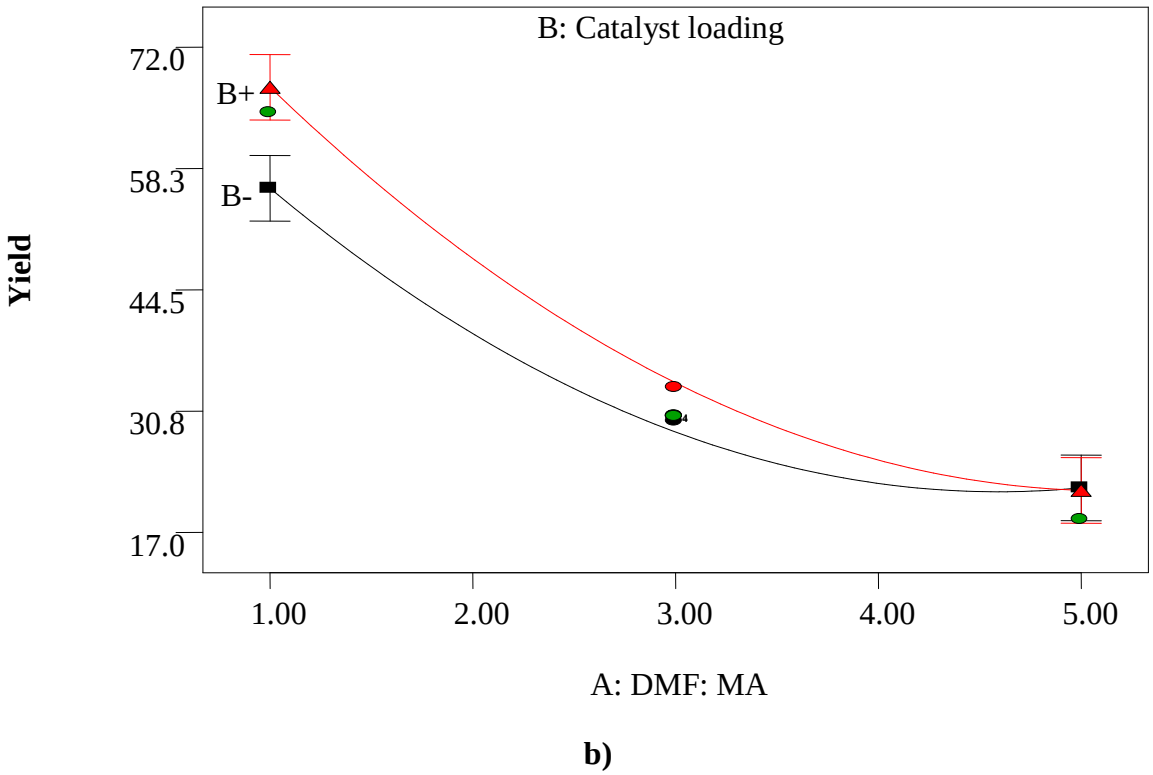

b)

Figure 4-12: a) Interaction effects of reactant molar ratio and catalyst loading on the conversion of DMF, and; b) Interaction effects of reactant molar ratio and catalyst loading on the yield of dimethyl benzoic acid respectively, at 8 hr reaction time.

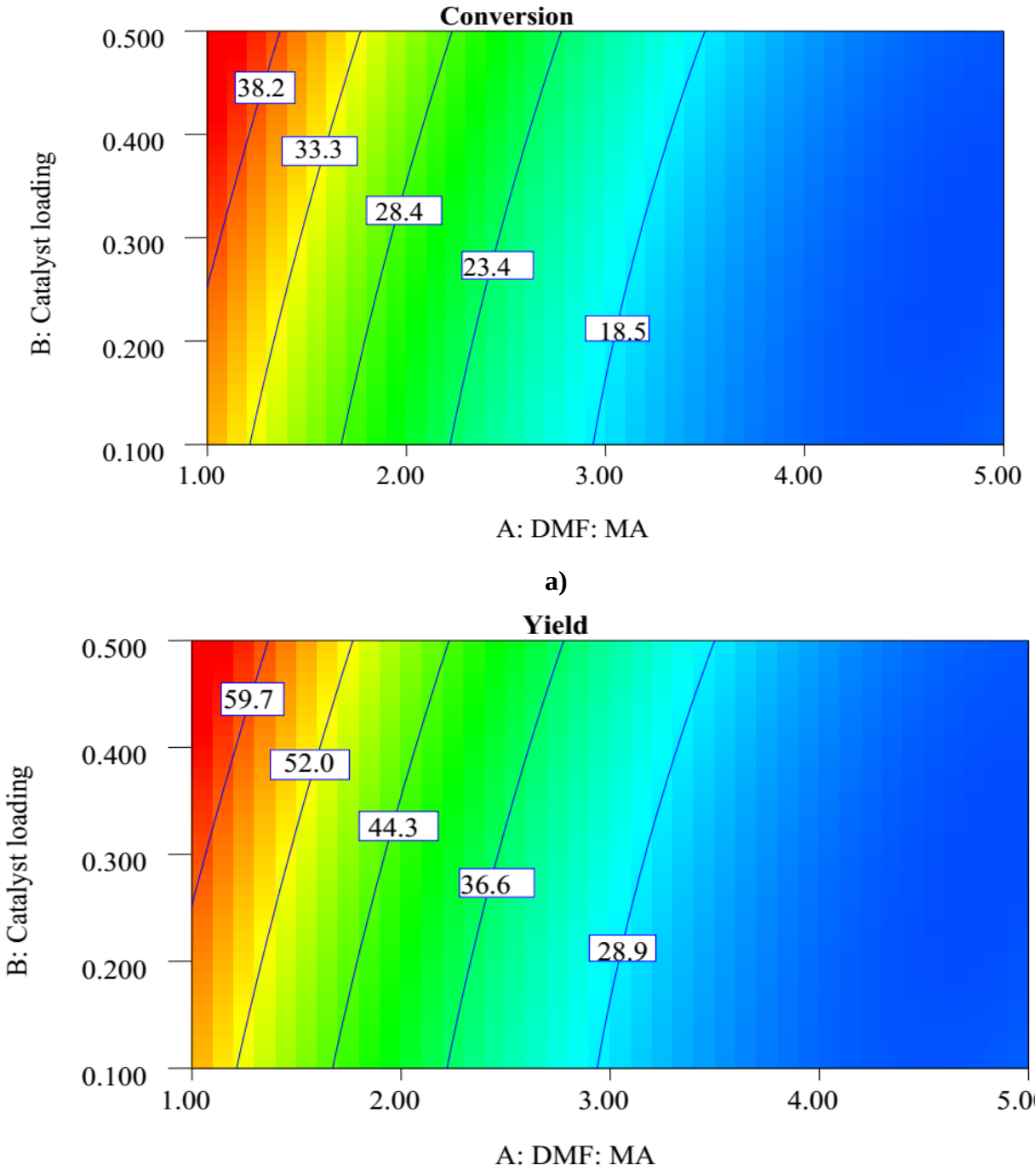

Figure 4-13: a) Contour plot for the effects of reactant molar ratio and catalyst loading on the conversion of DMF, and; b) Contour plot for the effects of reactant molar ratio and catalyst loading on the yield of dimethyl benzoic acid respectively, at 8 hr reaction time.

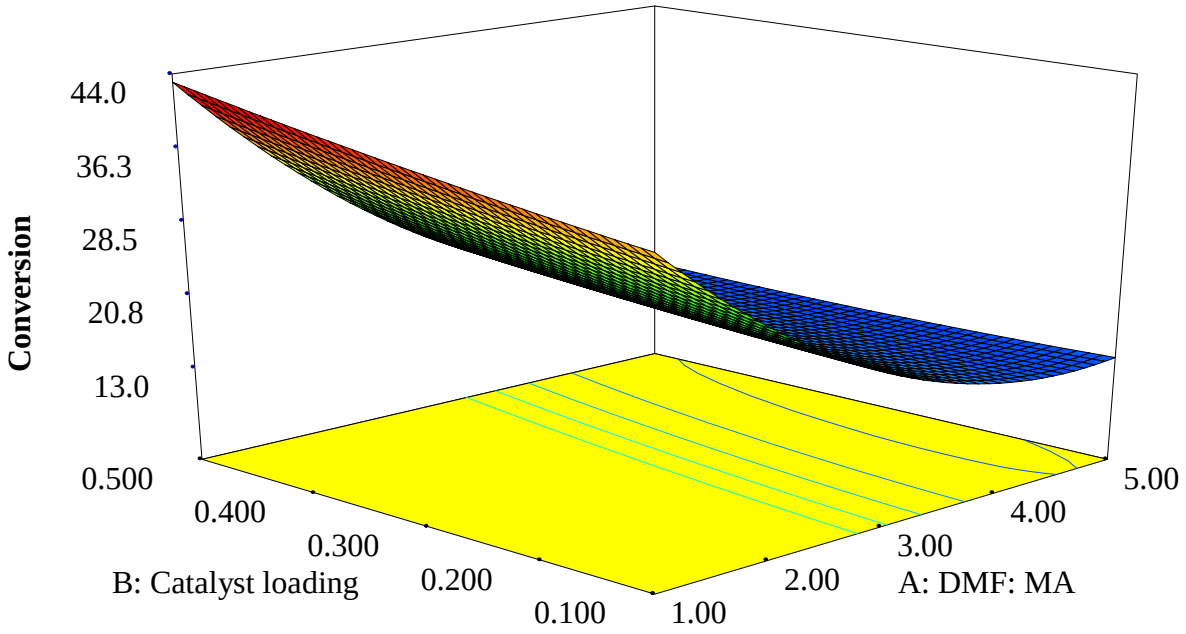

a)

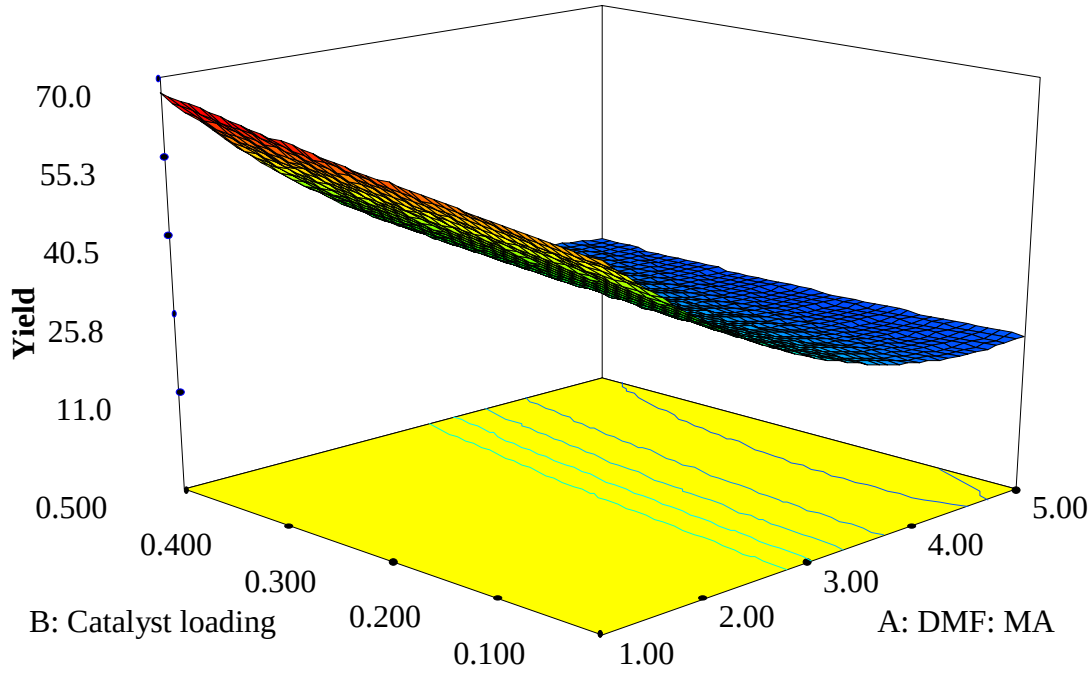

b)

Figure 4-14: a) Response surface plot for the effects of catalyst loading and reactant molar ratio on the conversion of DMF, and; b) Response surface plot for the effects of catalyst loading and reactant molar ratio on the yield of dimethyl benzoic acid respectively, at 8 hrs reaction time.

When we see the resulting plots of figure 4.12 a and b, the process is taking place at a constant reaction time (i.e. at the center point) with a variations of the other parameters such as reactant molar ratio and catalyst loading. And they are represented by the black and red lines, which are indicates low and high level of parameters respectively. As shown in figures 4.12 a and b, As the molar ratio of the reactants (i.e. DMF: Maleic anhydride) was increased from 1 to 5, the conversion of DMF and the yield of dimethyl benzoic acid were analyzed using 0.1, 0.2, 0.3, 0.4 and 0.5 moles of catalyst loading. These resulting figures show that, at a lower amount reactant molar ratio and high amount of catalyst loading, higher reactant conversion and product yield was obtained (i.e. 43.18 and 67.45% of conversion and yield was obtained respectively) and at higher levels of molar ratio of the reactants and lower value of catalyst loading, lower value of reactant conversion and product yield was obtained (i.e. 13.93 and 21.76% of conversion and yield was obtained respectively). This shows the factors such as the molar ratio of the reactants and the load of catalyst has inversely affected the Diels-Alder cycloaddition reaction. As the molar ratio increased from 1 to 5, the decrement in the conversion and yield may happen due to the limitation of the reagent (the dienophile) that was utilized in the chemical reaction to react with the DMF (i.e. Maleic anhydride, which is used as a dienophile in the chemical reaction). And, as the catalyst loading is increased from 0.1 to 0.5 moles, both increment in conversion and the yield may happen due to the reactivity nature of the catalyst at short period of time. Therefore, from the results, the molar ratio and the load of the catalyst have strong relationships and affects strongly to the conversion and the yield.

The resulting contour plots of figure 4.13 a and b shows the predicted response of the conversion and yield respectively. As increasing the load of the catalyst at the lower level reactant molar ratio and increased the molar ratio of the reactants at lower level load of catalyst gives a positive effect on both the conversion of DMF and the yield of the intermediate product (dimethyl benzoic acid), and they are linearly affects the process. From these plots, maximum amount of conversion and yields was obtained when the ratio of the reactants and catalyst loading are at 1.03, and 0.3 mol. As the result, 41.33% conversion and 64.57% yield was obtained.

As shown the results of the response surface figures 4.14 a and b obtained from the effects of reactant molar ratio and the load of the catalyst is looks like linear shape. Hence, as defined in the above contour results, as the molar ratio of the reactant was increased at lower level of catalyst loading, the conversion and the yield was decreased, and as the catalyst loading was

increased at lower levels of reactant molar ratio, the reactant conversion and product yield was increased linearly. Therefore, the response surface can be represented the exact property/effect of the parameters as defined in the contour plots, and it is possible to determine the optimum operating conditions simply from the plot at the interaction of the two parameters, and 41.33% conversion, and 64.57% yield was obtained at 0.3 mol of catalyst loading and a reactant molar ratio of 1, when the reaction time is constant (i.e. at the center point, which is equal to 8hr).

4.3.5. Effects of reactant molar ratio and reaction time on the conversion of DMF and the yield of dimethyl benzoic acid

In this section, the effect of reactant molar ratio and reaction time on the reactant conversion (DMF conversion) and product yield (yield of dimethyl benzoic acid) was investigated at a constant amount of catalyst (i.e. when the catalyst load is at the center point). To investigate the effect of these factors, look at the interaction, contour and surface response plots as shown in the following figures 4.15 up to 4.17 respectively.

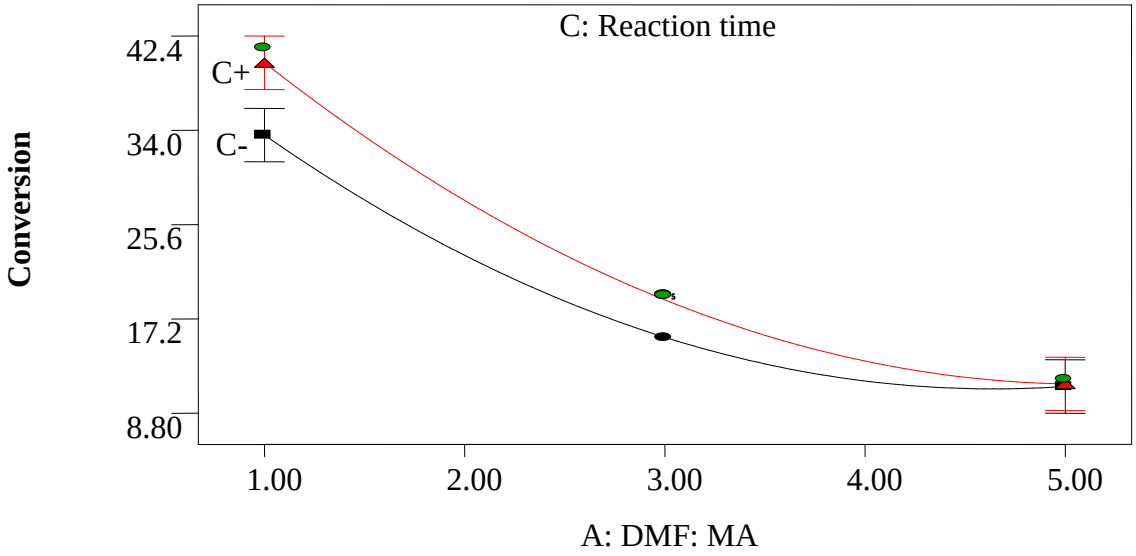

a)

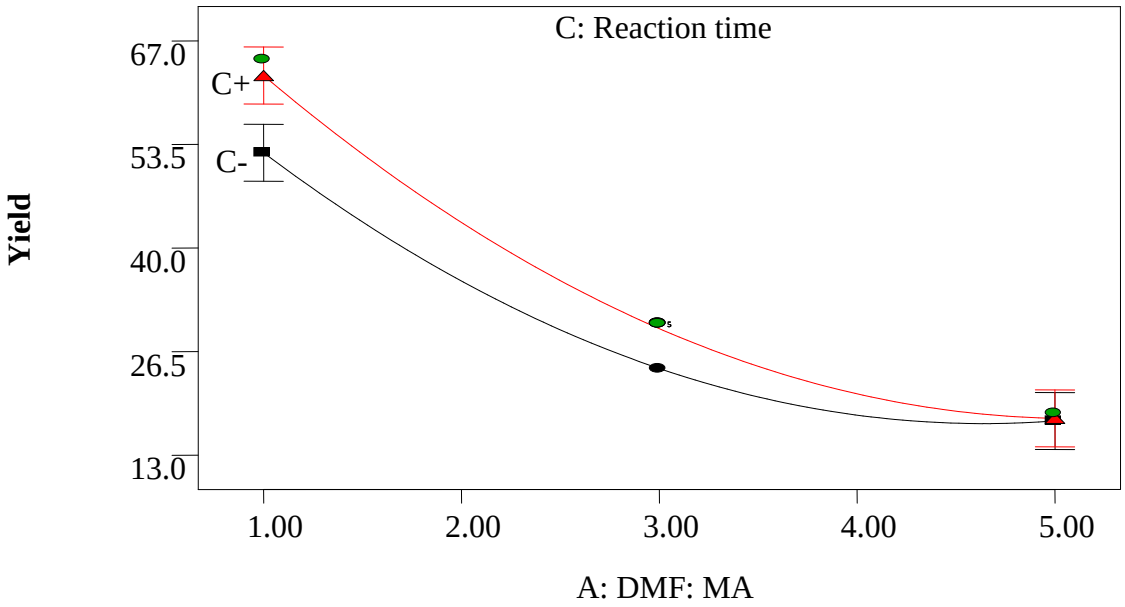

b)

Figure 4-15: a) Interaction effects of reactant molar ratio and reaction time on the conversion of DMF, and; b) Interaction effects of reactant molar ratio and reaction time on the yield of dimethyl benzoic acid respectively, at 0.3 mol of catalyst

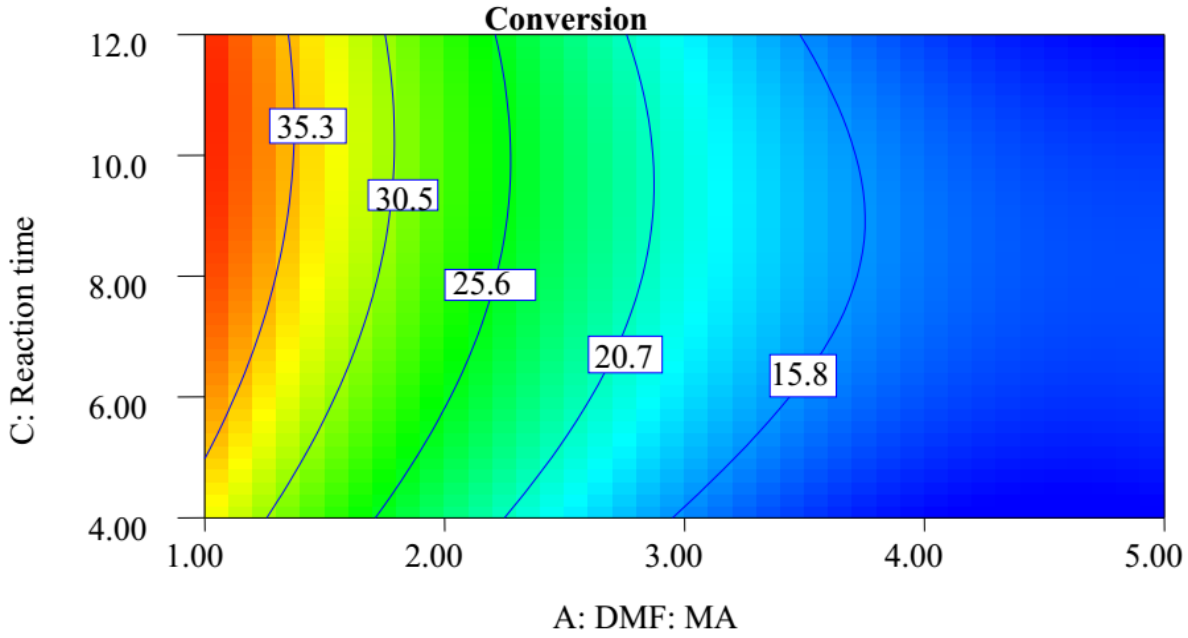

a)

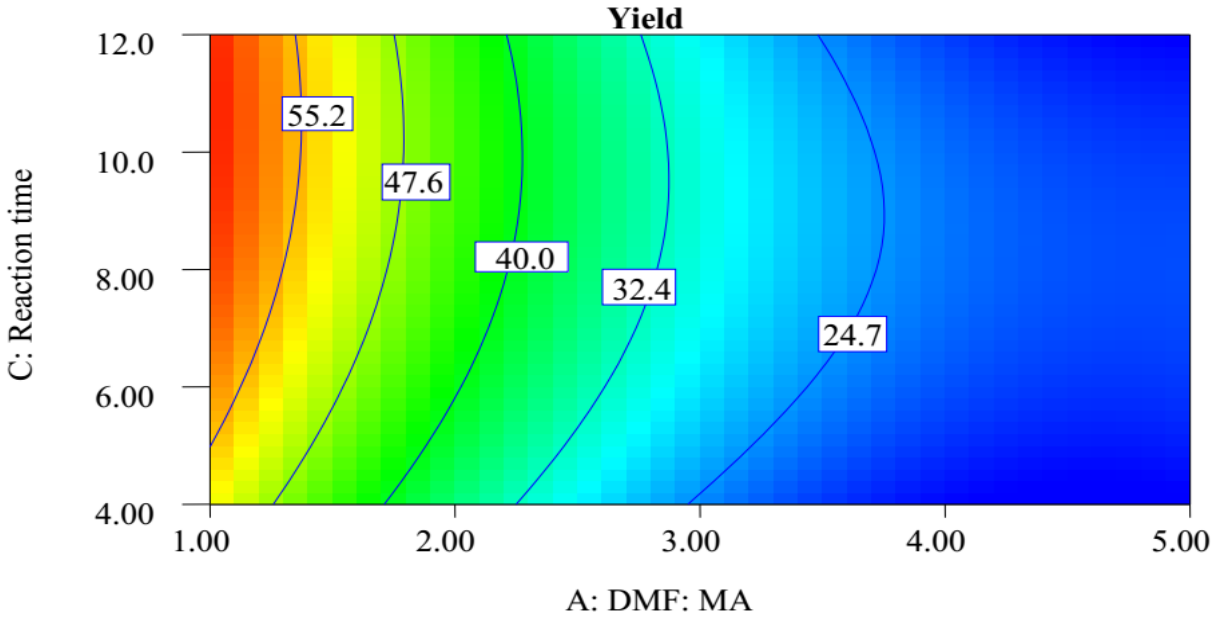

b)

Figure 4-16: a) Contour plot for the effects of reactant molar ratio and reaction time on the conversion of DMF, and; b) Contour plot for the effects of reactant molar ratio and reaction time on the yield of dimethyl benzoic acid respectively, at 0.3 mole of catalyst.

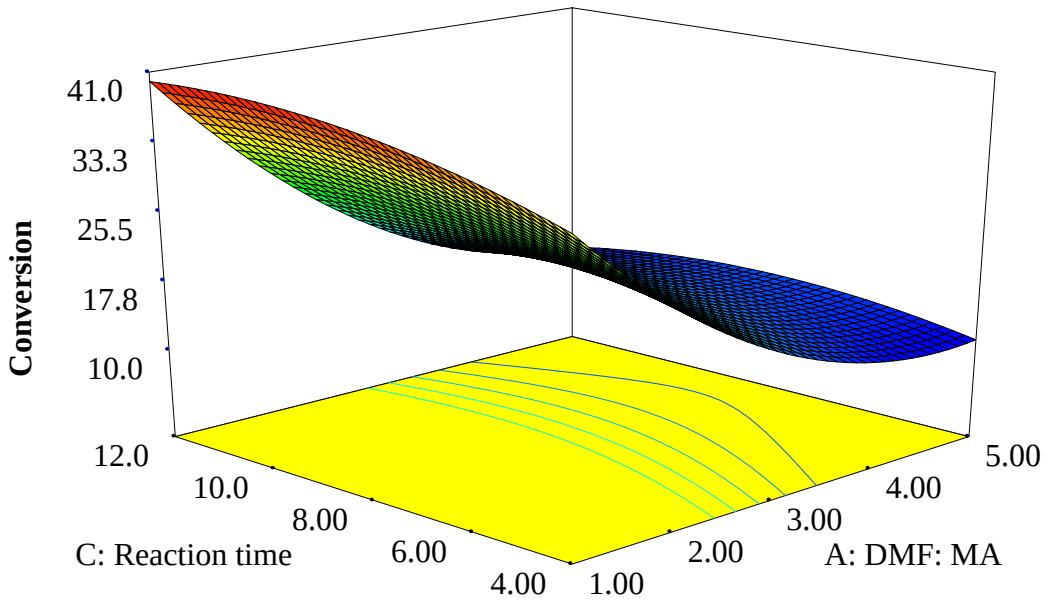

a)

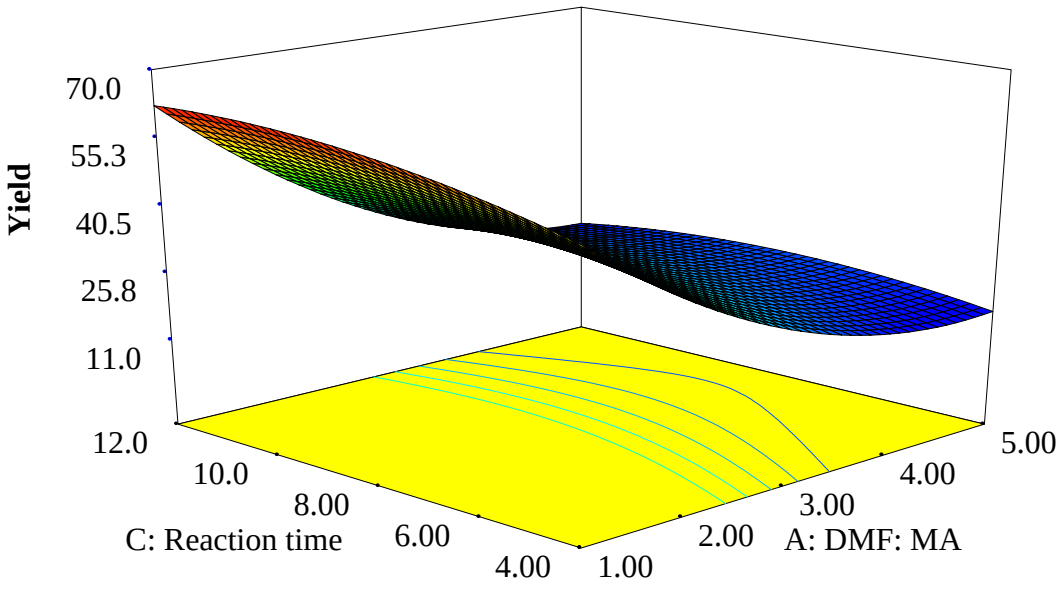

b)

Figure 4-17: a) Response surface plot for the effects of reactant molar ratio and reaction time on the conversion of DMF, and; b) Response surface plot for the effects of reactant molar ratio and reaction time on the yield of dimethyl benzoic acid respectively, at 0.3 mol of catalyst.

The resulting plots of figures 4.15, 4.16 and 4.17 (i.e. plots in terms of interaction, contour and response surfaces, respectively), shows how the molar ratio of the reactants and the reaction time can affects the conversion and the yield of the process at constant load of catalyst (i.e. at the center point). When we see the interaction effects of the two variables figure 4.15 a and b, at the lower level of molar ratios of reactants and higher level of reaction time, high amount of conversion and yield was obtained, and also, at the higher level of the molar ratio and reaction time both the conversion and the yield was slowly decreased. From the plots, the maximum amount of conversion and yield was obtained at 8 hr reaction time and the reactant molar ratio equal to one, which are 41.33 and 64.57%, respectively, due to these resolutions, both the factors has a strong relationship with the conversion and the yield. Therefore, the decrement in the conversion and yield as increment in time may happen due to the limited amount of catalyst used in the reaction and limitation of the reagent (i.e. the dienophile) that was utilized to take place the reaction, and may happen due to formation of by-products such as leovinoic acid, formic acid,

toluene, benzene etc. In addition to this, as the cooking time is increased, it leads to catalyst deactivation, that is the way to decrease the responses as increasing time.

The contour plots showing the predicted responses of DMF conversion and yield of dimethyl benzoic acid as a function of the molar ratio of the reactants and the reaction time were shown in the figures 4.16 a and b. As the molar ratio of reactants increased at lower levels of reaction time, and as the reaction time increases at lower levels of molar ratio, both the conversion of the reactant and the yield of the intermediate product deceased and increased respectively, this implies, the factors gives a positive effect on the corresponding responses.

The response surface plots as shown in the figure 4.17 a and b was obtained from the effects of the molar ratio of the reactant and reaction time in the process, and it gives looks like a conical shape with interaction at the center of the plane. Hence, these plots are exactly represented the effects of the given parameters on the required response as defined previously in the interaction and contour plots, and there were well defined the optimum operating conditions which give the maximum amount of responses. As shown in the above figures 4.17 a and b, as the molar ratio of reactants increased at lower levels of reaction time and as time increases at lower levels of molar ratios of reactants all the responses can slowly decrease and increased respectively, and at the optimum values of the molar ratio of reactants which is equal to one and reaction time of 8hr, 41.33% conversion and 64.57% yield was obtained.

4.3.6. Effect of catalyst loading and reaction time on the conversion of DMF and yield of dimethyl benzoic acid

In the above two interpretations such as the effects of the molar ratio of the reactant and catalyst loading as well as the effects of molar ratio and reaction time on the conversion of the main reactant and the yield of the intermediate product was investigated in form of interaction, contour and response surface plots. In this, the interaction of catalyst loading and reaction time is also another factor which affects the responses (i.e. both the conversion and the yield) and their effects are represented as shown in the following figures 4.18 up to 4.20 in the interaction, contour and response surface plots respectively.

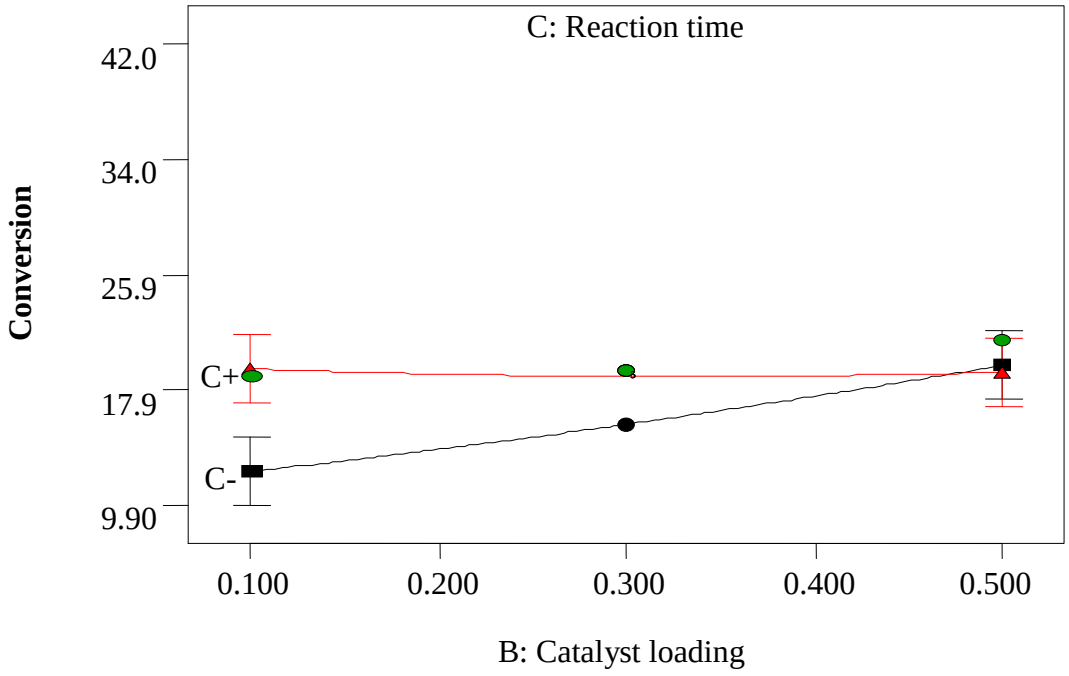

a)

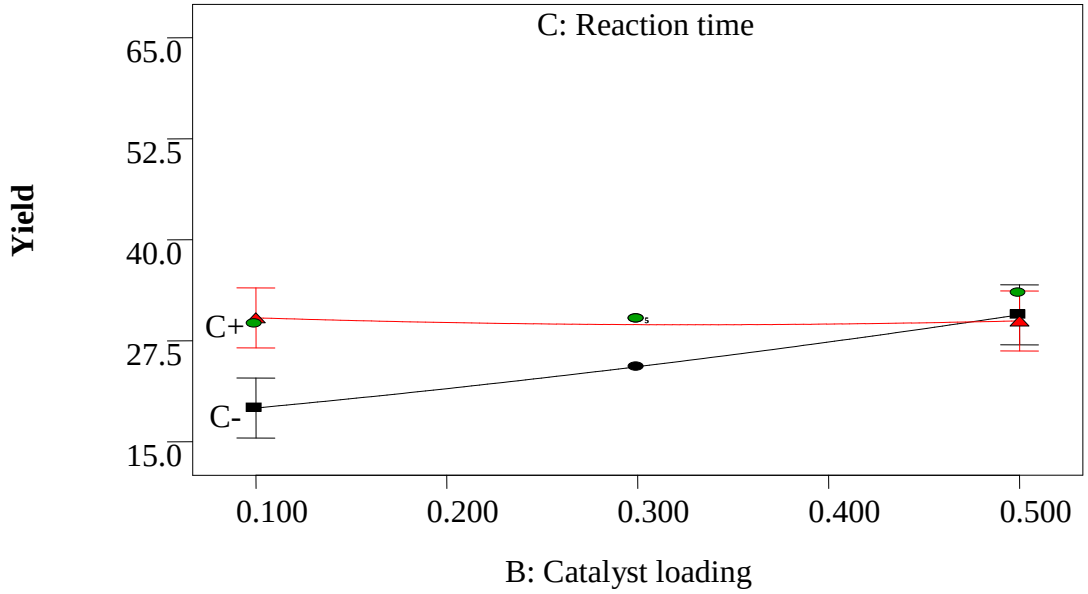

b)

Figure 4-18: a) Interaction effects of reaction time and catalyst loading on the conversion of DMF, and; b) Interaction effects of reaction time and catalyst loading on the yield of dimethyl benzoic acid respectively, at 3 mole/mole ratios of reactants.

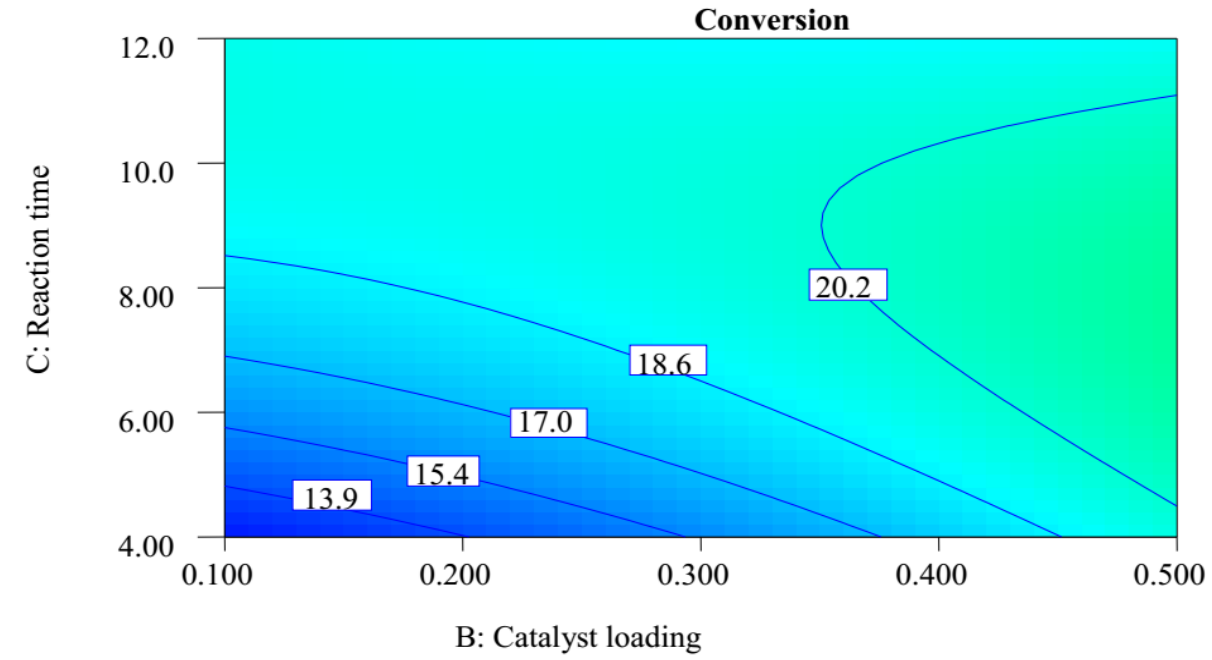

a)

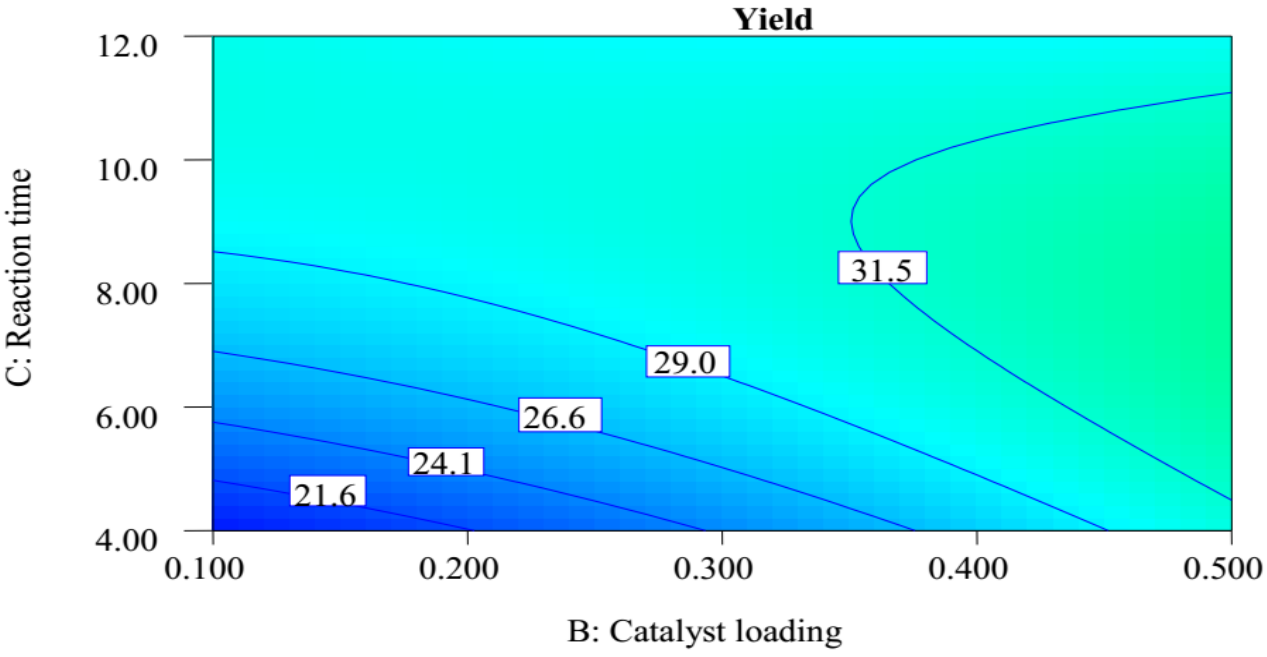

b)

Figure 4-19: a) Contour plot for the effects of reaction time and catalyst loading on the conversion of DMF, and; b) Contour plot for the effects of reaction time and catalyst loading on the yield of dimethyl benzoic acid respectively, at 3 mole/mole ratios of reactants.

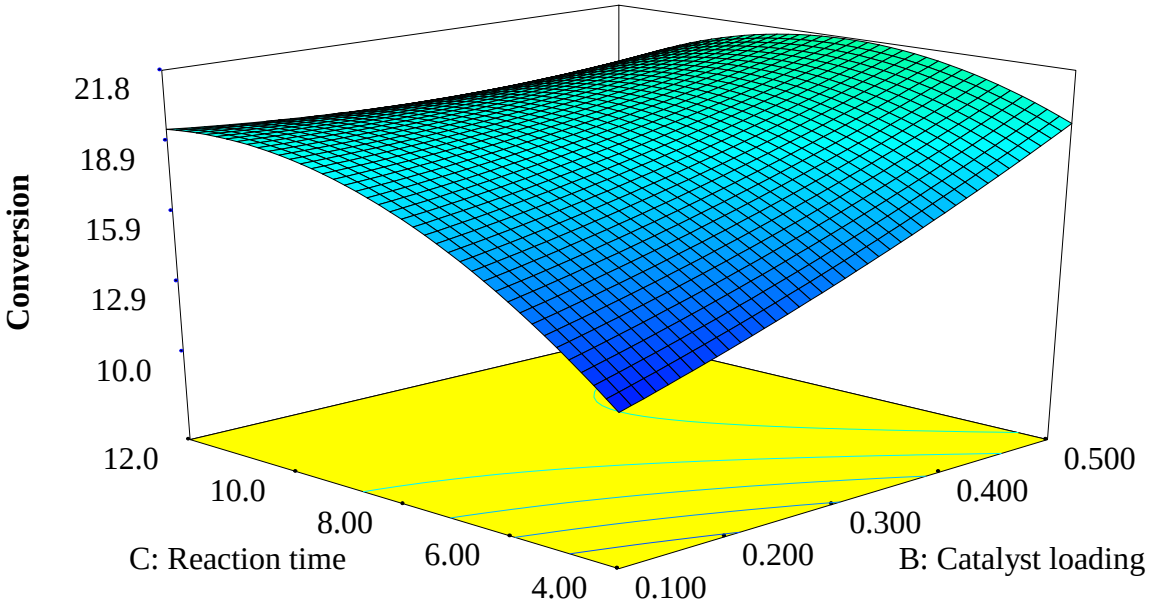

a)

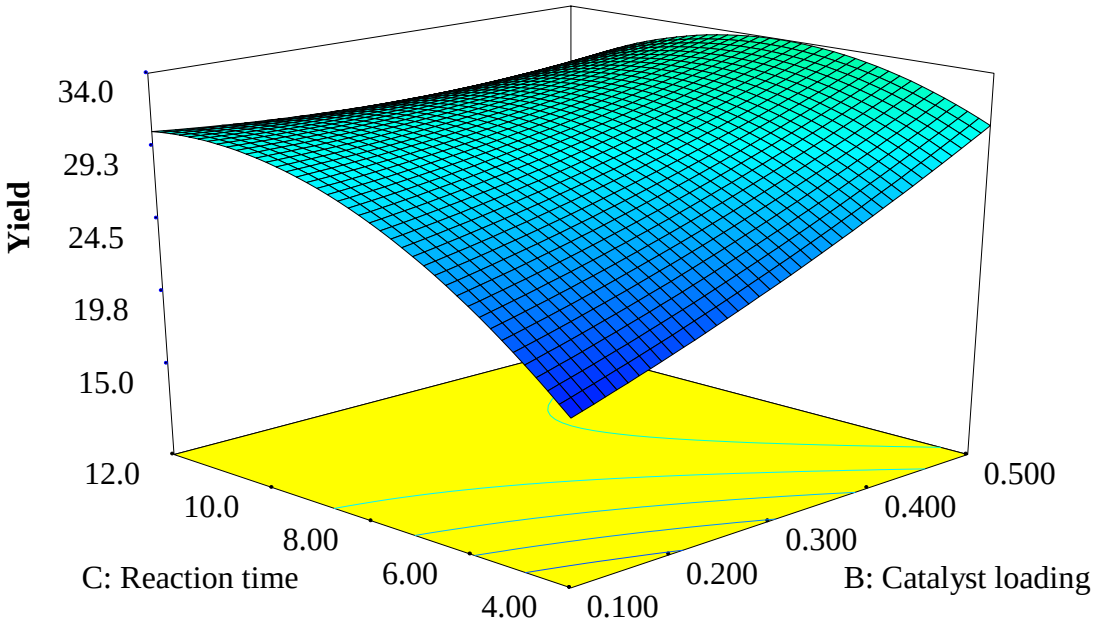

b)

Figure 4-20: a) Response surface plot for the effects of catalyst loading and reaction time on the conversion of DMF, and; b) Response surface plot for the effects of catalyst loading and reaction time on the yield of dimethyl benzoic acid respectively, at 3 mole/mole ratios of reactants.

From the resulting plots of figures 4.18 up to 4.20, shows the effect of catalyst loading and reaction time on the conversion of the main reactant and the yield of the intermediate product in the form of interaction, contour and response surface plots. The interaction effects of catalyst loading and reaction time on the conversion and yield were as shown in figures 4.18 a and b respectively, when the molar ratio of the reactants were constant (i.e. at the center point). In this plot, when the level of the catalyst loading was increased at a higher level of reaction time the conversion as well as the yield was increased slowly to some extent and finally slowly decreased, but the maximum amount of conversion and yield was obtained at a high level of catalyst loading and medium level of reaction time. Hence, both the catalyst loading and the reaction time have strong relationship for the conversion of the reactant and the yield of the intermediate product.

The contour plot in figures 4.19 a and b shows the predicted responses of the reactant conversion and yield of the intermediate product. As the catalyst loading increases at higher levels of reaction time, both the conversion and the yield were linearly increased until the reaction time was equal to 8hr, then after, as the time was increased from 8 to 12 hrs, the conversion and yield were decreased from 21.4 to 19.35 and 33.43 to 30.23% respectively. From this relation all the factors at high and low level give a positive effect on the reactant conversion as well as the yield of the product.

The response surface figures 4.20 a and b was obtained from the effects of the catalyst loading and the reaction time of the process. As the catalyst loading increases at high levels of the reaction time, higher amount of conversion and product yield was obtained, and at lower levels of reaction time with increasing loads of catalyst, both the conversion and the yield was rapidly increased until 8hr reaction time, and finally looks like triangular shape was formed. As increasing reaction time at high level of catalyst loading the decrement in the conversion and yield may happen due to the unstable nature of the catalyst and limited amount of the reagent that was utilized in the chemical reaction, because the reagents are present in small amount as compared to the main reactant (i.e. DMF). And also, as increasing reaction time at a lower level of catalyst, the decrement in the response happens due to the fact that the catalyst activation decreases as increasing the cooking formation (cooking time).

4.4. Optimization of DMF Conversion and Dimethyl Benzoic Acid Yield

Optimization is a process/method of determining the optimum values of parameters that gives maximum productivity or minimum cost depending on the objective function, and the parameters are called design variables. In the Diels-Alder cycloaddition reaction, the parameters such as the molar ratio of reactants, reaction time and catalyst loads are the design variables to perform the objective function (i.e. Maximization of both the reactant conversion and production yield of the intermediate product at the optimum values of the required parameters such as the amount of the reactant molar ratio, catalyst loading and reaction time). The values of the design variables as well as their corresponding responses (ranges in table 4.12) are selected from table 4.2.

Table 4-12: Optimization criteria for determination of maximum conversion and yield

Constraints			
Parameters	Goal	Lower limit	Upper limit
Molar ratio of reactants (mole ratio)	In the range	1	5
Catalyst loading (mole)	In the range	0.1	0.5
Reaction time (hrs)	In the range	4	12
Conversion of DMF (%)	Maximize	11.4	41.39
Yield of dimethyl benzoic acid (%)	Maximize	17.8	64.6
Objective functions			
Maximization of DMF conversion based on the actual equation 4.2			
Maximization of dimethyl benzoic acid yield based on the actual equation 4.4			

The optimum possible solutions of the design variables (i.e. reactant molar ratio, catalyst loading and reaction time) and the corresponding responses (i.e. the conversion and yield) are presented as shown in the following tables 4.13 and 4.14, and also their corresponding plots are presented as shown in the figures 4.21 up to 4.26.

Table 4-13: Optimum possible solutions for the Diels-Alder cycloaddition process using Design expert®7 software

Run №	DMF: MA	Catalyst loading	Reaction time	Conversion	Yield	Desirability
1	1.03	0.48	6.46	41.38	64.65	1 (Selected)
2	1.05	0.46	8.67	41.70	65.15	1.00
3	1.02	0.44	10.7	41.77	65.25	1.00
4	1.00	0.48	6.98	42.10	65.78	1.00
5	1.09	0.48	8.47	41.65	65.06	1.00
6	1.01	0.40	9.01	41.39	64.67	1.00
7	1.00	0.39	10.3	41.34	64.58	1.00
8	1.01	0.42	10.5	41.68	65.11	1.00
9	1.00	0.42	11.3	41.54	64.89	1.00
10	1.00	0.42	8.23	41.45	64.75	1.00
11	1.01	0.43	9.58	41.99	65.59	1.00
12	1.03	0.47	11.8	41.50	64.83	1.00
13	1.02	0.43	9.43	41.67	65.10	1.00
14	1.02	0.44	9.07	42.01	65.63	1.00
15	1.01	0.45	10.1	42.15	65.85	1.00
16	1.03	0.48	7.12	41.87	65.40	1.00
17	1.00	0.48	10.2	42.83	66.90	1.00
18	1.01	0.46	11.5	41.91	65.47	1.00
19	1.03	0.48	11.9	41.65	65.06	1.00
20	1.03	0.45	9.05	41.93	65.50	1.00
21	1.03	0.49	7.38	42.21	65.95	1.00
22	1.06	0.46	8.09	41.46	64.76	1.00
23	1.07	0.46	10.2	41.49	64.82	1.00
24	1.00	0.50	5.35	41.29	64.50	1.00
25	1.00	0.35	11.4	40.67	63.54	0.98
26	1.00	0.34	12.0	40.37	63.06	0.97
27	1.00	0.16	12.0	39.00	60.92	0.92
28	1.00	0.10	12.0	38.67	60.41	0.91
29	1.00	0.10	10.6	38.21	59.69	0.90
30	1.16	0.10	12.0	36.61	57.20	0.84

Table 4-14: Optimization design summary using design expert®7 software

Factor	Name	Level	Low Level	High Level	Coding
A	DMF:MA	1.03	1	5	Actual
B	Catalyst loading	0.48	0.1	0.5	Actual
C	Reaction time	6.46	4	12	Actual
Response	**Prediction**	**SE Mean**	**95% CI low**	**95% CI high**	**SE Pred**
Conversion	41.38	1.31	38.37	44.39	2.16
Yield	64.65	2.04	59.94	69.35	3.38

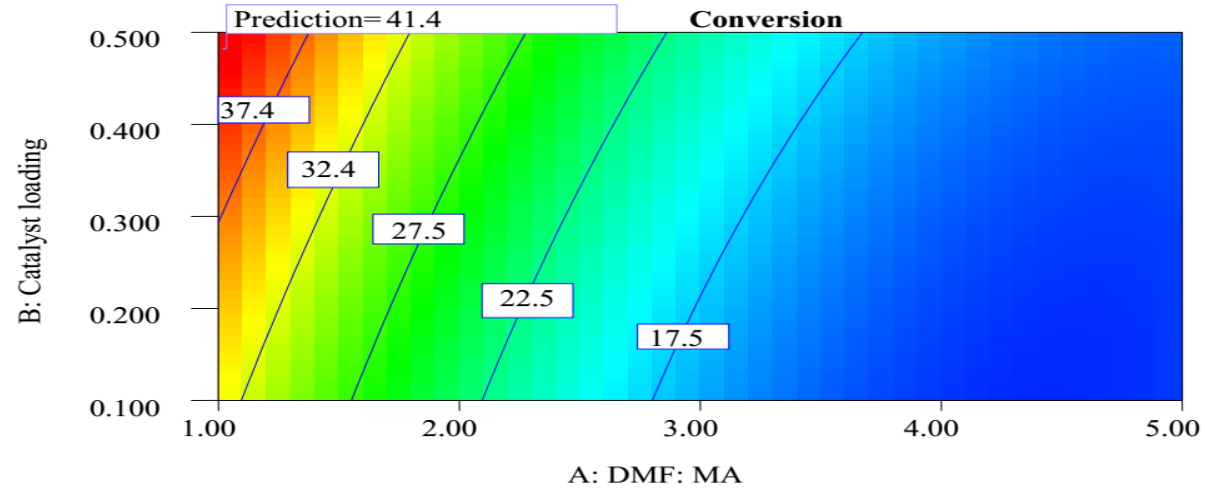

a)

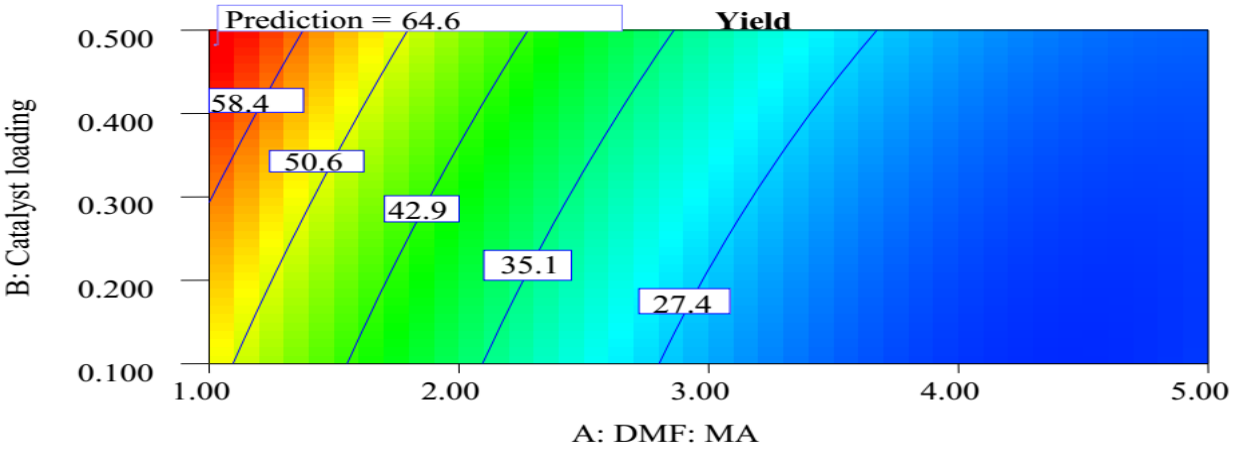

b)

Figure 4-21: a) Contour plot for the effects of reactant molar ratio and catalyst loading on the conversion of DMF, and; b) Contour plot for the effects of reactant molar ratio and catalyst loading on the yield of dimethyl benzoic acid respectively, at 6.46 hr reaction time.

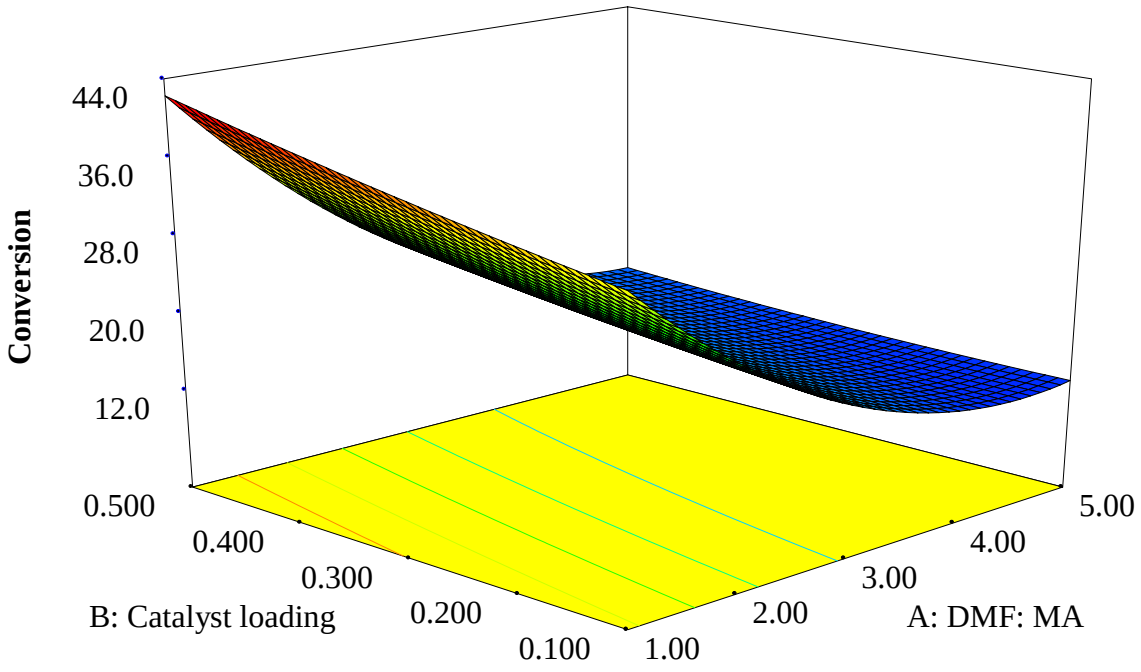

a)

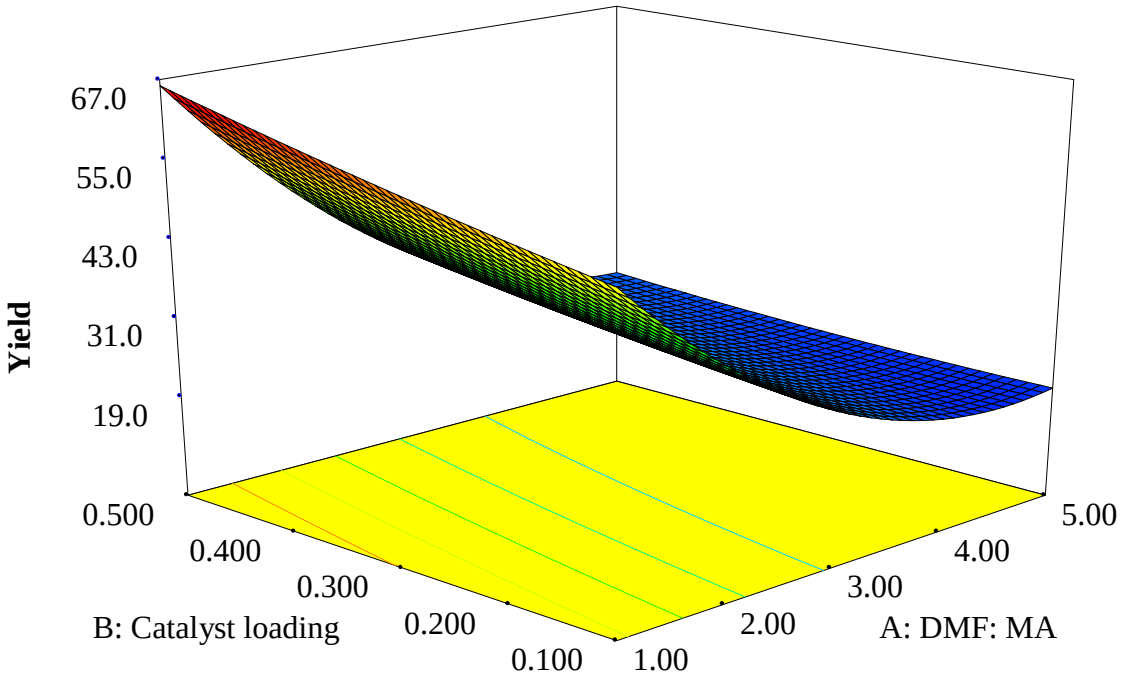

b)

Figure 4-22: a) Response surface plot for the effects of reactant molar ratio and catalyst loading on the conversion of DMF, and; b) Response surface plot for the effects of reactant molar ratio and catalyst loading on the yield of dimethyl benzoic acid respectively, at 6.46 hr reaction time.

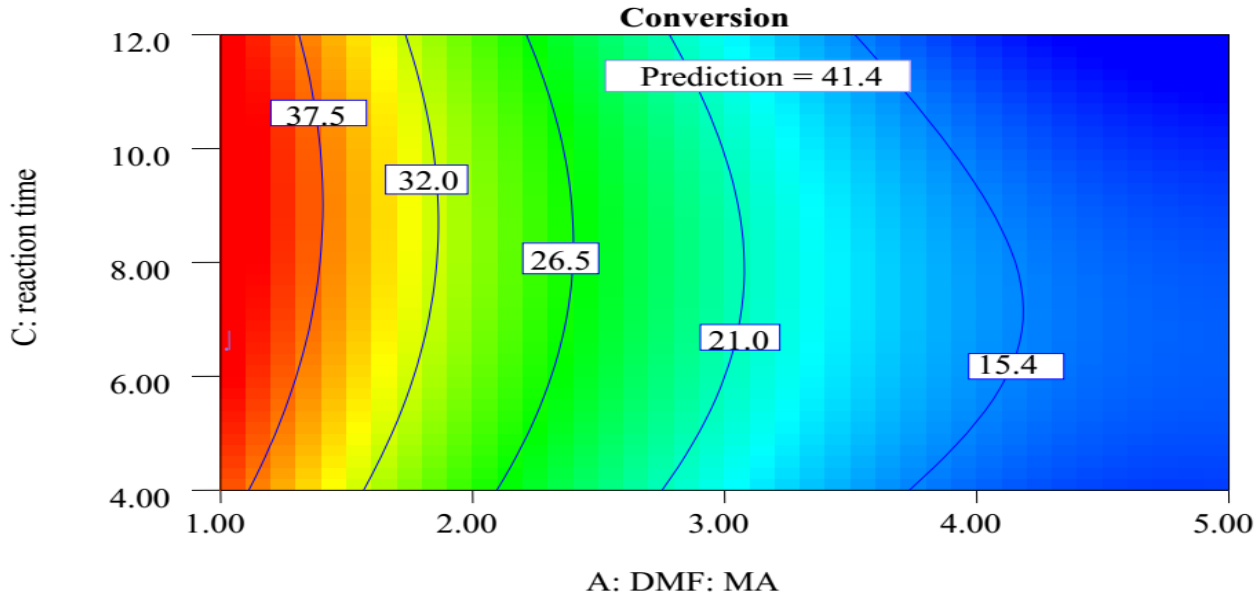

a)

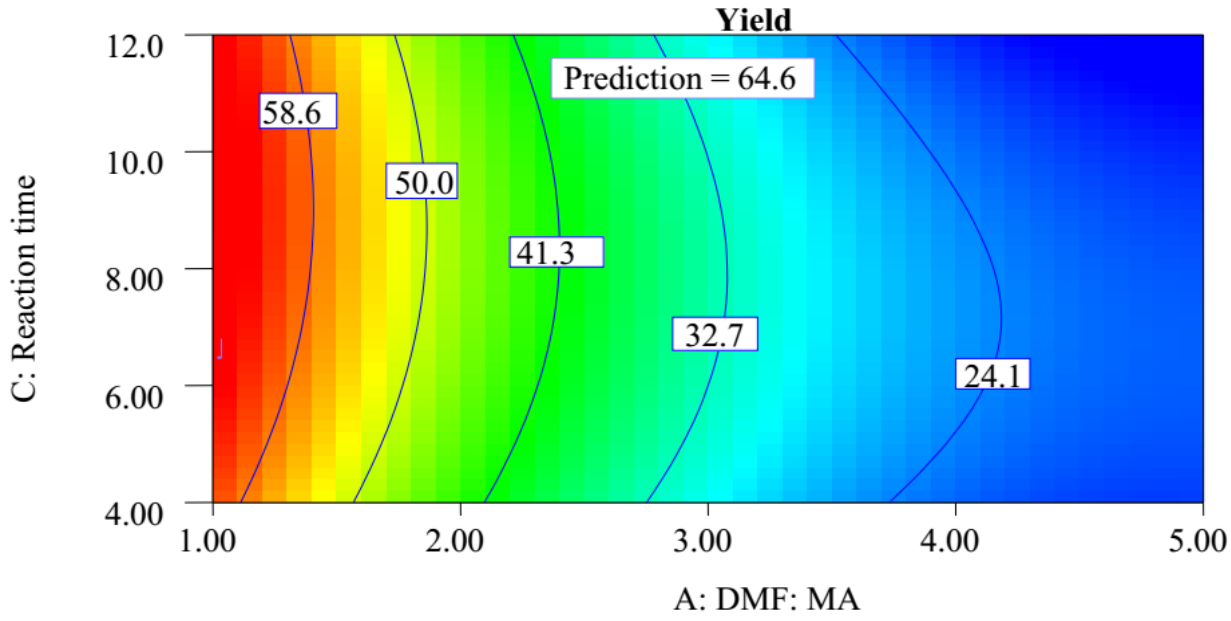

b)

Figure 4-23: a) Contour plot for the effects of reactant molar ratio and reaction time on the conversion of DMF, and; b) Contour plot for the effects of reactant molar ratio and reaction time on the yield of dimethyl benzoic acid respectively, at 0.482 mole of catalyst loading.

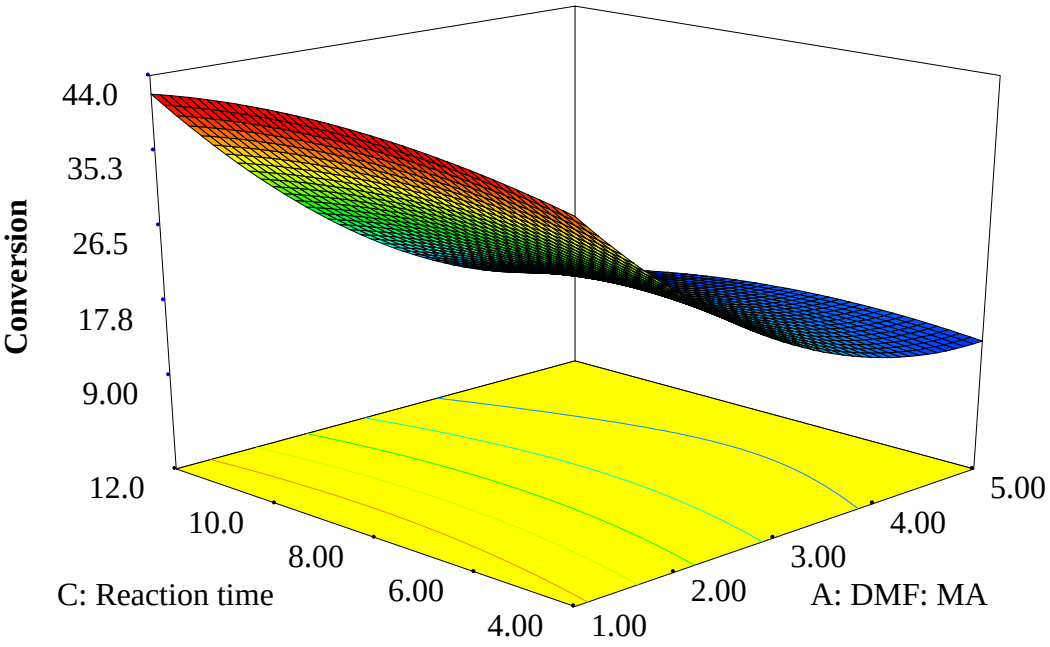

a)

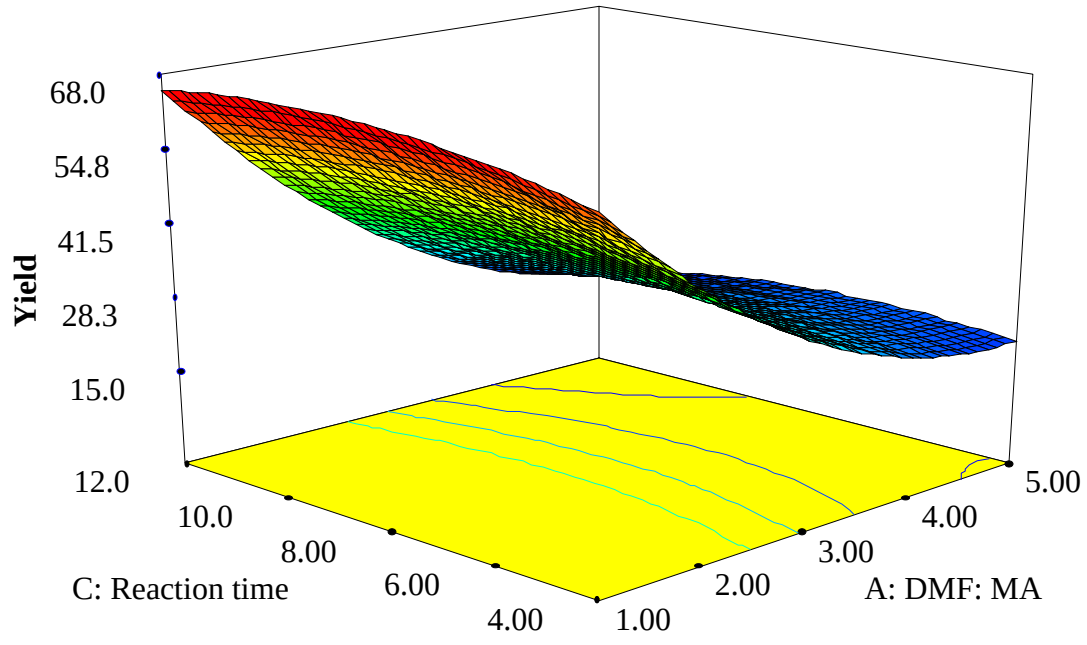

b)

Figure 4-24: a) Response surface plot for the effects of reactant molar ratio and reaction time on the conversion of DMF, and; b) Response surface plot for the effects of reactant molar ratio and reaction time on the yield of dimethyl benzoic acid respectively, at 0.482 mol of catalyst loading.

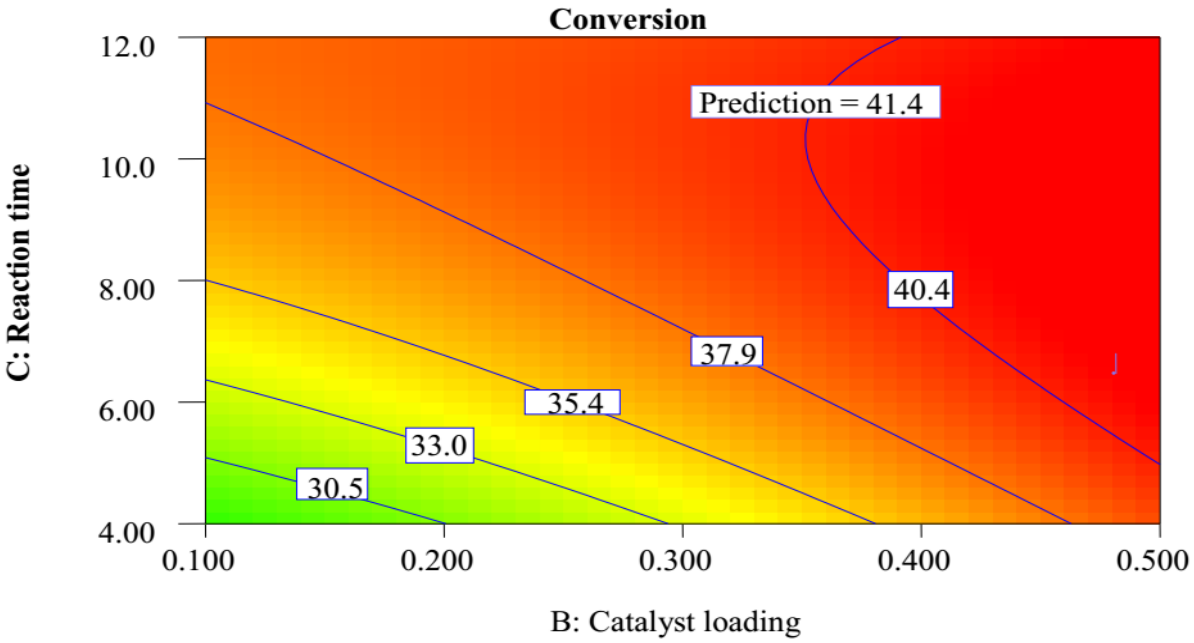

a)

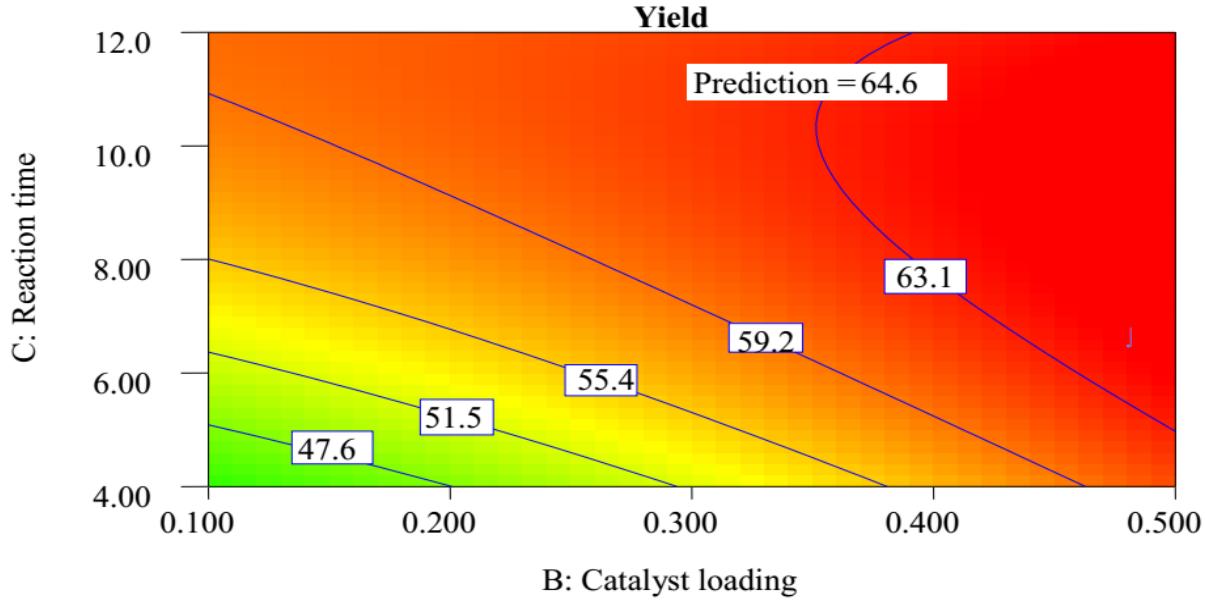

b)

Figure 4-25: a) Contour plot for the effects of catalyst loading and reaction time on the conversion of DMF, and; b) Contour plot for the effects of catalyst loading and reaction time on the yield of dimethyl benzoic acid respectively, at 1.03 mole/mole ratios of reactants.

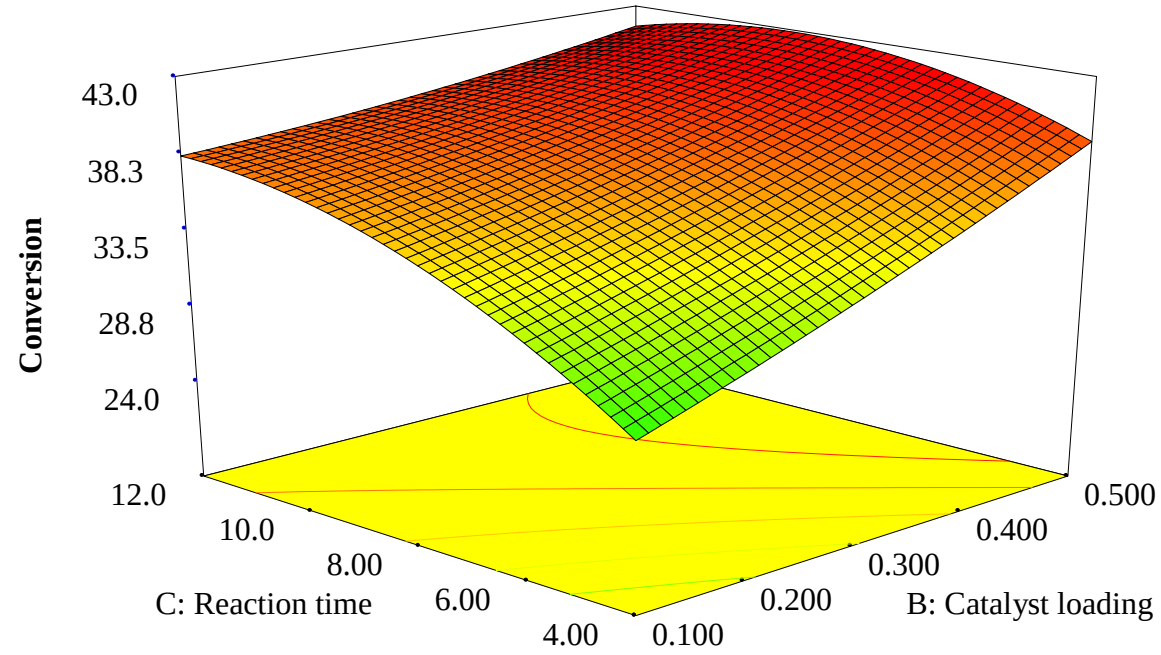

a)

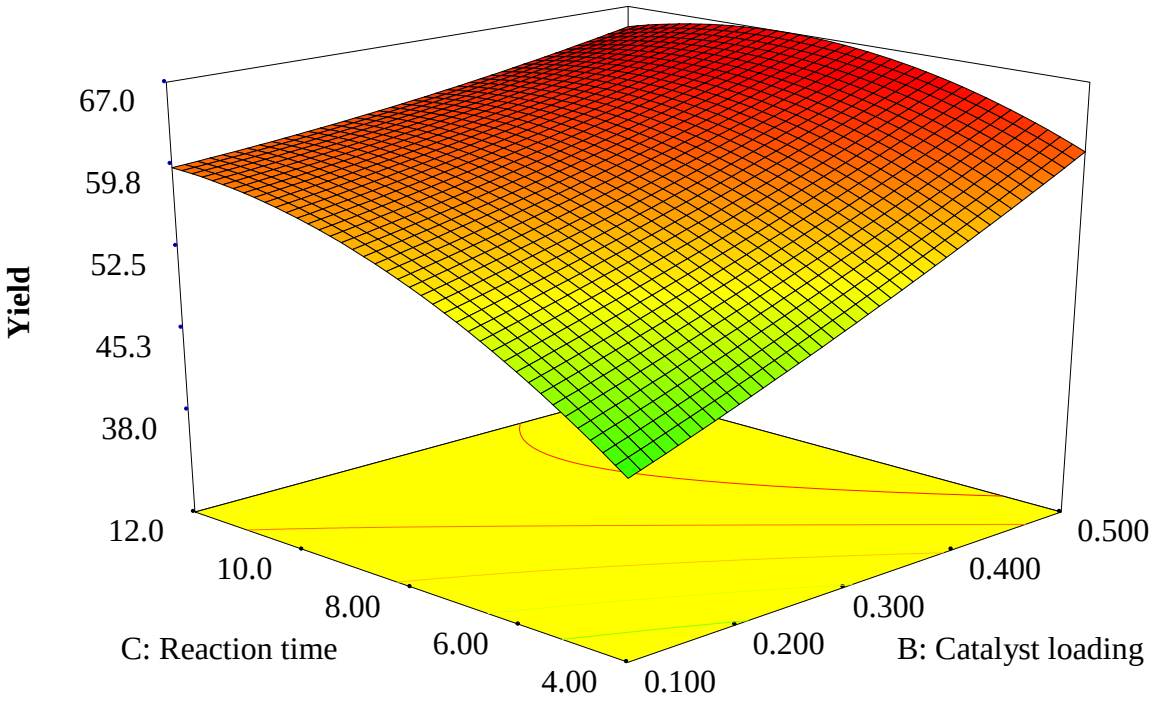

b)

Figure 4-26: a) Response surface plot for the effects of catalyst loading and reaction time on the conversion of DMF, and; b) Response surface plot for the effects of catalyst loading and reaction time on the yield of dimethyl benzoic acid respectively, at 1.03 mole/mole ratio of reactants.

From the overall optimization process in the Diels-Alder cycloaddition reaction as shown in table 4.13 and representative figures starting from 4.21-4.26, the optimum values of the parameters which gives the maximum dimethyl furan conversion and dimethyl benzoic acid yield was obtained when the molar ratio of the reactants (i.e. DMF: MA = 1.03), 0.48 moles of catalyst loading and at 6.46 hour reaction time. As the result, under these conditions, the model predicted values of 41.38% conversion of DMF and 64.64% yield of dimethyl benzoic acid was obtained with a desirability value of 1. According to *Wijaya et al.,* (*2015*), 91% conversion of DMF and 86% of dimethyl benzoic acid have been reported using $Sc(OTf)_3$ catalyst at 12 hrs. But in this study, 41.4% conversion of DMF and 64.4% yield of dimethyl benzoic acid were obtained using $AlCl_3$ as a catalyst at 6.46 hrs; this variation may happen due to personal error and measurement error. In addition to this, the variation may happen due to difference in character of the catalysts such as reactivity, selectivity as well stability natures, which means that, since catalysts are substances, in which they facilitates the rate of the chemical reaction based on the nature of their reactivity and stability. Therefore, in this study, metal halides are more reactive than of the transition metal catalysts such as $Sc(OTf)_3$, that was utilized by the other researcher, since it give moderate amount of yield as well as high conversion within a short period of time, but it is more less stable than of the transition metal catalysts that was utilized by the other researcher.

4.5. Model Validation

In this study, model validation was carried out to check the calculated values of reactant conversion and product yields that was obtained in table 4.2 and values after optimization using the Design expert software (this software evaluates to ensure that it complies with the requirements). According to the response surface (i.e. central composite design) result using design expert®7 software, the experiment was conducted in the Diels-Alder cycloaddition reaction to investigate the effects of reactant molar ratio, catalyst loading and reaction time on the conversion of DMF and the yield of dimethyl benzoic acid next to Para-xylene by a series of steps such as dehydration and aromatization of dimethyl benzoic acid. In this, the experiment was conducted to maximize the conversion of DMF and the yield of dimethyl benzoic acid using the numerical optimization response optimizer in the design expert®7 software. From the above table 4.13 or 4.14 the analysis shows that, the conversion of DMF and dimethyl benzoic acid yield of average predicted values are 41.4 and 64.6% respectively at the optimal values of test

variables (i.e. DMF: MA = 1.03, 0.482 mole of catalyst and 6.46 hrs of reaction time). Therefore, the model was considered to be accurate and reliable for predicting the yield of the intermediate product such as dimethyl benzoic acid next to Para-xylene, and, will be expected that, this product will give a higher yield to the final product.

4.6. The effect of acid concentration on the dehydration of dimethyl benzoic acid to PX

The dehydration reaction of dimethyl benzoic acid to Para-xylene was conducted at 115 ℃ (i.e. above the boiling points of water, formic acid, toluene and benzene, which are the by-products) for 1-3 hours of reaction time in the presence of 2-6 M acid concentration (i.e. 98% H_2SO_4) through a continues string at 400 rpm. In this study, the effects of acid concentration on the conversion of dimethyl benzoic acid and yield of dimethyl benzene (Para-xylene) was investigated, and the effects were represented using the following table 4.17, in this table, the values of dimethyl benzoic acid conversion and the yield of dimethyl benzene was obtained using equations 3.15 and 3.16 respectively after determination of the unknown concentration of the sample using equation 3.14). And the effect of the acid concentration was represented graphically as shown below in figures 4.27 and 4.28.

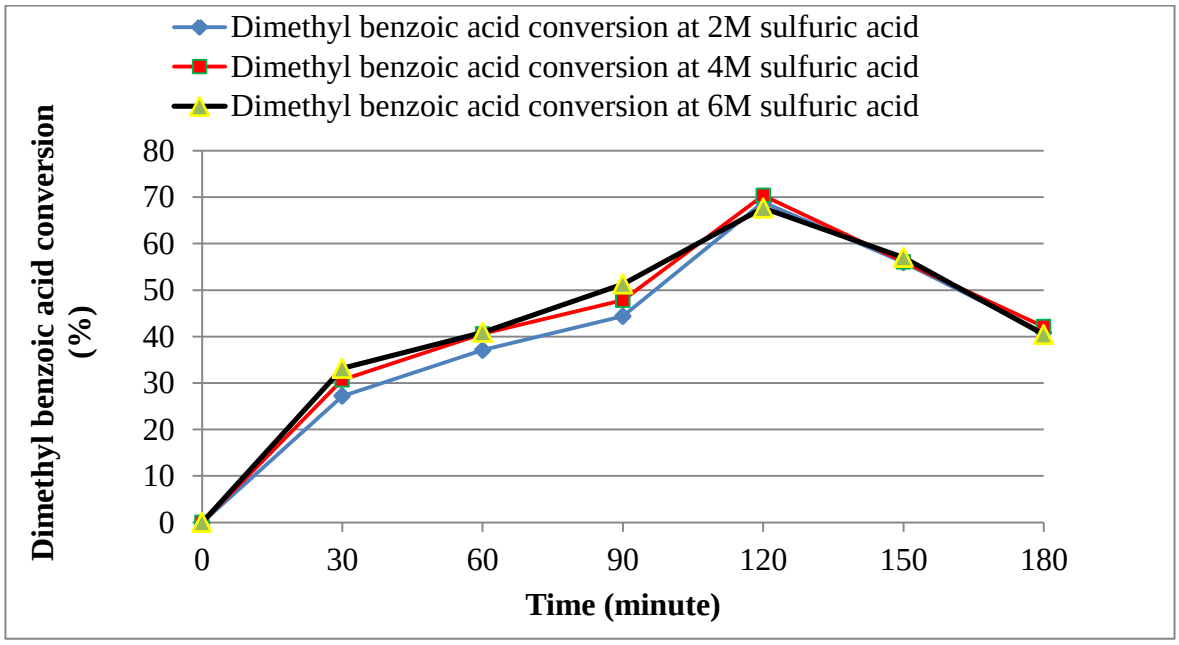

Figure 4-27: The effect of H_2SO_4 concentration on dimethyl benzoic acid conversion in the dehydration of dimethyl benzoic acid to PX (reaction conditions: 50 ml of dimethyl benzoic acid in 2-6 M H_2SO_4, at 115 ℃, 1 to 3 hrs.

Table 4-15: The effect of $H_2 SO_4$ on dimethyl benzoic acid conversion and PX yields, in the dimethyl benzoic acid dehydration to PX (reaction conditions: 50 ml of dimethyl benzoic acid in 2-6 M, 98% $H_2 SO_4$, at 115 ℃, 1 to 3 hrs.)

Run №	Acid Concentration (98%, H_2SO_4)	Time (minutes)	Absorbance @ 192 nm	Conversion of dimethyl benzoic acid (%)	Yield of dimethyl benzene (%)
1	2	30	0.21	27.20	19.20
2	4	30	0.24	30.66	21.64
3	6	30	0.26	33.15	23.40
4	2	60	0.28	37.08	26.17
5	4	60	0.31	40.58	28.65
6	6	60	0.31	40.91	28.87
7	2	90	0.34	44.37	31.32
8	4	90	0.36	47.83	33.76
9	6	90	0.39	51.29	36.21
10	2	120	0.52	68.88	48.62
11	4	120	0.53	70.36	49.66
12	6	120	0.51	67.66	47.76
13	2	150	0.42	55.94	39.49
14	4	150	0.43	56.09	39.59
15	6	150	0.43	57.00	40.23
16	2	180	0.31	40.85	28.83
17	4	180	0.32	42.14	29.74
18	6	180	0.31	40.44	28.54

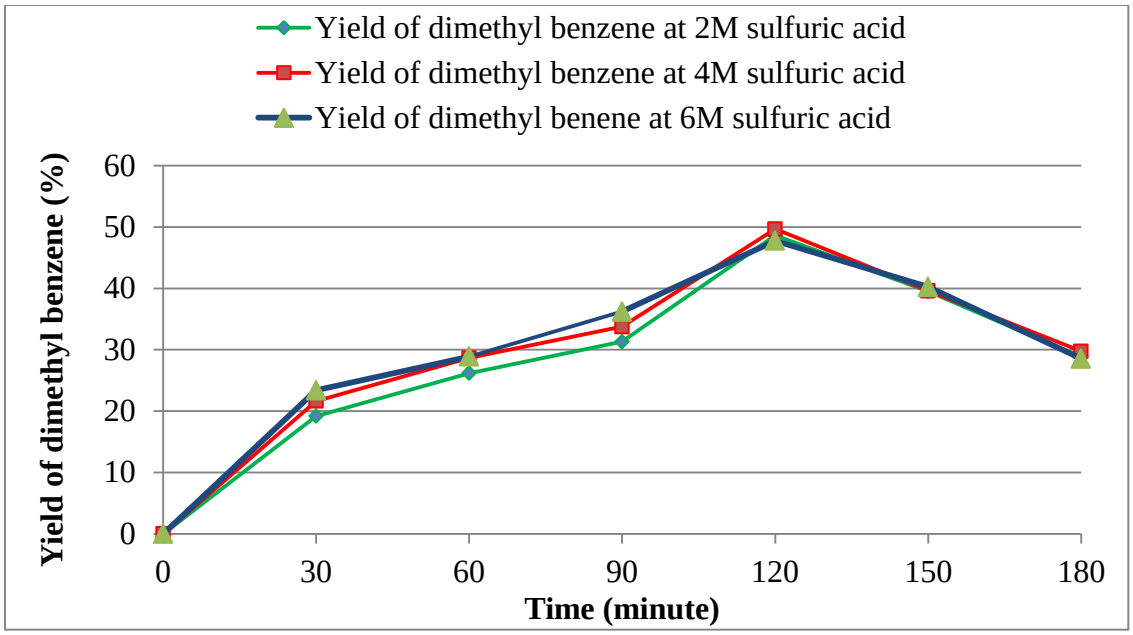

Figure 4-28: The effect of H_2SO_4 concentration on the yields of PX in the dimethyl benzoic acid dehydration to PX (reaction conditions: 50 ml of dimethyl benzoic acid in 2-6 M H_2SO_4, at 115 ℃, 1 to 3 hrs).

From the above figures 4.27 and 4.28, the dehydration or decomposition of dimethyl benzoic acid to Para-xylene was performed at 115 ℃. Initially, both the conversion of dimethyl benzoic acid and the Para-xylene yield was increased with increasing the acid concentration and reaction time, as the result, 70.36% conversion of dimethyl benzoic acid and 49.66% yield of Para-xylene were obtained at 120 minutes and 4M acid concentration. As the acid concentration and the reaction time was further increases, both the dimethyl benzoic acid conversion and Para-xylene yield was decreased. The lowering in the yield of the intermediate product may happen due to increasing formation rate of the by-products (i.e. at long reaction time, concurrently increased in the by-product formation rate led to lowering the rate formation of the intermediate products such as PX). Which means that, as the acid concentration was increased; the final product yield was decreased, demonstrating that the acid can promote for undesired product formation in the dehydration of organic compounds (*Pacheco et al., 2014*). From the previous studies of the Diels Alder cycloaddition reaction between the biomass derived DMF and maleic anhydride followed by dehydration of dimethyl benzoic acid to Para-xylene, 97% conversion of dimethyl benzoic acid and 91% yield of dimethyl benzene have been reported by (*Lin et al., 2013*). In this study, the lowering in the reactant conversion as well product yield may happen due to lowering

production of the dimethyl benzoic acid in the Diels-Alder cycloaddition reaction before dehydration, the reasons are as mention before may be due to personal error, measurement error as well as due to utilization of different catalyst from the previous researcher, which means that, since catalysts are substances, in which they can speed up the rate of the chemical reaction based on the nature of their reactivity and stability. Therefore, the catalyst (i.e. $Sc(OTf)_3$, the transition metal catalyst) that was utilized by the other researcher is more strongly stable, but it is less reactive than of metal halides such as $AlCl_3$, that was utilized in this study.

4.7. Characterization results of the intermediate products using FTIR

Infrared spectroscopy is an important and a crucial characterization technique used to understand easily the structure of matter at the molecular scale. In general, the chemical composition and the bonding arrangement of constituents in the homopolymer, copolymers, and polymeric materials can be obtained using IR spectroscopy.

During Para-xylene production from the biomass particularly sugarcane bagasse, a number of intermediate products was produced such as glucose, HMF, DMF, dimethyl benzoic acid and finally Para-xylene. And these intermediate products were characterized using FTIR to check the functional groups whether the intermediate products are formed in each step or not.

Glucoses have characteristic FTIR absorptions associated with the O-H, C-O and the C-H stretching vibrations. In this, the region 2900-3450 cm^{-1} with a very intense and broad band assigned to CH and OH vibration groups, while the region from 600-1500 cm^{-1} in which C-O and C-C groups vibration modes are present and the carbohydrates generally shows their characteristic bands. The bands at around 2880 and 2930 cm^{-1} were assigned as the symmetric stretching modes of the $–CH_2$ and$–CH_3$ groups, respectively (*Ibrahim et al., 2006*).

The HMF and DMF's (aldehydes), are characteristic FTIR absorptions associated with the –OH, C-H, C = C, and C = C–H stretching vibrations. When the stretching vibration region is between 3700-3000 cm^{-1}, it indicates the -OH functional group, between 1700-1500 cm^{-1}, it indicates the C=C and C=C–H of the furan ring, and also the stretching vibration between 1400-900 cm^{-1} indicates the C-C-H, C-O-H and O-C-H of the furan ring (*Esmaeili et al., 2017*).

Dimethyl benzoic acids (benzene carboxylic acids) have characteristic FTIR absorptions associated with the O-H, C-H, C=O and C = C stretching vibrations. Aromatic systems exhibits the C-H stretching vibrations in the region between 3100-3000 cm^{-1}, and the O-H group is

identified by the region between 2500-3300 cm^{-1}, the region between 1680-1750 cm^{-1} indicates the C=O group and the stretch vibration frequencies of C = C of the benzene nucleus is obtained around 1454-1506 $cm^{-1}$and absorption around 900-1100 cm^{-1} could be due to carbon-oxygen bound of the acid grouping. And also, the C-C stretching vibrations are observed to medium intensity sharp bands in the region 1300-1000 cm^{-1} (*Doncea et al., 2012).*

Dimethyl benzene's have characteristic FTIR absorptions associated with the C = C−C and the C−H stretching vibrations. Aromatic ring exhibits the C = C−C stretching vibrations in the region between 1615-1580 cm^{-1} and 1510-1450 cm^{-1}, while the C−H stretching vibration is observed around 3130-3070 cm^{-1}. Furthermore, the C-H of the aromatic in the plane bend and 1,4-disubstitution (Para position) was observed at region between 1225-950 cm^{-1} and 860-800 cm^{-1} respectively (*Coates, 2006*). This assures that the product obtained from sugarcane bagasse was glucose, HMF, DMF, dimethyl benzoic acid and finally the Para-xylene in each step of the production process due to the confirmation of these regions as shown below.

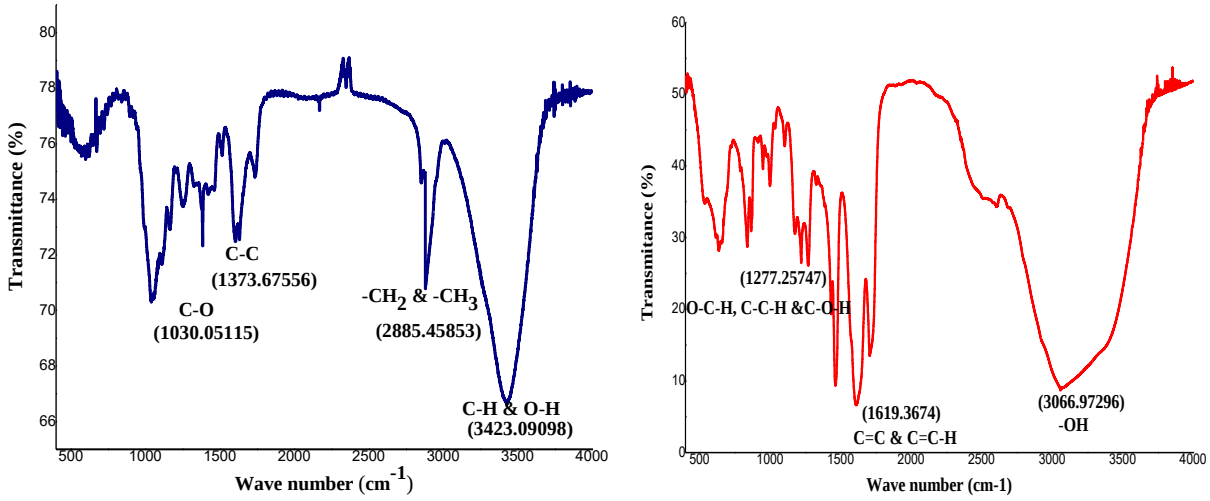

a) **b)**

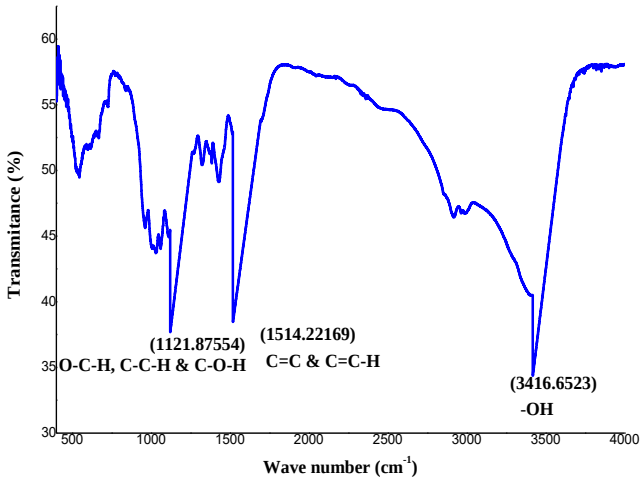

c)

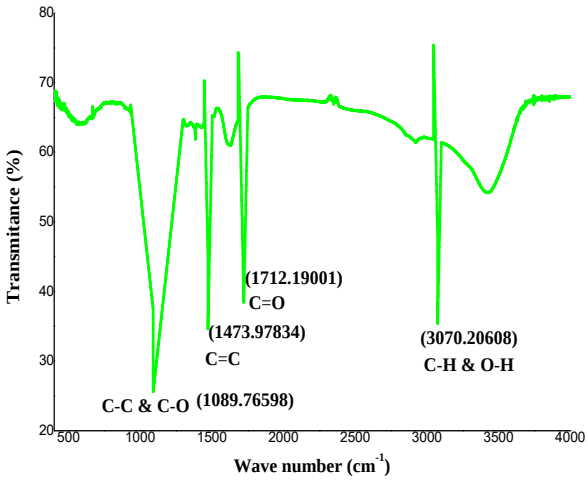

d)

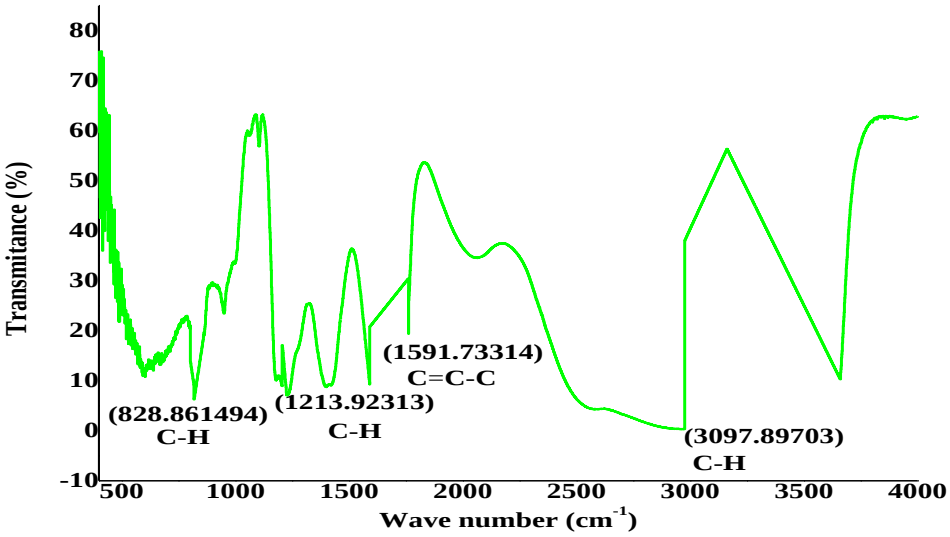

e)

Figure 4-29: FT-IR results of; a) glucose, b) HMF, c) DMF, d) dimethyl benzoic acid, and; e) Para-xylene respectively.

4.8. Gas chromatography-mass spectroscopy results of 1, 4-dimethyl benzene

The resulting sample was analyzed using GC-MS to identify the composition of components in the sample, and it identifies the atomic composition of components based on their relative volatility or boiling point. The mass spectral data were recorded with electron impact ionization at 70 eV. And the results were as follows:

Table 4-16: GC-MS result of the sample

Retention time (min)	Molecular Weight, m/e (g/mol)	Abundance (%)	Compound name
13.50	92.14	12.31	Toluene
18.95	106.17	30.88	P-xylene
22.35	106.17	12.85	O-xylene
25.30	120.20	35.13	n-propyl benzene
27.40	156.31	9.83	Methyldecane

From the above table 4-16, five organic compounds were identified based on their boiling point. And the name of the compounds are identified based on their molecular weight (i.e. m/e), where e is the charge detected during the experimental analysis with respect to time. From these results, dimethyl benzene is obtained at 18.95 minutes with its molecular weight (i.e. m/e = 106 g/mol). From these results, 30.88% of dimethyl benzene/Para-xylene was obtained. According to *Mohameed et al.,* (*2007*), 91% yield of dimethyl benzene/Para-xylene was reported without optimization using GC-MS. In this study the decrement may happens due to lack of proper purification techniques (e.g. personal error). So, in order to increase the selectivity of PX, it is better to use separation (purification) techniques that can separate the other components easily.

4.9. Thermodynamics of Diels-Alder cycloaddition reaction

The Diels-Alder reaction is one of the most notable and utilized cycloaddition organic chemistry. It was first discovered by Otto Diels and Kurt Alder in 1928. And the reaction is a [4 + 2] cycloaddition that proceeds through a concerted reaction. Diels–Alder cycloaddition of biomass-derived furanic compounds (e.g. dimethyl furan) with dienophile chemicals has significant potential for high yield chemical production of renewable aromatic chemicals such as xylene, benzene and toluene. Furanic compounds then undergo a symmetry-allowed [4 + 2] Diels–Alder cycloaddition reaction with the dienophile such as Maleic anhydride, Acrolein, ethylene, acrylic acid and others to form a six-membered cyclohexene ring in thermally reversible condition (*Thiyagarajan et al., 2016*). Generally, the reaction involves the addition of an alkene or alkyne to the 1, 4 positions of diene. And in this study, the reaction occurs by symmetry-allowed [4 + 2] Diels–Alder cycloaddition of DMF with Maleic anhydride and subsequent aromatization by

acid-catalyzed dehydration and decarboxylation processes. In this study, we are mostly interested in being able to predict the equilibrium and rate constants. These are always related to the change in the Gibbs free energy of the system, ΔG, which can be estimated from both quantum chemical and molecular dynamics simultaneously. For any chemical reaction can viewed as an equilibrium, in which the extent of conversion of the reactant into products is determined by the law of mass action. For example, for the generic reaction,

$$\mathrm{aA + bB} \underset{\mathrm{K_{-1}}}{\overset{\mathrm{K_1}}{\rightleftharpoons}} \mathrm{cC} \quad \ldots\ldots \quad (4.14)$$

When the reaction is at equilibrium, both the forward and backward rates of reaction are equal (i.e. $r_1 = r_{-1}$). Because, $r_1 = K_1\{A\}^a\{B\}^b$, and $r_{-1} = K_{-1}\{C\}^c$, it follows that

$$\mathrm{K} = \frac{\mathrm{K_1}}{\mathrm{K_{-1}}} = \frac{\{\mathrm{C}\}^\mathrm{c}}{\{\mathrm{A}\}^\mathrm{a}\{\mathrm{B}\}^\mathrm{b}} \quad \ldots\ldots \quad (4.15)$$

Where, [A], [B], and [C], refers to the molar concentration of the respective functional groups (i.e. the DMF, dienophile, the products respectively). When the reaction or other change of state occurs under constant temperature and pressure, the energy exchange between molecules and/or the environment is denoted by the change in Gibbs free energy (i.e. ΔG) and it is expressed as:

$$G = H - TS \quad \ldots\ldots \quad (4.16)$$

Where, H and S are the enthalpy (heat) and entropy of the reaction respectively. At equilibrium, ΔG = 0. And since it is a state function, the change in G is independent of the path between two particular states. Hence, The Gibbs free energy change at temperature T is expressed as,

$$\Delta G = \Delta H - T\,\Delta S \quad \ldots\ldots \quad (4.17)$$

In terms of standard states, when reactants and products at 1M concentrations (or 1 atmosphere pressure), the free energy change is expressed as,

$$\Delta G^0 = \Delta H^0 - T\Delta S^0 \quad \ldots\ldots \quad (4.18)$$

The relationship between the standard Gibbs free energy ΔG^0 *and* K comes from the statistical thermodynamic using the following equation:

$$\Delta G^O = -RT\, ln\, K_{eq} = -2.303\, RT\, log\, K_{eq} \quad \ldots\ldots \quad (4.19)$$

Where, R is the universal gas constant = 8.314 J/mol.K, and

T is the temperature in ^{O}K.

The standard free energy change refers to the change in energy between two systems in their standard states. To estimate the relative rates of these two reactions in the forward and the reverse reactions $(K_1/K_{-1})_f$ and $(K_{-1}/K_1)_r$. this requires the assumption that the entropy of activation (ΔS^0) of these processes is approximately equal.

From equation 4.16 the change in Gibbs free energy is the same as with the change in enthalpy of the reaction. This implies from equation 4.17 the equilibrium constant of the reaction can also possible to calculate using the following equation:

$$K = \frac{K_1}{K_{-1}} = exp(-\Delta G^0/RT) \quad \ldots \ldots \ldots \quad (4.20)$$

If K =1, reactants and products are in the same amount, $\Delta G^0 = 0$, implies that neither product, nor reactants are formed.

If K > 1, the equilibrium shifts to the right, $\Delta G^0 =$ negative and also the reaction is an exothermic and it is spontaneous, implies that products are favored.

If K < 1, the equilibrium shifts to the left, $\Delta G^0 =$ positive and also the reaction is an endothermic and it is non-spontaneous, implies that reactants are favored.

This study deals specifically with the Diels–Alder reaction to the thermo-reversible crosslinking of monomers or polymers incorporating furan (i.e. 2, 5-dimethyl furan) and Maleic anhydride (dienophile).

The choice of these particular systems stems from the fact that the furan/maleic anhydride Diels-Alder adduct displays a relatively low temperature of decoupling through its retro Diels-Alder reaction, which therefore opens the way to interesting applications such as recyclable networks, self-healing materials. In this study, the Diels Alder cycloaddition reaction is represented by the following chemical equation.

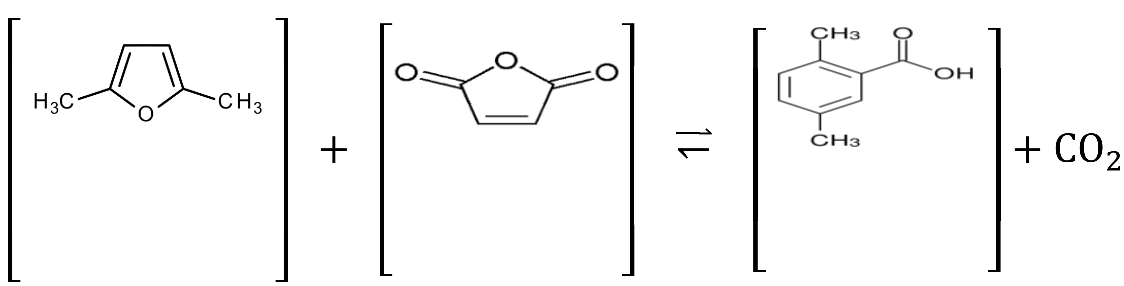

When the system is at equilibrium, the maximum amount of products is obtained at the optimum values of the parameters (i.e. the points in which maximum yield was obtained). Therefore, from the overall optimization process of the Diels Alder cycloaddition reaction the maximum yield of dimethyl benzoic acid as well maximum conversion of DMF was obtained when the reactant molar ratio (DMF: MA = 1.03), at 0.48 moles of catalyst loading and 6.46 hr reaction time. Implies that, the equilibrium concentrations of each component are at the points in which the maximum productivity was obtained. Then from the analysis of variance results the equilibrium concentrations are listed in the following table 4-17.

Table 4-17: Stochiometrically obtained equilibrium concentration of each component

Components	Amount of components at equilibrium (mole)	Equilibrium concentration (mole/liter)
Dimethyl furan (C_6H_8O)	0.29	4.63
Maleic anhydride ($C_4H_2O_3$)	0.30	4.72
Dimethyl benzoic acid ($C_9H_{10}O_2$)	0.46	7.23
Carbon dioxide (CO_2)	0.13	2.12

From the above table 4.13, using equation 4.14, the value of the equilibrium constant K_{eq} of the reaction is:

$$K_{eq} = \frac{[C_6H_8O]^1[C_4H_2O_3]^1}{[C_9H_{10}O_2]^1[CO_2]^1} = 0.70$$

And, the Gibbs free energy of the reaction was determined using equation 4.19 as follows:

$$\Delta G^O = -RT\ ln\, K_{eq} = -2.303\, RT\, log\, K_{eq} = -8.314 \frac{J}{mol.K} * 323.15K\ ln(0.7012) = 953.67\, J/mol$$

Therefore, from the above results, Since K < 1, and $\Delta G^0{}_{Rxn}$ = positive, the reaction is an endothermic and it is non-spontaneous, and also, the equilibrium shifts to the left, implies that reactants are favored.

5. CONCLUSIONS AND RECOMMENDATIONS

5.1. Conclusions

Lignocellulosic biomass-derived celluloses have a great potential to form biofuels and high value added chemical compounds such as benzene, toluene, xylene and others in an economically feasible way. Therefore, this study has been focused on the production of the most valuable chemicals, particularly Para-xylene, which is used as a major raw material for the production of high value purified polyethylene terephthalate, which is used for production of plastic materials. This study deals with the possibility of converting the lignocellulosic biomass particularly sugarcane bagasse into value-added chemicals particularly Para-xylene using two-step acid-catalyzed hydrolysis reaction, acid-catalyzed dehydration, hydrogenation, Diels-Alder cycloaddition reaction and dehydration followed by decarboxylation steps. The experiment was conducted using design expert®7 software, central composite design (CCD) method in quadratic model to investigate the effect of process parameters such as molar ratio of the reactant, catalyst loading and reaction time on the Diels-Alder cycloaddition reaction step. Based on the analysis of the experimental result (ANOVA), all these parameters and their interactions have significant effects on the responses such as conversion of DMF and the yield of dimethyl benzoic acid. During the experiment we investigate that, as the reactant molar ratio was increased from 1 to 5 both the conversion of DMF and the yield of dimethyl benzoic acid was slowly decreased from 39.1 to 13.6 and from 61.1 to 21.3 respectively. And also, as the catalyst loading was increased from 0.1 to 0.5 moles, both the conversion of DMF and the yield of dimethyl benzoic acid was slowly increased from 18.2 to 21.7 and from 28.4 to 34 respectively. Moreover, as the reaction time increased from 4 to 12 hrs, both the conversion of DMF and the yield of dimethyl benzoic acid was slowly increased until it reaches 8hr and slowly decreased as the time is above 8 hrs. In this, initially the conversion and the yield was increased from 15.5 to 19.3 and 24.3 to 30.2, and as the time is increased above 8 hr, the conversion and the yield was decreased to 18.3 and 29.5 respectively. As the result, a maximum of 41.4% DMF conversion and 64.6% yield of dimethyl benzoic acid were obtained at a lower concentration of DMF using small amount of Lewis acid catalyst (i.e. $AlCl_3$). And also the effects of acid concentration on the dehydration of dimethyl benzoic acid was investigated at different reaction times, and finally, 70.36% conversion of

dimethyl benzoic acid and 49.66% yield of Para-xylene (1,4-dimethyl benzene) was obtained at 4M H_2SO_4 and 120 minutes reaction time.

In this study, the intermediate products in each of the process steps were characterized using FTIR to check whether the required products such as glucose, HMF, DMF, dimethyl benzoic acid and 1, 4-dimethyl benzoic acid are formed or not. And from the FTIR results, the functional group of all the required products was observed, which indicates, the presence of these intermediate products in each step of the production process. And also, the final product was characterized using GC-MS to determine the composition of the intermediate product in the sample, and finally, 30.88% composition of 1, 4-dimethyl benzene was obtained.

5.2. Recommendations

In this study, there are many difficulties to investigate all the process steps starting from the size reduction of the sample up to the final product. In this work, the effects of operating variables on the Diels-Alder cycloaddition reaction was investigated and optimized, but it is necessary to optimize the other parameters in each step of the process such as in the material pretreatment, dehydration reaction of glucose conversion to HMF, hydrogenation reaction of HMF conversion to DMF and decarboxylation of dimethyl benzoic acids. In addition to this, in this study, chemical pretreatment method was used to extract the reducing sugars using concentrated strong acids, since chemicals are highly toxic and corrosive, future works will better to select biological methods rather than chemical pretreatment methods, which is the environmentally friendly method to minimize risks and environmental challenges.

Furthermore, in this study, the intermediate products were analyzed only using FTIR and GC-MS, but, it is necessary to characterize using NMR, to analyze the detailed structure of the substances as well as to identify the reaction mixtures, side products, and intermediate product of the sample, which was not included in this study. Therefore, future studies should include NMR analysis and various kinetics and optimization of the reactions on the main steps of the reaction such as hydrolysis, dehydration, and hydrogenation reactions.

REFERENCES

Abdel-Halim, E. S. (2014). Chemical modification of cellulose extracted from sugarcane bagasse: Preparation of hydroxyethyl cellulose. *Arabian Journal of Chemistry*, *7*(3), 362–371. https://doi.org/10.1016/j.arabjc.2013.05.006

Agbor, V. B., Cicek, N., Sparling, R., Berlin, A., & Levin, D. B. (2011). Biomass pretreatment: Fundamentals toward application. *Biotechnology Advances*, *29*(6), 675–685. https://doi.org/10.1016/j.biotechadv.2011.05.005

Agustina, D., Kumagai, S., Nonaka, M., & Sasaki, K. (2013). Production of 5-hydroxymethyl Furfural from Sugarcane Bagasse Under Hot Compressed Water. *Procedia Earth and Planetary Science*, *6*, 441–447. https://doi.org/10.1016/j.proeps.2013.01.058

Aigbodion, V. S., Hassan, S. B., Ause, T., & Nyior, G. B. (2010). Potential Utilization of Solid Waste (Bagasse Ash), *9*(1), 67–77.

Allison, B. D., Brandt, M. E., & Devasher, R. B. (2011). Infrared Spectroscopy, 6(15), 24–28.

Amarasekara, A. S., Williams, L. D., & Ebede, C. C. (2008). Mechanism of the dehydration of D -fructose to 5-hydroxymethyl furfural in dimethyl sulfoxide at 150 °C : NMR study. *Carbohydrate Research*, *343*(18), 3021–3024. https://doi.org/10.1016/j.carres.2008.09.008

Amin, F. R., Khalid, H., Zhang, H., Rahman, S., Zhang, R., Liu, G., & Chen, C. (2017). Pre-treatment methods of lignocellulosic biomass for anaerobic digestion. *AMB Express*. Dec; 7(1), 72, https://doi.org/10.1186/s13568-017-0375-4

Aqilah, N., Fadzil, M., Hasbi, M., Rahim, A., & Maniam, G. P. (2014). A brief review of para - xylene oxidation to terephthalic acid as a model of primary C – H bond activation, *35*(10), 1641–1652. https://doi.org/10.1016/S1872

Aragaw, T. A. (2016). Proximate Analysis of Cane Bagasse and Synthesizing Activated Carbon: Emphasis on Material Balance. *Journal of Environmental Treatment Techniques*, *4*(4), 102–110.

Aransiola, E. F., Daramola, M. O., & Ojumu, T. V. (2013). Xylenes: Production technologies and uses, *Synthesis, Characterization and Physicochemical Properties*, (January 2016), pp 127-154, 978-1-62808-342-2.

Araujo, A. S., Domingos, T. B., Souza, M. J. B., & Silva, A. O. S. (2001). Xylene Isomerization In Sapo-11/Hzsm-5 Mixed Catalyst, *73*(2), 283–290.

Ashraf, M. T. (2013). Analysis and optimization of P-Xylene Production process by Highly Selective Methylation of Toluene, 52 (38), pp 13730–13737

Ayeni, A. O., Adeeyo, O. A., Oresegun, O. M., & Oladimeji, E. (2015). Compositional analysis of lignocellulosic materials : Evaluation of an economically viable method suitable for woody and non-woody biomass; American Journal of Engineering Research (AJER), (4), 14–19.

Ayeni, A. O., Hymore, F. K., Mudliar, S. N., Deshmukh, S. C., Satpute, D. B., Omoleye, J. A., & Pandey, R. A. (2013). Hydrogen peroxide and lime based oxidative pre-treatment of wood waste to enhance enzymatic hydrolysis for a bio-refinery: Process parameter optimization using response surface methodology. *Fuel*, *106*, 187–194. https://doi.org/10.1016/j.fuel.2012.12.078

Badiei, M., Asim, N., Jahim, J. M., & Sopian, K. (2014). Comparison of Chemical Pretreatment Methods for Cellulosic Biomass. *APCBEE Procedia*, *9*(Icbee 2013), 170–174. https://doi.org/10.1016/j.apcbee.2014.01.030

Barberio, A., Gallegos, A., & Liu, M. (2015). Para-xylene from Corn. 5-4-2015, 295.

Beers, K. (2005). Physico-chemical Analysis of Selected Biomass Materials in University of Hawaii, *29* (12), pp 7975–7984; doi**:** 10.1021/acs.energyfuels.5b01945

Betancur, G. J. V. (2010). Sugar cane bagasse as feedstock for second generation ethanol production. Part I : Diluted acid pre-treatment optimization. https://doi.org/10.2225/vol.13-issue.3-fulltext-3

Bhaumik, P., Deepa, A. K., & Kane, T. (2014). Value addition to lignocellulosics and biomass-derived sugars: An insight into solid acid-based catalytic methods, *126*(2), 373–385.

Biddy, M. J., Scarlata, C., & Kinchin, C. (2016). Chemicals from Biomass: A Market Assessment of Bio-products with Near-Term Potential. *NREL Technical Report NREL/TP-5100-65509*, 131. https://doi.org/10.2172/1244312

Bogliano, A. (2016). Lignin Valorization through Catalytic Lignocellulose Fractionation: A Fundamental Platform for the Future Biorefinery, 9(13), 1544-58. doi: 10.1002/cssc.201600237

Bujang, N., Najwa, M., Rodhi, M., Musa, M., & Subari, F. (2013). Effect of dilute sulfuric acid hydrolysis of coconut dregs on chemical and thermal properties. *Procedia Engineering*, *68*, 372–378. https://doi.org/10.1016/j.proeng.2013.12.194

Catrinck, M. N., Ribeiro, E. S., Monteiro, R. S., Ribas, R. M., Barbosa, M. H. P., & Teó, R. F. (2017). The direct conversion of glucose to 5-hydroxymethyl furfural using a mixture of novice acid and niobium phosphate as a solid acid catalyst, Vol. 210, 67–74. https://doi.org/10.1016/j.fuel.2017.08.035

Coates, J. (2006). Interpretation of Infrared Spectra, A Practical Approach. *Encyclopedia of Analytical Chemistry*, 1–23. https://doi.org/10.1002/9780470027318.a5606

Creation, M. J. (2014). Renewable Chemicals & Materials Opportunity Assessment Report Major Job Creation and Agricultural Sector Engine,1: 13. https://doi.org/10.1186/s40538-014-0013-1

Daramola, M. O. (2010). Characterization and Optimization of an Extractor-type Catalytic Membrane Reactor for Meta-xylene Isomerization over Pt-HZSM-5 Catalyst, Asia-Pac. J. Chem. Eng. 2010; 5: 815–837 doi: 10.1002/apj.414.

Dashtban, M., Technologies, A., & Dashtban, M. (2015). Production of Furfural from Process-Relevant Biomass-Derived Pentoses in a Biphasic Reaction System, *ACS Sustainable Chem. Eng.*, *5* (7), pp 5694–5701, doi: 10.1021/acssuschemeng.7b00215

Delidovich, I., Hausoul, P. J. C., Deng, L., Pfu, R., Rose, M., & Palkovits, R. (2016). Alternative Monomers Based on Lignocellulose and Their Use for Polymer Production, *Chem. Rev.*, 2016, *116* (3), pp 1540–1599; https://doi.org/10.1021/acs.chemrev.5b00354

Dhabhai, R., Jain, A., & Chaurasia, S. P. (2012). Production Of Fermentable Sugars By Dilute Acid Pretreatment And Enzymatic Saccharification Of Three Different Lignocellulosic Materials, *4*(4), 1497–1502.

Doncea, S., Virgil, B., Senin, R., & Ion, R. (2012). Spectral Identification and Hplc Quantification of Benzoic Acid From Natural Juices, *7*(7), 39–41.

Dussán, K. J., Silva, D. D. V, Moraes, E. J. C., Priscila, V., & Felipe, M. G. A. (2014). Dilute-acid Hydrolysis of Cellulose to Glucose from Sugarcane Bagasse, *38*, 433–438. https://doi.org/10.3303/CET1438073

Dutta, S., & Mascal, M. (2014). Novel Pathways to 2, 5-Dimethylfuran via Biomass-Derived 5-(Chloromethyl) furfural, ChemSusChem. 2014 Nov; 7(11): 3028-30. https://doi.org/10.1002/cssc.201402702. Epub 2014 Sep 5.

Edhirej, A., Sapuan, S. M., Jawaid, M., & Zahari, N. I. (2017). Preparation and Characterization of Cassava Bagasse Reinforced Thermoplastic Cassava Starch, *18*(1), 162–171. https://doi.org/10.1007/s12221-017-6251-7

Elgharbawy, A. A., Alam, Z., Moniruzzaman, M., & Goto, M. (2016). Ionic liquid pre-treatment as emerging approaches for enhanced enzymatic hydrolysis of lignocellulosic biomass. *Biochemical Engineering Journal*, *109*, 252–267. https://doi.org/10.1016/j.bej.2016.01.021

Eriksson, N. (2013). Production of four selected renewable aromatic chemicals. *Division of Forest Products and Chemical Engineering*, Vol.42, 1–33.

Esmaeili, N., Zohuriaan-Mehr, M. J., Mohajeri, S., Kabiri, K., & Bouhendi, H. (2017). Hydroxymethyl furfural-modified urea–formaldehyde resin: synthesis and properties. *European Journal of Wood and Wood Products*, *75*(1), 71–80. https://doi.org/10.1007/s00107-016-1072-8

Ferreira, L., Almeida, P. De, Vanderley, A., Sola, H., & Jairo, J. (2017). Acta Scientiarum Sugarcane bagasse pellets: characterization and comparative analysis, 461–468. https://doi.org/10.4025/actascitechnol.v39i4.30198

Fms, D., Jgc, G., & Lf, S. (2017). Exploring the Microbial Production of Aromatic Fine Chemicals to Overcome the Barriers of Traditional Methods, *8*(1), 94–109.

Gallo, J. M. R., & Trapp, M. A. (2017). The chemical conversion of biomass-derived saccharides. *Journal of the Brazilian Chemical Society*, *28*(9), 1586–1607. https://doi.org/10.21577/0103-5053.20170009

Ghasemzadeh, R., Kargar, A., & Lotfi, M. (2014). Comparison of pretreatment methods for biofuel production, Vol. 8(1), 15–16.

Gobinath, E., Jeyavijayan, S., & Xavier, R. J. (2017). Spectroscopic investigations, DFT computations and other molecular properties of 2, 4-dimethyl benzoic acid, *55*, 541–550.

Goyal, R., Sarkar, B., Bag, A., Siddiqui, N., Dumbre, D., Lucas, N., Bordoloi, A. (2016). Studies of synergy between metal – support interfaces and selective hydrogenation of HMF to DMF in water. *Journal of Catalysis*, *340*, 248–260. https://doi.org/10.1016/j.jcat.2016.05.012

Harmsen, P., & Huijgen, W. (2010). Literature Review of Physical and Chemical Pre-treatment Processes for Lignocellulosic Biomass, Vol.7, 1–49.

Hong, K. O. H. M. A. Y. (2013). Preparation and characterization of carboxymethyl cellulose from sugarcane bagasse, 10:22, 110.

Ibrahim, M., Alaam, M., El-Haes, H., Jalbout, A. F., & Leon, A. De. (2006). Analysis of the structure and vibrational spectra of glucose and fructose. *Eclética Química*, *31*(3), 15–21. https://doi.org/10.1590/S0100-46702006000300002

Jaiswal, A. (2015). A Comprehensive Review on Pre-treatment Strategy for Lignocellulosic Food Industry Waste: Challenges and Opportunities, 199, 92-102. doi: 10.1016/j.biortech.2015.07.106. Epub 2015 Aug 4.

Jenness, G. R. (2015). Use of High Performance Computing in Modeling Biomass Refining, *54* (1), 324–337; doi: 10.1021/ci4005145.

Jönsson, L. J., & Martín, C. (2016). Pretreatment of lignocellulose: Formation of inhibitory by-products and strategies for minimizing their effects. *Bioresource Technology*, *199*, 103–112. https://doi.org/10.1016/j.biortech.2015.10.009

Journal, B. (2012). Effect of acid hydrolysis and fungal bio-treatment on Agro-industrial wastes for obtainment of free sugars for bio-ethanol production; Egypt; Department of Agricultural Chemistry, Faculty of Agriculture, Ain Shams University, Shoubra El-Kheima, 43(4), 1523–1535. doi: 10.1590/S1517-838220120004000037.

Karp, S. G., Woiciechowski, A. L., Soccol, V. T., & Soccol, R. (2013). Pretreatment Strategies for Delignification of Sugarcane Bagasse: A Review, *56*, 679–689.

Kumar, A. K., & Sharma, S. (2017). Recent updates on different methods of pretreatment of lignocellulosic feedstocks. *Bioresources and Bioprocessing*, *4* (1), 7. https://doi.org/10.1186/s40643-017-0137-9

Kumar, P., Barrett, D. M., Delwiche, M. J., Stroeve, P., Kumar, P., Barrett, D. M., Stroeve, P. (2009). Methods for Pretreatment of Lignocellulosic Biomass for Efficient Hydrolysis and Biofuel Production. *48* (8), 3713–3729. https://doi.org/10.1021/ie801542g.

Lee, Y. -J. (2005). Oxidation of Sugarcane Bagasse Using a Combination of Hypochlorite and Peroxide, 100 (2): 935-941. https:// doi.org/10.1016/j.biortech.2008.06.043.

Limayem, A., & Ricke, S. C. (2012). Lignocellulosic biomass for bioethanol production : Current perspectives, potential issues and future prospects. *Progress in Energy and Combustion Science*, *38* (4), 449–467. https://doi.org/10.1016/j.pecs.2012.03.002

Lin, Z. (2015). Integrated Design, Evaluation and Optimization of Biomass Conversion to Chemicals. Retrieved from https://doi.org/doi:10.7282/T3V40X5N.

Lin, Z., & Ierapetritou, M. (2013). Aromatic from Lignocellulosic Biomass : Economic Analysis of the Production of p-Xylene from 5-Hydroxymethyl furfural, *59* (6), 2079-2087. https://doi.org/10.1002/aic.13969

Liu, J., Tang, Y., Wu, K., Bi, C., & Cui, Q. (2012). Conversion of fructose into 5-hydroxymethyl furfural (HMF) and its derivatives promoted by inorganic salt in alcohol. *Carbohydrate Research*, *350*, 20–24. https://doi.org/10.1016/j.carres.2011.12.006

Löffler, E., & International, G. (2009). Why co-production is an important topic for local government, 424 (6944), 62.

Lyons, T. W., Guironnet, D., Findlater, M., & Brookhart, M. (2012). Synthesis of p - Xylene from Ethylene, 134 (38), 15708–15711. https://doi.org/10.1021/ja307612b

Maria, A., Galletti, R., & Antonetti, C. (2011). Mid infrared, FT-IR as a Tool for Monitoring Herbaceous Biomass Composition and Its Conversion to Furfural, Volume 2015, Article ID 719042, 12 pages.http://dx.doi.org/10.1155/2015/719042

Maryana, R., Ma'rifatun, D., Wheni, I. A., K.w., S., & Rizal, W. A. (2014). Alkaline pre-treatment on sugarcane bagasse for bio-ethanol production. *Energy Procedia*, *47*, 250–254. https://doi.org/10.1016/j.egypro.2014.01.221

Mathematik, V. D. F., & Rwth, N. Der. (2015). „ Oxidative Pretreatment and Biocatalytic Valorization of Lignocellulosic Biomass ", 480552_21 Jul 2015, 18:12

Mcfarlane, J., & Robinson, S. (2007). *Survey of Alternative Feedstocks for Commodity Chemical Manufacturing, 2(2):60-74.doi:10.3934/bioeng.2.60.*

Meng, Q., Qiu, C., Zheng, H., Li, X., & Zhu, Y. (2017). Efficient Decarbonylation of 5-hydroxymethylfurfural over Pd / Al_2O_3 catalyst : Preparation via electrostatic attraction between Pd (II) complex and anionic Al_2O_3. *Molecular Catalysis*, *433*, 111–121. https://doi.org/10.1016/j.mcat.2017.02.035

Meuwese, A. (2013). The sustainability of producing BTX from biomass, 1–77.

Miao, Z., Grift, T. E., & Ting, K. C. (2014). Size Reduction and Densification of Lignocellulosic Biomass Feedstock for Biopower, Bioproducts, and Liquid Biofuel Production, 10–13. https://doi.org/10.1081/E-EAFE2-120051298

Michelin, M., & Teixeira, J. A. (2016). Liquid hot water pre-treatment of multi feedstocks and enzymatic hydrolysis of solids obtained thereof. *Bioresource Technology*, *216*, 862–869. https://doi.org/10.1016/j.biortech.2016.06.018

Mohameed, H. A., Jdayil, B. A., & Takrouri, K. (2007). Separation of para -xylene from xylene mixture via crystallization, *46*, 25–36. https://doi.org/10.1016/j.cep.2006.04.002

Negi, S., & Pandey, A. K. (2014). Ionic Liquid Pretreatment. *Pretreatment of Biomass,Processes and Technologies*, 137–155. https://doi.org/10.1016/B978-0-12-800080-9.00008-6

Neifar, M., & Chouchane, H. (2016). Ligninases and Glycosyl Hydrolases in Developing a cellulosic Bioethanol Industry, *2*(5), 234–248.

Neto, D., & Dantas, C. (2011). Separation Of Xylene Isomers Through Adsorption On Microporous Materials, 255–268. https://doi.org/10.5419/bjpg2011-0024

Nikbin, N., Do, P. T., Caratzoulas, S., Lobo, R. F., Dauenhauer, P. J., & Vlachos, D. G. (2013). A DFT study of the acid-catalyzed conversion of 2 , 5-dimethylfuran and ethylene to p-xylene. *Journal of Catalysis*, *297*, 35–43. https://doi.org/10.1016/j.jcat.2012.09.017

Nizamoff, A. J. (2012). Bio-Routes to para-Xylene, (March). *134* (38), pp 15708–15711 doi: 10.1021/ja307612b

Pacheco, J. J., & Davis, M. E. (2014). Synthesis of terephthalic acid via Diels-Alder reactions with ethylene and oxidized variants of 5-hydroxymethylfurfural, (15). https://doi.org/10.1073/pnas.1408345111

Peleteiro, S., & Garrote, G. (2014). Utilization of Ionic Liquids in Lignocellulose Biorefineries as Agents for Separation, Derivatization, Fractionation, or Pretreatment, 63(37):8093-102. doi: 10.1021/acs.jafc.5b03461. Epub 2015 Sep 10.

Petre, M., Zarnea, G., Adrian, P., & Gheorghiu, E. (1999). Bio-degradation and bio-conversion of cellulose wastes using bacterial and fungal cells immobilized in radio polymerized hydrogels, *27*, 309–332.

Rocha, G. J. M., Gonçalves, A. R., Nakanishi, S. C., Nascimento, V. M., & Silva, V. F. N. (2015). Pilot scale steam explosion and diluted sulfuric acid pre-treatments: Comparative study aiming the sugarcane bagasse Saccharification. *Industrial Crops and Products*, *74*, 810–816. https://doi.org/10.1016/j.indcrop.2015.05.074

Saha, B., & Abu-omar, M. M. (2014). Advances in 5-hydroxymethylfurfural production from biomass in Biphasic solvents, 24–38. https://doi.org/10.1039/c3gc41324a

Salminen, E., Riittonen, T., Virtanen, P., Kumar, N., & Mikkola, J. (2012). The Challenge of Efficient Synthesis of Biofuels from Lignocellulose for Future Renewable Transportation Fuels, *2012*. https://doi.org/10.1155/2012/674761

Science, A. (2015). Synthesis Of Furfural From Bagasse, Hayelom. G, Kiros. F, Tsegalaul. K, Tsigehiwot. G, *57*, 72–84. https://doi.org/10.18052/www.scipress.com/ILCPA.57.72

Science, C., Chang, C., Xiong, R., & Technology, A. (2015). Kinetic Regimes in the Tandem Reactions of H- BEA Catalyzed Formation of p-Xylene from Dimethylfuran, (October). https://doi.org/10.1039/C5CY01320H

Settle, A. E., Berstis, L., Rorrer, N. A., Roman-Leshkóv, Y., Beckham, G. T., Richards, R. M., & Vardon, D. R. (2017). Heterogeneous Diels–Alder catalysis for biomass-derived aromatic compounds. *Green Chem.*, *19* (15), 3468–3492. https://doi.org/10.1039/C7GC00992E

Sheppard, S. T. D., & Hailes, H. C. (2016). As featured in *Green Chemistry*, *18*, 1855–1858. https://doi.org/10.1039/c5gc02935j

Singh, S., Varanasi, P., Singh, P., Adams, P. D., Auer, M., & Simmons, B. A. (2013). Understanding the impact of ionic liquid pretreatment on cellulose and lignin via thermo-chemical analysis. *Biomass and Bioenergy*, *54*, 276–283. https://doi.org/10.1016/j.biombioe.2013.02.035

Singhvi, M. S., Chaudhari, S., & Gokhale, D. V. (2014). Lignocellulose Processing: A Current Challenge, 8271–8277. https://doi.org/10.1039/C3RA46112B

Sn, W. (2008). Sugarcane Bagasse : How Easy Is It To Measure Its Constituents? Vol.81, 266–273, Ref.30.

Souza, A. P. De, Leite, D. C. C., & Buckeridge, M. S. (2012). Composition and Structure of Sugarcane Cell Wall Polysaccharides: Implications for Second-Generation Bioethanol Production. https://doi.org/10.1007/s12155-012-9268-1

Srivastava, M., Sengupta, S., Das, P., & Datta, S. (2017). Novel Pre Treatment Techniques for Extraction of Fermentable Sugars from Natural Waste Materials for Bio Ethanol Production, 1–7. https://doi.org/10.19080/IJESNR.2017.07.555713.

Thiyagarajan, S., Genuino, H. C., Van Der Waal, J. C., De Jong, E., Weckhuysen, B. M., Van Haveren, J., … Van Es, D. S. (2016). A Facile Solid-Phase Route to Renewable Aromatic Chemicals from Bio-based Furanics. *Angewandte Chemie - International Edition*, *55*(4), 1368–1371. https://doi.org/10.1002/anie.201509346

Toribio-Cuaya, H., Pedraza-Segura, L., Macías-Bravo, S., Vasquez-Medrano, R., & Favela-Torres, E. (2014). Characterization of Lignocellulosic Biomass Using Five Simple Steps. *Journal of Chemical , Biological and Physical Sciences*, *4*(5), 28–47.

Tsai, T. (1999). Disproportionation and transalkylation of alkylbenzenes over zeolite catalysts. *Applied Catalysis A: General*, *181*(2), 355–398. https://doi.org/10.1016/S0926-860X(98)00396-2

Tucker, M. (2017). Dilute acid pretreatment of sorghum biomass to maximize the hemicellulose hydrolysis with minimized levels of fermentative inhibitors for bio-ethanol production. 7:139. https://doi.org/10.1007/s13205-017-0752-3

Upare, P. P., Hwang, D. W., Hwang, Y. K., Lee, U., Hong, D., & Chang, J. (2015). An integrated process for the production of 2,5-dimethylfuran from fructose, 3310–3313. https://doi.org/10.1039/c5gc00281h

Vardon, D. R. (2017). Heterogeneous Diels–Alder catalysis for biomass-derived aromatic compounds. *Green Chemistry*, *19* (15), 3468–3492. https://doi.org/10.1039/c7gc00992e

Wang, Tianfu,. (2014). "Catalytic conversion of glucose to 5-hydroxymethylfurfural as a potential bio-renewable platform chemical". *217,* https://lib.dr.iastate.edu/etd/13721

Weber, R., & Keller, W. D. (2016a). "Para-Xylene Derived from Biorenewable Feedstock". *Honors Theses AY 15/16*. 80. Retrieved from http://repository.uwyo.edu/ honors_theses_15-16/80

Weber, R., & Keller, W. D. (2016b). "Para-Xylene Derived from Biorenewable Feedstock". *Honors Theses AY 15/16*. 80. http://repository.uwyo.edu/honors_theses_15-16/80

Wijaya, Y. P., Suh, D. J., & Jae, J. (2015). Production of renewable p-xylene from 2,5-dimethylfuran via Diels-Alder cycloaddition and dehydrative aromatization reactions over silica-alumina aerogel catalysts. *Catalysis Communications*, *70*, 12–16. https://doi.org/10.1016/j.catcom.2015.07.008

Williams, C. L. (2014). Cycloaddition of biomass-derived furans for catalytic production of renewable p-xylene, 2 (6), 935-939

Winner, N. P. (1994). Sustainability / Green Design " Sustainability means living on nature ' s income rather Principles of Sustainability, *1*, 1412-1430; doi: 10.3390/su1041412

Yang, S. G., & Tsubaki, N. (2017). As featured in Chemical Science. *Chemical Science*, *8*, 7941–7946. https://doi.org/10.1039/C7SC03427J

Yasuhiko, A. (2013). LCA comparison of 100% bio-based PET synthesized from different PTA pathways.Michigan State University. https://doi.org/10.25335/m5hx2s.

Zhao, X., Cheng, K., & Liu, D. (2009). Organosolv pretreatment of lignocellulosic biomass for enzymatic hydrolysis. *Applied Microbiology and Biotechnology*, *82*(5), 815–827. https://doi.org/10.1007/s00253-009-1883-1

Zheng, Y., Pan, Z., & Zhang, R. (2009). Overview of biomass pretreatment for cellulosic ethanol production, *2*(3), 51–68. https://doi.org/10.3965/j.issn.1934-6344.2009.03.051-068

Zhou, C., Zhao, J., Elgasim, A., Yagoub, A., & Ma, H. (2017). Conversion of glucose into 5-hydroxymethylfurfural in different solvents and catalysts : Reaction kinetics and mechanism. *Egyptian Journal of Petroleum*, *26*(2), 477–487. https://doi.org/10.1016/j.ejpe.2016.07.005

APPENDICES

Appendix A: Chemical identity and properties of xylene isomers

Characteristics	**m-xylene**	**o-xylene**	**p-xylene**
Synonyms/trade name	1,3-dimethyl benzene; m-dimethyl benzene; m-methyl toluene	1,2-dimethylbenzene; o-dimethyl benzene; o-methyl toluene	1,4-dimethyl benzene; p-dimethyl benzene; p-methyl toluene
Chemical formula	C_8H_{10}	C_8H_{10}	C_8H_{10}
Molecular weight	106.16 gr/mol	106.16 gr/mol	106.16 gr/mol
Color	Colorless	Colorless	Colorless
Physical state	Liquid	Liquid	Liquid
Melting point	-47.8 ℃	-25.2 ℃	13.2 ℃
Boiling point	139.1 ℃	144.5 ℃	138.4 ℃
Density at 20 ℃	0.864 g/cm^3	0.880 g/cm^3	0.861 g/cm^3
Odor	Sweet	Sweet	Sweet
Solubility @25 ℃	161 mg/L miscible with alcohol, ether and other organic solvents	178 mg/L miscible with alcohol, ether and other organic solvents	162 mg/L soluble in alcohol, ether and other organic solvents
Vapour pressure	8.29 mmHg at 25 ℃	6.61 mmHg at 25 ℃	8.84 mmHg at 25 ℃
Henry's law constant	7.18*10^{-3} atm.m^3/mol	5.18*10^{-3} atm.m^3/mol	6.90*10^{-3} atm.m^3/mol
Autoignition temperature	527 ℃	463 ℃	528 ℃
Flash point	27 ℃	32 ℃	27 ℃
Flammability limits	1.1-7.0%	1.0-7.0%	1.1-7.0%

(Sources:*(Aransiola et al., 2013)***)**

Appendix-B: Infrared Spectroscopy Correlation Table by frequency regions

4000-3000 cm^{-1}				
Bond	**Frequency**	**Functional group**	**Type of vibration**	**Intensity**
O-H	3700-3584	Alcohol	Stretching	Medium, sharp
	3550-3200	Alcohol	Stretching	Strong, broad
N-H	3500	Primary amine	Stretching	Medium
	3400			
	3400-3300	Aliphatic primary amine		Medium
	3330-3250			
	3350-3310	Secondary amine	Stretching	Medium
O-H	3300-2500	Carboxylic acid	Stretching	Strong, broad
	3200-2700	Alcohol	Stretching	Week, broad
3000-2500 cm^{-1}				
C-H	3333-3267	Alkyne	Stretching	Strong, sharp
	3100-3000	Alkene	Stretching	Medium
	3000-2840	Alkane	Stretching	Medium
	2830-2695	Aldehyde	Stretching	Medium
2400-2000 cm^{-1}				
O=C=O	2349	Carbon dioxide	Stretching	Strong
$C \equiv N$	2260-2222	Nitrile	Stretching	Week
$C \equiv C$	2260-2190	Alkyne	Stretching	Week
C=C=O	2150	Ketene	Stretching	
$C \equiv C$	2140-2100	Alkyne	Stretching	Week
C=C=C	2000-1900	Allenes	Stretching	Medium
2000-1650 cm^{-1}				
C-H	2000-1650	Aromatic compound	Bending	Week
1870-1540 cm^{-1}				
C=O	1818	Anhydride	Stretching	Strong
	1750			
	1815-1785	Acid halides	Stretching	Strong
	1800-1770	Conjugated acid halide	Stretching	Strong
	1775	Conjugated anhydride	Stretching	Strong
	1720			
	1770-1780	Vinyl /phenyl	Stretching	Strong
	1760	Carboxylic acid	Stretching	Strong
	1750-1735	Esters	Stretching	Strong
	1740-1720	Aldehyde	Stretching	Strong
	1720-1706	Carboxylic acid	Stretching	Strong
	1685-1666	Conjugated ketone	Stretching	Strong
1670-1600 cm^{-1}				
C=C	1678-1668	Alkene, Disubstituted (trans)	Stretching	Week
	1675-1665	Trisubstituted	Stretching	Week

		Tetra substituted	Stretching	Week
	1662-1626	Disubstituted	Stretching	Medium
	1658-1648	Vinylidene	Stretching	Medium
1600-1300 cm^{-1}				
N-O	1550-1500	Nitro compound	Stretching	Strong
	1372-1290			
C-H	1465	Alkane, methyl group	Bending	Medium
	1375			
	1390-1380	Aldehyde		
	1385-1380	Alkane		
	1370-1365			
1400-1000 cm^{-1}				
O-H	1440-1395	Carboxylic acid	Bending	Medium
	1420-1330	Alcohol	Bending	Medium
S=O	1415-1380	Sulfate	Stretching	Strong
	1200-1185			
	1410-1380	Sulfonyl chloride	Stretching	Strong
C-H	1310-1250	Aromatic ester	Stretching	Strong
CO-O-CO	1050-1040	Anhydride	Stretching	Strong, broad
1000-650 cm^{-1}				
C=C	995-985	Alkene, Monosubstituted	Bending	Strong
	915-905			
	980-960	Disubstituted (trans)		
	840-790	Trisubstituted	Bending	Medium
900-700 cm^{-1}				
C-H	880±20	1,2,4-trisubstituted	Bending	Strong
	810±20			
	880±20	1,3-disubstituted		
	780±20			
	700±20			
	810±20	1,4-disubstituted 1,2,3,4-tetrasubstituted		
	780±20	1,2,3-trisubstituted		
	700±20			
	755±20	1,2-disubstituted		
	750±20	Mono-substituted		
	700±20	Benzene derivative		

(**Sources**: *(Allison et al., 2011)*)

Appendix-C: Experimental Result calculation

Table C-1: proximity analysis

Physical composition	Initial Mass (W_1, g)	Final Mass (W_2, g)	Mass percentage
Moisture content	4.230	4.05446	$\text{MC} = \frac{(W_1 - W_2)}{W_1} * 100 = \frac{(4.23 - 4.0545)}{4.23} * 100 = 4.15\%$
Volatile Matter	3.930	0.981	$\text{VM} = \frac{(W_1 - W_2)}{W_1} * 100 = \frac{(3.93 - 0.981)}{3.93} * 100 = 75.04\%$
Ash Content	4.350	0.3506	$\text{Ash} = \frac{W_2}{W_1} * 100 = \frac{0.3506}{4.350} * 100 = 8.06\%$
Fixed Carbon	$\text{FC} = 100 - \text{Ash}(\%) - \text{VM}(\%) - \text{MC}(\%) = 100 - 8.06 - 75.04 - 4.15 = 12.75\%$		

Table C-2: Chemical composition analysis results

Chemical Composition	Initial Mass (W_1, g)	Final Mass (W_2, g)	Mass Percentage
Extractives	10	9.7795	$\text{Extra.} = \frac{(W_1 - W_2)}{W_1} * 100 = \frac{(10 - 9.78)}{10} * 100 = 2.205\%$
Hemicellulose	3.0	2.0040	$\text{Hem.} = \frac{(W_1 - W_2)}{W_1} * 100 = \frac{(3.0 - 2.00)}{3.0} * 100 = 33.20\%$
Lignin	3.0	2.3760	$\text{Lig.} = \frac{(W_1 - W_2)}{W_1} * 100 = \frac{(3.0 - 2.376)}{3.0} * 100 = 20.80\%$
Cellulose	$\text{WC} = 100 - (\text{WE} + \text{WH} + \text{WL}) = 100 - 2.205 - 33.20 - 20.80 = 43.795\%$		